



National Library
of Canada

Bibliothèque nationale
du Canada

Canadian Theses Service

Services des thèses canadiennes

Ottawa, Canada
K1A 0N4

CANADIAN THESES

NOTICE

The quality of this microfiche is heavily dependent upon the quality of the original thesis submitted for microfilming. Every effort has been made to ensure the highest quality of reproduction possible.

If pages are missing, contact the university which granted the degree.

Some pages may have indistinct print especially if the original pages were typed with a poor typewriter ribbon or if the university sent us an inferior photocopy.

Previously copyrighted materials (journal articles, published tests, etc.) are not filmed.

Reproduction in full or in part of this film is governed by the Canadian Copyright Act, R.S.C. 1970, c. C-30. Please read the authorization forms which accompany this thesis.

THIS DISSERTATION
HAS BEEN MICROFILMED
EXACTLY AS RECEIVED

THÈSES CANADIENNES

AVIS

La qualité de cette microfiche dépend grandement de la qualité de la thèse soumise au microfilmage. Nous avons tout fait pour assurer une qualité supérieure de reproduction.

S'il manque des pages, veuillez communiquer avec l'université qui a conféré le grade.

La qualité d'impression de certaines pages peut laisser à désirer, surtout si les pages originales ont été dactylographiées à l'aide d'un ruban usé ou si l'université nous a fait parvenir une photocopie de qualité inférieure.

Les documents qui font déjà l'objet d'un droit d'auteur (articles de revue, examens publiés, etc.) ne sont pas microfilmés.

La reproduction, même partielle, de ce microfilm est soumise à la Loi canadienne sur le droit d'auteur, SRC 1970, c. C-30. Veuillez prendre connaissance des formules d'autorisation qui accompagnent cette thèse.

LA THÈSE A ÉTÉ
MICROFILMÉE TELLE QUE
NOUS L'AVONS REÇUE



PERMISSION TO MICROFILM — AUTORISATION DE MICROFILMER

• Please print or type / Ecrire en lettres moulees ou dactylographier

Full Name of Author — Nom complet de l'auteur

ROBIN FREDRICK BRUCE TURNER

Date of Birth — Date de naissance

16 AUGUST 1956

Country of Birth — Lieu de naissance

Permanent Address — Residence fixe

1205 - 11135 - 83 AVENUE
EDMONTON ALBERTA T6E 2C6

Title of Thesis — Titre de la these

SPHERICAL DISTRIBUTION AND DENSITY
OF ELECTROMAGNETIC MODES IN
RECTANGULAR CAVITIES

University — Université

UNIVERSITY OF ALBERTA

Degree for which thesis was presented — Grade pour lequel cette these fut presentee

MASTER OF SCIENCE

Year this degree conferred — Année d'obtention de ce grade

1984

Name of Supervisor — Nom du directeur de these

W.A.G. VOSS / W.R. TINBA

Permission is hereby granted to the NATIONAL LIBRARY OF CANADA to microfilm this thesis and to lend or sell copies of the film.

The author reserves other publication rights, and neither the thesis nor extensive extracts from it may be printed or otherwise reproduced without the author's written permission.

L'autorisation est, par la presente, accordée à la BIBLIOTHÈQUE NATIONALE DU CANADA de microfilmer cette thèse et de prêter ou de vendre des exemplaires du film.

L'auteur se réserve les autres droits de publication; ni la thèse ni de longs extraits de celle-ci ne doivent être imprimés ou autrement reproduits sans l'autorisation écrite de l'auteur.

Date

12 OCTOBER 1984

Signature

THE UNIVERSITY OF ALBERTA

SPECTRAL DISTRIBUTION AND DENSIT.

OF ELECTROMAGNETIC MODES IN RECTANGULAR CAVITIES

by

ROBIN F.B. TURNER

A THESIS

SUBMITTED TO THE FACULTY OF GRADUATE STUDIES AND RESEARCH
IN PARTIAL FULFILMENT OF THE REQUIREMENTS FOR THE DEGREE OF

MASTER OF SCIENCE

DEPARTMENT OF ELECTRICAL ENGINEERING

EDMONTON, ALBERTA

FALL, 1984

DEPARTMENT OF
ELECTRICAL ENGINEERING
TELEPHONE (403) 432-3332 AND 432-3393



THE UNIVERSITY OF ALBERTA
EDMONTON, CANADA
T6G 2E1

THE UNIVERSITY OF ALBERTA

RELEASE FORM

NAME OF AUTHOR: Robin F.B. Turner

TITLE OF THESIS: Spectral Distribution and Density of
Electromagnetic Modes in Rectangular
Cavities

DEGREE FOR WHICH THESIS WAS PRESENTED: Master of Science

YEAR THIS DEGREE GRANTED: 1984

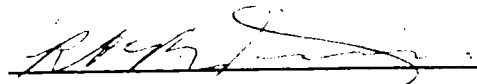
Permission is hereby granted to

THE UNIVERSITY OF ALBERTA LIBRARY

to reproduce single copies of this thesis, and to lend or
sell such copies for private, scholarly or scientific
research purposes only.

The author reserves other publication rights, and
neither the thesis nor extensive extracts from it may be
printed or otherwise reproduced without the author's written
permission.

(Signed)



PERMANENT ADDRESS: College Plaza Tower 1
No. 1205, 11135 83 Avenue
Edmonton, Alberta T6G 2C6

DATED: September 13, 1984

THE UNIVERSITY OF ALBERTA

FACULTY OF GRADUATE STUDIES AND RESEARCH

The undersigned certify that they have read, and recommend to the Faculty of Graduate Studies and Research, for acceptance, a thesis entitled

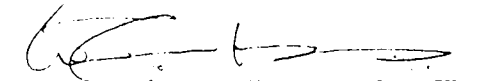
Spectral Distribution and Density
of Electromagnetic Modes in Rectangular Cavities

submitted by

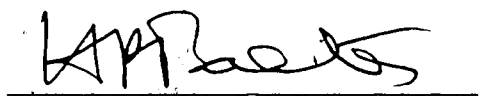
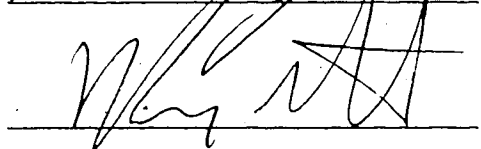
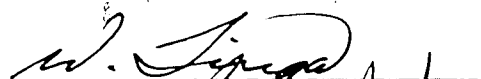
Robin F.B. Turner

in partial fulfilment of the requirements for the degree of
Master of Science

(Co-Supervisor)



(Co-Supervisor)



Date: September 13, 1984

ABSTRACT

The spectral distribution and spectral density of electromagnetic modes are perceived to be of value in the design and analysis of rectangular multimode cavities. However, these mode distributions have never been determined correctly in the engineering literature. Serious errors have been discovered in both numerical and analytical mode distribution calculations which have survived, apparently undetected, partly due to a lack of experimental measurements. The nature of the errors suggests that misunderstandings exist regarding the partial distributions of TM and TE modes.

A brief introduction is given which corrects a deficiency in the engineering literature regarding references to fundamental theoretical work. The introduction is followed by a review of the essential physics of electromagnetic boundary value problems in rectangular geometry.

A numerical algorithm is presented which enumerates TM and TE modes separately, and thereby yields the correct number of modes in an empty rectangular cavity for any finite bandwidth. This algorithm is used to generate corrected versions of previously published cavity design tables which were based on faulty algorithms. Numerical

mode distributions are computed for a number of hypothetical cavities which illustrate some important characteristics of these distributions not previously considered. These characteristics affect the utility of mode distribution calculations in the design of microwave heating cavities.

The first experimental measurements of mode distributions are reported for an empty rectangular laboratory cavity which are in good agreement with computed distributions obtained using the correct algorithm. Additional results for the same cavity fitted with a mode stirrer indicate that the mode distributions are substantially perturbed by such loading.

Certain versions of the scalar asymptotic mode distribution formulae, which are valid for acoustic modes, have been incorrectly applied to microwave cavity problems in engineering. The correct formulae are derived by considering the number of lattice points in an ellipsoid in p -space. Approximate eigenfrequency distributions obtained from these formulae are compared with the numerically and experimentally determined distributions. The results of these comparisons verify the analytical formulae at microwave frequencies and, therefore, are of interest to both physicists and engineers. The accuracy of these formulae are discussed in terms of their role in the design and analysis of microwave power applicators.

ACKNOWLEDGMENTS

The author wishes to express his sincere appreciation to the following people and council:

Professors W.A.G. Voss and W.R. Tinga for encouragement, guidance and support, and for allowing me the opportunity to pursue this project (and others) during the course of my program.

Professor H.P. Baltes for providing the impetus which substantially changed the direction and emphasis of my work, and for his interest and input since.

Professor G.B. Walker, Dr. G. Walker, Mr. T.M. Curran and Mr. R.B. Paranjape for many valuable philosophical and technical discussions.

Miss M.K. Gowan for moral support and invaluable assistance with the typing and proof reading of this thesis.

The University of Alberta Department of Electrical Engineering for providing financial support through yearly Graduate Teaching Assistantships. And the Natural Sciences and Engineering Research Council of Canada for providing financial assistance through the grants A2272 (W.A.G. Voss) and A7626 (W.R. Tinga).

TABLE OF CONTENTS

CHAPTER	PAGE
1. INTRODUCTION	1
1.1 Properties of Eigenvalue Spectra	1
1.2 Overview of Physics Literature	3
1.3 Overview of Engineering Literature	6
1.4 Objectives	9
1.5 Scope	10
2. THEORETICAL BACKGROUND	12
2.1 Rectangular Waveguide Modes	12
2.2 Rectangular Cavity Modes	17
2.3 Rectangular Cavity Field Components	19
2.4 Eigenmode Distributions	20
3. NUMERICAL EIGENMODE DISTRIBUTIONS	25
3.1 Numerical Mode Counting	25
3.2 A Mode Counting Algorithm	28
3.3 Computer Aided Cavity Design	33
3.4 Numerical Case Studies	36
3.5 Revised Cavity Design Tables	45
3.6 Discussion	46
4. EXPERIMENTAL EIGENMODE DISTRIBUTIONS	48
4.1 Materials and Methods	48

4.2 Results for the Empty Cavity	52
4.3 Results for the Cavity with a Mode Stirrer	55
4.4 Discussion	57
5. ANALYTICAL EIGENMODE DISTRIBUTIONS	60
5.1 Asymptotic Eigenmode Distributions	60
5.2 Asymptotic Spectral Distribution of EM Modes ...	64
5.3 Asymptotic Spectral Density of EM Modes	68
5.4 Verification of the Asymptotic Formulae	69
5.5 Exact Spectral Density of EM Modes	73
5.6 Discussion	76
6. SUMMARY AND CONCLUSIONS	78
6.1 Regarding Calculated Mode Distributions	78
6.2 Regarding Measured Mode Distributions	80
6.3 Some Topics for Further Research	81
6.4 Concluding Remarks	81
BIBLIOGRAPHY AND REFERENCES	84
APPENDICES	
APPENDIX A. COMPUTER PROGRAM LISTINGS	94
APPENDIX B. CAVITY MODE COUNT REFERENCE TABLES ...	123
APPENDIX C. ON THE CROSS-COUPLING PROBLEM	135
APPENDIX D. ASYMPTOTIC FORMULAE FOR WAVEGUIDES ...	140

LIST OF TABLES

TABLE	PAGE
3.1 Truth table for the Boolean output variables E, H, B, N.	31
3.2 Karnaugh maps for the Boolean output variables E, H, B, N.	32
5.1 Comparison of the figures E and A for the asymptotic formulae applied to the hypothetical cavities discussed in Chapter 3.	74
B.1 Numerically determined mode count reference data for several rectangular cavities excited by frequencies within the range $2425 \leq f \leq 2475$ MHz.	123
B.2 Numerically determined mode count reference data for several rectangular cavities excited by frequencies within the range $900 \leq f \leq 930$ MHz.	128
B.3 A comparison of mode count data for several cavities of typical sizes used in domestic microwave ovens.	133
B.4 Variations in the mode count data presented in Tables B.1, 2, 3.	134

LIST OF FIGURES

FIGURE	PAGE
2.1 Venn diagram representation of the solution space of Eq.(2.38) for finite bandwidth.	23
3.1 Flow chart representation of a mode counting algorithm for rectangular cavities.	34
3.2 The theoretical spectral distribution of electromagnetic modes in an empty cubic cavity.	37
3.3 The theoretical spectral distribution of electromagnetic modes in an empty rectangular cavity..	38
3.4 The theoretical spectral density of electromagnetic modes in an empty cubic cavity for a bandwidth of 100 MHz.	39
3.5 The theoretical spectral density of electromagnetic modes in an empty rectangular cavity for a bandwidth of 100 MHz.	40
3.6 The theoretical spectral density of electromagnetic modes in an empty (nearly) cubic cavity for a bandwidth of 100 MHz.	41
3.7 The theoretical spectral density of electromagnetic modes in an empty rectangular cavity for a bandwidth of 100 MHz.	42
3.8 - The theoretical spectral density of electromagnetic modes in an empty cubic cavity for	43

	a bandwidth of 50 MHz.	
3.9	The theoretical spectral density of electromagnetic modes in an empty rectangular cavity for a bandwidth of 50 MHz.	44
4.1	Schematic diagram of the measurement system used to obtain experimental mode distribution data.	50
4.2	Comparison of the theoretical (N^t) and measured (N^m) spectral distribution of modes in an empty rectangular cavity.	53
4.3	Comparison of the theoretical (D^t) and measured (D^m) spectral density of modes in an empty rectangular cavity for a bandwidth of 50 MHz.	54
4.4	Comparison of the measured spectral distribution of modes in a rectangular cavity with (N^m), and without (N^m), a mode stirrer.	56
5.1	Comparison of the exact and approximate spectral distribution of EM modes for a particular rectangular cavity.	71
5.2	Comparison of the exact and approximate spectral density of EM modes for a particular rectangular cavity for a bandwidth of 50 MHz.	72
C.1	Measured spectral distribution of modes (N^m), for the experimental cavity discussed in Chapters 4 and 5, showing the relative cross-coupling between top and side mounted antennae.	137

LIST OF SYMBOLS AND ABBREVIATIONS

- x_1, x_2, x_3 orthogonal spatial coordinates in meters, in three dimensional space.
- a_1, a_2, a_3 unit vectors directed along the x_1, x_2, x_3 axes respectively.
- L_1, L_2, L_3 fixed linear dimensions in meters, in the x_1, x_2, x_3 directions respectively.
- t time in seconds.
- E, D electric field intensity in volts per meter, and electric flux density in Coulombs per meter² respectively.
- H, B magnetic field intensity in amps per meter, and magnetic flux density in Webers per meter² respectively.
- n unit normal vector directed inward from a bounding surface.
- J, ρ_s surface current density in amps per meter, and surface charge density in Coulombs per meter² respectively, at a dielectric-conductor interface.
- μ_0, ϵ_0 magnetic permeability in Henries per meter, and electric permittivity in Farads per meter respectively, of free space.
- k_0, k_0 free space wave vector and its modulus or wave number respectively, in radians per meter.
- λ, ω, c wave length in meters, angular frequency in radians per second, and phase velocity in meters

per second respectively, of propagating waves.

∇_t^2, ∇_t transverse components only of the Laplacian and gradient operators respectively.

TE, TM, EM abbreviations for the terms "transverse electric", "transverse magnetic" and "electromagnetic" respectively.

TS, NL abbreviations for "total number of solutions" and "non-longitudinal solutions" respectively.

$A|_{s_i, s_j}$ indicates that the quantity or expression A is to be evaluated at the surfaces i and j .

p_1, p_2, p_3 nonnegative, dimensionless, integral quantum numbers referred to the x_1, x_2, x_3 dimensions respectively.

P_1, P_2, P_3 Boolean variables which are true if p_1, p_2, p_3 respectively are non-zero, and false if they are zero.

E, H, B, N Boolean variables which are true if the triplet (p_1, p_2, p_3) describes a TM mode, a TE mode, both or neither respectively.

ω_c, k_c cutoff angular frequency in radians per second, and cutoff wave number in radians per meter respectively.

$\delta\omega, \delta k$ bandwidth in radians per second and radians per meter respectively.

N, D exact spectral distribution and spectral density respectively, of electromagnetic modes.

N^m, D^m measured spectral distribution and spectral

density respectively, of electromagnetic modes.

N', D' theoretical spectral distribution and spectral density respectively, of electromagnetic modes.

$N(\omega), D(\omega)$ asymptotic spectral distribution and spectral density functions respectively, of electromagnetic modes.

V, S volume in meters³ and internal surface area in meters² respectively, of a particular rectangular cavity.

E, A average (signed) error and average absolute error respectively, between exact and approximate mode distributions.

CHAPTER 1. INTRODUCTION

The first section of this chapter is intended to provide a qualitative description of the nature of eigenvalue spectra, and to introduce functional definitions of the two types of mode distribution. Proper mathematical definitions will be given in Chapter 2. The next two sections comprise a brief overview of some of the important existing literature, which is necessary in order to understand the origin of the problems addressed in later chapters. The final two sections describe the objectives of the present work and define the scope of the thesis.

1.1 Properties of Eigenvalue Spectra

The electromagnetic forms of the wave equation follow directly from Maxwell's equations and are therefore inherently involved in virtually every problem in electrodynamics. The classical solution to these equations in a domain completely bounded by perfectly conducting surfaces yields an infinite set of eigenvalues representing the allowable modes of oscillation. These eigenvalues are quasi-randomly spaced throughout the spectrum and exhibit finite degeneracy at each of the eigenfrequencies. For any of the simple geometries in which the wave equation is separable, any arbitrary number of the eigenvalues can be calculated analytically. However, it is virtually

impossible to predict, by strictly analytical means, the exact number of modes that will occur within a given bandwidth. Yet this spectral density is of considerable importance in many scientific and engineering applications.

The spectral density is derived from the more fundamental spectral distribution of eigenmodes. Simply stated, the spectral distribution of the eigenvalues for a particular bounded domain (e.g. waveguide or cavity) is the cumulative total number of eigenvalues, or modes, with eigenfrequencies not exceeding some upper limit, as a "function" of the limit frequency. If the spectral distribution "function" is evaluated at two different marker frequencies, the difference yields the number of modes in the bandwidth defined by these two frequencies. This result is equivalent to evaluating a spectral density "function"—which describes the number of modes per interval of bandwidth—at the same marker frequencies. If the two frequencies are allowed to be arbitrary, but their separation is held constant, then this differential number of modes can be (and usually is) also presented as a distribution in the statistical sense.

In order to simplify the discussions to follow, the term "density" will be used throughout this thesis in reference to both the evaluated spectral density (i.e. the differential number of modes) and the unevaluated or true

spectral density of modes†. It should be clear from the context which form, if a particular one, is required.

In many contexts, the discussion applies equally well to either the spectral distribution or the spectral density of modes. It is therefore convenient to introduce an ambiguous term "eigenmode distribution" or simply "mode distribution", which could mean either or both of these distributions.

Of course, given the nature of the eigenvalues described above, neither the spectral distribution nor the spectral density of modes can, strictly speaking, be true functions. The reason for this phraseology will become clear when the exact mode distributions are defined mathematically in the next chapter. Also it will be helpful to dispense with the semantic distinction when the exact mode distributions are compared graphically to the asymptotic approximations, which are true functions of frequency.

1.2 Overview of Physics Literature

There are two methods of determining the exact eigenmode distributions for a given cavity: numerical

†For most engineering applications, the bandwidth must be specified in order to extract useful quantitative information.

computation and experimental measurement. It is important to realize that both are relatively modern methods†. But near the turn of the century, long before the advent of programmable computing machinery and electronic measuring equipment, there was a scientific need for an understanding of the behavior of eigenvalue spectra [1-4]. Calculus and analytical methods were the most powerful theoretical tools of the day, and theorists therefore approached the problem by studying the asymptotic behavior of eigenvalue spectra in the limit of large wave numbers. That is, the average cumulative number of modes, as a function of frequency, in the high frequency limit.

The first detailed investigation of this kind was undertaken more than seven decades ago by Weyl [5-8] who considered the mathematical problem‡ of calculating the asymptotic distribution of the eigenvalues of Laplacian operators. Weyl obtained the first term of an asymptotic expansion of the mode distribution and proved its independence of the shape of the domain. Later investigators, notably Courant [9], Courant and Hilbert [10], Carleman [11], Pleijel [12,13], Brownell [14,15], and

†Although a student of H.A. Lorentz, Johanna Reudler, actually calculated (by hand) portions of the exact mode distributions for a few simple geometries [Leiden dissertation, 1912].

‡Weyl at first considered some nonphysical boundary conditions which resembled those of the electromagnetic problem, but this did not detract from the mathematical importance of the work.

Agmon [16,17], extended Weyl's results and improved the accuracy of the asymptotic expansion. Most of these authors considered the special case of electromagnetic boundary conditions, but the emphasis of this early research was more on mathematical rigor than physical applications of the theory. The references given above are representative but by no means constitute a complete list. An excellent and thorough review of the important (mathematical) developments up to the time of its publication in 1967 is given by Clark [18].

Some early work which focused more on the electromagnetic problem was done by Müller [19], Müller and Niemyer [20], Niemyer [21,22] and Pathria [23]. It was not until the early seventies, however, that the electromagnetic problem was fully understood theoretically. Also by this time, numerical and experimental methods were well-developed, which permitted the theoretical work to be tested. Some of the important results from this era will be discussed in some detail in Chapter 5, but Case and Chiu [24], Balian and Bloch [25], Balian and Duplantier [26], Baltes and Kneubühl [27], Baltes and Hilf [28], Baltes [29,30], and Steinle and Baltes [31,32] were eminent contributors. The theoretical results obtained for the electromagnetic case have been applied mainly to infrared and optical [30-37] problems in physics. Comprehensive literature reviews which include both theoretical and

applied research on the electromagnetic (and other) problems are given in several articles by Baltes, *et al.* [27,28,30,38].

The physics literature cited above is all "well connected" in the sense that subsequent papers built on the results of previous research and adequate references were provided to assist later researchers. However, two papers by Bolt [39] and Maa [40], which appeared simultaneously in 1939, were not quite so "well connected". Bolt and Maa treated the scalar (acoustic) problem and derived asymptotic formulae for the mode distributions that were presented as extensions to those given in the texts by Courant and Hilbert [10] and Morse [41]. No other references to prior research were given. This apparently singular breach of continuity may have contributed to some of the problems which later developed in the engineering literature.

1.3 Overview of Engineering Literature

The interests of (electrical) engineers are mainly in the electromagnetic applications of mode distributions. The most common of which being the investigation of the characteristics of rectangular cavities used in microwave heating systems. Of course, the precise shape of the (exact) mode distributions in a loaded cavity are

necessarily different from those in an empty cavity†. Hence it would seem that, from an engineering point of view, the empty-cavity (or intrinsic) mode distributions may or may not be important characteristics. But the consensus among microwave oven designers appears to be that the intrinsic mode distributions are indeed helpful in predicting the performance of the loaded cavity [42-49]. However, it is interesting to note that these mode distributions have yet to be determined correctly—by numerical, experimental or analytical means—in the engineering literature.

It was not until the early sixties that mode distributions were really considered in the context of microwave applicator design. Philips Research Labs published a set of tables [42] giving the (incorrect) number of modes, within the ISM band at 2450 MHz, for several rectangular cavities. These tables were later reprinted in a book by Püschner [43], accompanied by a discussion of exact and approximate mode distributions. Unfortunately, the asymptotic formulae quoted by Püschner are also incorrect. They are actually the acoustic formulae given in the second edition of the text by Morse [41], which incorporated the work of Bolt and Maa mentioned previously. Püschner simply doubled each of the terms in Maa's formulae

†In nearly all practical applications, cavity loads consist of inhomogeneous, irregularly shaped, lossy dielectric materials and therefore substantially change the boundary value problem.

in order to account for the two different wave types. The errors in both the numerical data (tables) and the analytical formulae will be explained and corrected in later chapters.

James, *et al.* [44,45] also quoted Maa's formulae in articles on multimode theory. These articles have been cited in several later engineering works, including the recent text by Metaxas and Meredith [46] where both [45] and [40] are cited.

Copson and Decareau [47] avoid the mistake of quoting Maa's formulae by giving instead only the first term (for which the doubling is valid). But this too is misleading since the first term is only accurate for infinitely high frequencies. No references are provided.

The only known attempt (in English) to point out these problems is unfortunately buried within an article on microwave applications in China [49], and is itself marred by a serious typographical error in the "corrected" spectral distribution formula†. Again, no references are given which direct the reader to the copious physics literature on the subject. In fact, ironically, the only direct link between the engineering literature and the physics literature is via

†A more explicit account in Chinese [50] gives the correct asymptotic formulae, but does not contain any references to the fundamental physics papers.

the papers by Bolt and Maa, which have nothing to do with the electromagnetic problem, and which do not provide adequate references to gain access to the EM work.

1.4 Objectives

Partly due to the lack of a theoretical literature base, and partly due to the lack of experimental data, long-standing errors abound in the engineering literature on multimode cavities. These errors have accumulated for over two decades without definitive action to correct them. Because the errors are of a theoretical nature, misunderstandings regarding the physics of mode distributions have resulted among engineers working in the field of microwave power.

It is a major objective of this thesis to draw attention to these problems, and to correct the errors by presenting the proper theoretical arguments along with the pertinent (correct) results. Attention is given to both the numerical computation of exact mode distributions, and the analytical calculation of approximate mode distributions. Also, the bibliographic references bridge a long-standing gap between the engineering and physics literature, and should provide other scholars and researchers with a sufficient literature base to begin more detailed studies of this important subject.

A second objective is to report the results of experimental measurements which substantiate the physical theory at microwave frequencies, and which reveal something of the nature of mode distributions in the presence of light metallic structures (e.g. mode stirrers). These measurements were performed on rectangular cavities but the technique is applicable to more complicated geometries.

A third objective is to discuss some of the characteristics of exact and approximate mode distributions which have been discerned from the experimental measurements and a number of numerical case studies. These characteristics must be understood in order to evaluate the roles and the utility of both exact and approximate mode distribution calculations in engineering research and design applications.

1.5 Scope

Most of the existing problems in the engineering literature involve mode distributions in empty, rectangular, ideal microwave cavities. Accordingly, this thesis concentrates on electromagnetic modes in perfectly conducting rectangular cavities which, for theoretical purposes, enclose a free space medium and, for practical (e.g. experimental) purposes, are air-filled. Although much of the physics of these cavities also applies to other

geometries, loading conditions and wave phenomena, these cases will not be studied in detail here. Where appropriate, generalizations will be mentioned, but not discussed unless there are direct ramifications in the field of microwave power engineering. Further limitations to the scope of certain sections will be given in the text pertaining to that material.

CHAPTER 2. THEORETICAL BACKGROUND

It is essential to understand the basic physics involved in electromagnetic boundary value problems in order to correctly obtain and interpret eigenmode distributions. It is therefore the purpose of this chapter to review these principles and to present, in a mathematical context, some important equations used in subsequent chapters. The two dimensional eigenvalue problem is introduced in the first section which leads to the definition and classification of waveguide modes. The analysis is extended in the next section to include cavity modes. The eigenfunctions which describe the actual field components are presented in the third section. Rigorous (mathematical) definitions of the mode distributions are given in the last section, along with a discussion of how and why the partial distributions of TM and TE modes are different.

2.1 Rectangular Waveguide Modes

Consider a three dimensional semi-infinite domain in free space defined, in Cartesian coordinates (x_1, x_2, x_3) , by

$$0 < x_1 < L_1 \tag{2.1}$$

$$0 < x_2 < L_2 \tag{2.2}$$

$$-\infty < x_3 < +\infty \tag{2.3}$$

and bounded by perfectly conducting plane surfaces.

Electromagnetic fields in this domain must satisfy the appropriate form of Maxwell's equations, viz.

$$\nabla \times \mathbf{E} = -\frac{\partial \mathbf{B}}{\partial t} \quad (2.4)$$

$$\nabla \times \mathbf{H} = \frac{\partial \mathbf{D}}{\partial t} \quad (2.5)$$

$$\nabla \cdot \mathbf{D} = 0 \quad (2.6)$$

$$\nabla \cdot \mathbf{B} = 0 \quad (2.7)$$

where $\mathbf{B} = \mu_0 \mathbf{H}$ and $\mathbf{D} = \epsilon_0 \mathbf{E}$ and, since the domain is enclosed by perfect conductors, the appropriate boundary conditions are

$$\mathbf{n} \times \mathbf{E} = 0 \quad (2.8)$$

$$\mathbf{n} \times \mathbf{H} = \mathbf{J}_s \quad (2.9)$$

$$\mathbf{n} \cdot \mathbf{D} = \rho_s \quad (2.10)$$

$$\mathbf{n} \cdot \mathbf{B} = 0 \quad (2.11)$$

where \mathbf{n} is the unit normal vector directed inward (toward the free-space medium) from the boundaries. It can easily be shown [51-53] that Eqs.(2.4-2.7) are equivalent to the EM wave equations

$$\nabla^2 \mathbf{E} - \mu_0 \epsilon_0 \frac{\partial^2 \mathbf{E}}{\partial t^2} = 0 \quad (2.12)$$

$$\nabla^2 \mathbf{H} - \mu_0 \epsilon_0 \frac{\partial^2 \mathbf{H}}{\partial t^2} = 0 \quad (2.13)$$

subject to the same boundary conditions described by Eqs.(2.8-2.11). And if the time dependence is assumed to be harmonic, then Eqs.(2.12,2.13) further reduce to the vector Helmholtz equations

$$\nabla^2 \mathbf{E} + k_0^2 \mathbf{E} = 0 \quad (2.14)$$

$$\nabla^2 \mathbf{H} + k_0^2 \mathbf{H} = 0 \quad (2.15)$$

where $k_0^2 = \mu_0 \epsilon_0 \omega^2$ the infinite-medium, free space wave number. It is common to view k_0 as the modulus of a so-called wave vector \mathbf{k}_0 with components in each of the coordinate directions, *viz.*

$$\mathbf{k}_0 = k_1 \mathbf{a}_1 + k_2 \mathbf{a}_2 + k_3 \mathbf{a}_3 \quad (2.16)$$

from which

$$|\mathbf{k}_0|^2 = k_0^2 = k_1^2 + k_2^2 + k_3^2 \quad (2.17)$$

and the direction of \mathbf{k}_0 is everywhere normal to the electric and magnetic field vectors.

Due to the infinite extent of the domain in the $\pm x_3$ directions, it is useful (and reasonable) to assume propagating wave functions of the form

$$\mathbf{E}(x, t) = \mathbf{E}(x_1, x_2) e^{-i(\omega t \pm k_3 x_3)} \quad (2.18)$$

$$\mathbf{H}(x, t) = \mathbf{H}(x_1, x_2) e^{-i(\omega t \pm k_3 x_3)} \quad (2.19)$$

where the plus/minus signs indicate forward/backward propagating waves. Furthermore, since the boundary conditions on \mathbf{E} and \mathbf{H} are different, the eigenvalues will, in general, be different. Thus it is natural to divide the field solutions into two distinct classes: transverse magnetic (TM or E-type) for which $H_3 \equiv 0$, and transverse

electric (TE or H-type) for which $E_3 \equiv 0$ †. For the present case, these TM and TE wave functions together constitute a complete orthonormal solution set from which arbitrary EM disturbances in a waveguide can be fully described.

Hence, a substantial simplification of the solution procedure can be achieved by converting the vector Eqs.(2.14,2.15) to equivalent scalar equations. This conversion is accomplished by separating the x_1, x_2 dependent parts of the wave functions (2.18,2.19) into axial (E_3 and H_3) and transverse ($E_{1,2}$ and $H_{1,2}$) components. It is then sufficient to solve

$$\nabla_{\perp}^2 E_3 + \gamma^2 E_3 = 0 \quad (2.20)$$

$$\nabla_{\perp}^2 H_3 + \gamma^2 H_3 = 0 \quad (2.21)$$

where $\gamma^2 = k_0^2 - k_z^2$, subject to the boundary conditions

$$E_3 |_{s_{1,2}} = 0 \quad (2.22)$$

$$\left. \frac{\partial H_3}{\partial n} \right|_{s_{1,2}} = 0 \quad (2.23)$$

respectively, since the transverse field components can be obtained directly from the axial components according to the relations

†A third species—the transverse electromagnetic (TEM) wave—should be considered in a general discussion of guided waves. However, the TEM mode cannot exist inside a single, hollow duct of infinite conductivity (i.e. the present case) and is therefore neglected here.

$$H_t = \pm i \frac{k_0}{\gamma^2} Z_0' (a_3 \times \nabla_t E_3) \quad (2.24)$$

$$E_t = \mp \frac{k_3}{k_0} Z_0 (a_3 \times H_t) \quad (2.25)$$

for TM waves, and

$$E_t = \mp i \frac{k_0}{\gamma^2} Z_0 (a_3 \times \nabla_t H_3) \quad (2.26)$$

$$H_t = \pm \frac{k_3}{k_0} Z_0' (a_3 \times E_t) \quad (2.27)$$

for TE waves, where $Z_0 = \sqrt{\mu_0/\epsilon_0}$, and the plus/minus signs again indicate forward/backward propagating waves.

The Eqs.(2.20,2.21), together with the boundary conditions (2.22,2.23) respectively, specify eigenvalue problems in two dimensions. In general, there will be two doubly infinite sets of eigenvalues—one for the TM waves and one for the TE waves—that emerge, and the corresponding eigenfunctions describe distinct field patterns or eigenmodes (or simply "modes") which propagate in the guide. However, due to the mathematical symmetry of the eigenfunctions with respect to differentiation, the resulting equation for the eigenvalues is

$$\gamma^2 = k_0^2 - k_3^2 = \frac{p_1^2 \pi^2}{L_1^2} + \frac{p_2^2 \pi^2}{L_2^2} \quad (2.28)$$

where p_1, p_2 are nonnegative integers, regardless of whether TM or TE modes are sought. Although, the particular

combinations of p_1, p_2 which yield nontrivial solutions may be different for TM and TE modes. From Eq.(2.28) it is easily seen that the wave number k_3 is real only if the condition

$$\mu_0 \epsilon_0 \omega^2 > \frac{p_1^2 \pi^2}{L_1^2} + \frac{p_2^2 \pi^2}{L_2^2} \quad (2.29)$$

is satisfied. Values of p_1, p_2 that do not satisfy Eq.(2.29) describe nonpropagating or evanescent modes. Eq.(2.29) thus defines the low-frequency limit or cutoff frequency of propagating modes. Also note that there is no upper limit imposed on propagating waveguide modes. Cavity modes do not share this characteristic.

2.2 Rectangular Cavity Modes

The formulation given above for waveguide modes can be extended to cavity modes by considering plane short circuits placed transverse to the x_3 axis at $x_3=0$ and $x_3=L_3$. Then the domain of interest is completely bounded by perfect conductor and the assumed harmonic x_3 dependence is no longer valid. The correct form of the x_3 dependence is in fact the same as that for a standing wave, as would be expected for the fields in a waveguide between perfectly reflecting planes. Also, an additional set of boundary conditions must now be applied at $x_3=0, L_3$. These are essentially the same as Eqs.(2.22,2.23), but with E_3 and H_3 interchanged, viz.

$$\left. \frac{\partial E_3}{\partial n} \right|_{s_3} = 0 \quad (2.30)$$

$$H_3|_{s_3} = 0 \quad (2.31)$$

which are satisfied for all x_3 only if the wave number is given by

$$k_3^2 = \frac{p_3^2 \pi^2}{L_3^2} \quad (2.32)$$

which is now discrete rather than quasi-continuous as in the waveguide case. Also, the relationships between the axial and transverse field components are now given [51] by

$$H_t = \pm i \frac{k_0}{\gamma^2} Z_0' \cos \frac{p_3 \pi x_3}{L_3} (a_3 \times \nabla_t E_3) \quad (2.33)$$

$$E_t = \pm \frac{p_3 \pi}{L_3 \gamma^2} \sin \frac{p_3 \pi x_3}{L_3} \nabla_t E_3 \quad (2.34)$$

for TM waves, and

$$E_t = \mp i \frac{k_0}{\gamma^2} Z_0 \sin \frac{p_3 \pi x_3}{L_3} (a_3 \times \nabla_t H_3) \quad (2.35)$$

$$H_t = \mp \frac{p_3 \pi}{L_3 \gamma^2} \cos \frac{p_3 \pi x_3}{L_3} \nabla_t H_3 \quad (2.36)$$

for TE waves.

The cavity case is thus an eigenvalue problem in three dimensions and the discrete field patterns (or modes) are stationary and characterized by triply infinite sets of line spectra. Substituting Eq.(2.32) into Eq.(2.28) yields

$$k_0^2 = \frac{p_1^2 \pi^2}{L_1^2} + \frac{p_2^2 \pi^2}{L_2^2} + \frac{p_3^2 \pi^2}{L_3^2} \quad (2.37)$$

or, since $k_0^2 = \epsilon_0 \mu_0 \omega^2$,

$$\mu_0 \epsilon_0 \omega_p^2 = \frac{p_1^2 \pi^2}{L_1^2} + \frac{p_2^2 \pi^2}{L_2^2} + \frac{p_3^2 \pi^2}{L_3^2} \quad (2.38)$$

which again applies to both TM and TE modes. Note that Eq.(2.38) is an equality (compared with Eq.(2.29) which is an inequality). The subscript p has been added to the angular frequency in order to emphasize that the spectra are now discrete. The resonant frequencies ω_p are hence appropriately called eigenfrequencies.

The foregoing does not change substantially if the cavity is completely filled with a perfect (i.e. linear, nondispersive) dielectric material. Essentially, the quantities ϵ_0 and μ_0 would have to be replaced by the actual ϵ and μ which characterize the particular dielectric under consideration. However, if the dielectric is not perfect, or does not completely fill the cavity, then the boundary value problem is changed significantly and the analysis presented here is no longer adequate.

2.3 Rectangular Cavity Field Components

The eigenfunctions are given (for several geometries) in most texts but in order to facilitate later discussions, it is useful to list the rectangular cavity eigenfunctions in a form consistent with the notation used here. Hence, following the procedure outlined in the two previous

sections, the actual field components (eigenfunctions) for a rectangular cavity are:

$$E_1 = -\frac{C}{\gamma^2} \frac{p_1 \pi}{L_1} \frac{p_3 \pi}{L_3} \cos \frac{p_1 \pi x_1}{L_1} \sin \frac{p_2 \pi x_2}{L_2} \sin \frac{p_3 \pi x_3}{L_3} \quad (2.39)$$

$$E_2 = -\frac{C}{\gamma^2} \frac{p_2 \pi}{L_2} \frac{p_3 \pi}{L_3} \sin \frac{p_1 \pi x_1}{L_1} \cos \frac{p_2 \pi x_2}{L_2} \sin \frac{p_3 \pi x_3}{L_3} \quad (2.40)$$

$$E_3 = C \sin \frac{p_1 \pi x_1}{L_1} \sin \frac{p_2 \pi x_2}{L_2} \cos \frac{p_3 \pi x_3}{L_3} \quad (2.41)$$

$$H_1 = i\omega\epsilon_0 \frac{C}{\gamma^2} \frac{p_2 \pi}{L_2} \sin \frac{p_1 \pi x_1}{L_1} \cos \frac{p_2 \pi x_2}{L_2} \cos \frac{p_3 \pi x_3}{L_3} \quad (2.42)$$

$$H_2 = -i\omega\epsilon_0 \frac{C}{\gamma^2} \frac{p_1 \pi}{L_1} \cos \frac{p_1 \pi x_1}{L_1} \sin \frac{p_2 \pi x_2}{L_2} \cos \frac{p_3 \pi x_3}{L_3} \quad (2.43)$$

for TM waves, and

$$H_1 = -\frac{D}{\gamma^2} \frac{p_1 \pi}{L_1} \frac{p_3 \pi}{L_3} \sin \frac{p_1 \pi x_1}{L_1} \cos \frac{p_2 \pi x_2}{L_2} \cos \frac{p_3 \pi x_3}{L_3} \quad (2.44)$$

$$H_2 = -\frac{D}{\gamma^2} \frac{p_2 \pi}{L_2} \frac{p_3 \pi}{L_3} \cos \frac{p_1 \pi x_1}{L_1} \sin \frac{p_2 \pi x_2}{L_2} \cos \frac{p_3 \pi x_3}{L_3} \quad (2.45)$$

$$H_3 = D \cos \frac{p_1 \pi x_1}{L_1} \cos \frac{p_2 \pi x_2}{L_2} \sin \frac{p_3 \pi x_3}{L_3} \quad (2.46)$$

$$E_1 = i\omega\mu_0 \frac{D}{\gamma^2} \frac{p_2 \pi}{L_2} \cos \frac{p_1 \pi x_1}{L_1} \sin \frac{p_2 \pi x_2}{L_2} \sin \frac{p_3 \pi x_3}{L_3} \quad (2.47)$$

$$E_2 = -i\omega\mu_0 \frac{D}{\gamma^2} \frac{p_1 \pi}{L_1} \sin \frac{p_1 \pi x_1}{L_1} \cos \frac{p_2 \pi x_2}{L_2} \sin \frac{p_3 \pi x_3}{L_3} \quad (2.48)$$

for TE waves; where C and D are arbitrary constants, and harmonic time dependence is understood.

2.4 Eigenmode Distributions

Any finite number of the eigenfrequencies defined by Eq.(2.38) can be calculated and arranged in ascending order,

viz.

$$0 < \omega_1 \leq \omega_2 \leq \omega_3 \leq \dots \leq \omega_p \dots \leq \omega \quad (2.49)$$

where ω is some arbitrary upper-limiting frequency to be considered. The total number of eigenfrequencies not exceeding ω is then

$$N = \sum_{\omega_p \leq \omega} 1 \quad (2.50)$$

where each term in the series represents one eigenfrequency in the sequence (2.49). And the total number of eigenfrequencies within the bandwidth $\delta\omega$ is

$$D\delta\omega = \sum_{\omega_p \leq \omega + \delta\omega} 1 - \sum_{\omega_p \leq \omega} 1 \quad (2.51)$$

where $\delta\omega$ is a (finite) real constant. Note that Eqs.(2.50,2.51) can be viewed as implicit "functions" of frequency since ω is arbitrary and can therefore be a continuous variable. In this sense, Eq.(2.50) serves as a mathematical definition† of a spectral distribution of the eigenfrequencies. And Eq.(2.51) serves as a definition for the spectral density of eigenfrequencies, per $\delta\omega$ of

†A slightly different definition is used in some of the physics literature, viz.

$$N = \sum_{\omega_p < \omega} 1 + \sum_{\omega_p = \omega} 1/2$$

but this work is mostly concerned with the asymptotic value of N in the high frequency limit, in which case the above definition and Eq.(2.50) are practically equivalent.

bandwidth. Notice that Eq.(2.51) closely resembles the definition of the derivative of the "function" N . In fact, if $\delta\omega \rightarrow 0$, then D represents a sum of Dirac delta functions $\delta(\omega - \omega_p)$ which would be the result obtained from the differentiation of the step function described by Eq.(2.50).

Since Eq.(2.38) holds equally well for TM and TE modes, it would be reasonable to define N_{TM}, N_{TE} and D_{TM}, D_{TE} using Eqs.(2.50,2.51) respectively, where only the actual ω_p are different. Hence, the total number of electromagnetic modes not exceeding ω would be

$$N_{EM} = N_{TM} + N_{TE} \quad (2.52)$$

and the number of modes within the bandwidth $\delta\omega$ would be

$$D_{EM}\delta\omega = D_{TM}\delta\omega + D_{TE}\delta\omega \quad (2.53)$$

where N_{TM} and N_{TE} are the partial distributions of TM and TE modes respectively, and D_{TM} and D_{TE} are the partial spectral densities of TM and TE modes respectively.

It is extremely important to realize that N_{TM} and N_{TE} are not, in general, equal over any given range of frequencies, and likewise for D_{TM} and D_{TE} . This is due to the fact that some combinations of p_1, p_2, p_3 uniquely identify certain modes as either TM or TE. That is, the solution space of Eq.(2.38) is "partitioned" into three unequal sets of triplets (p_1, p_2, p_3) which correspond to TM, TE

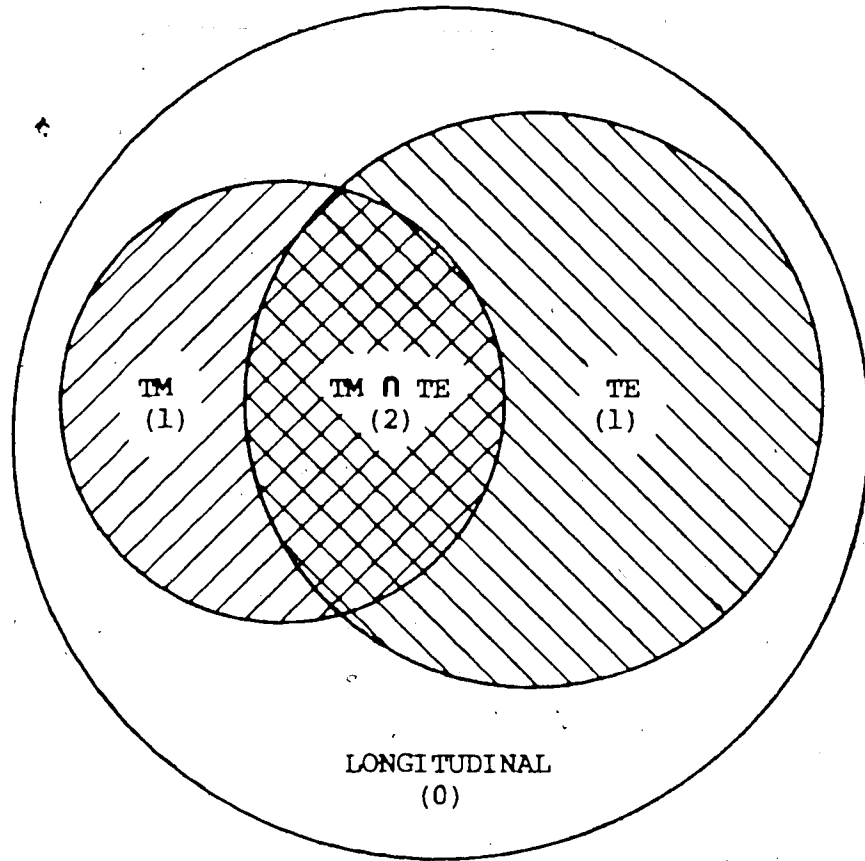


Figure 2.1 Venn diagram representation of the solution space of Eq.(2.38) for finite bandwidth. The numbers in parentheses indicate the multiplicities with which each member occurs in the distributions described by Eqs.(2.52,2.53).

and longitudinal (or forbidden) modes. Although the TM and TE sets do overlap, there are members which are unique to each set. This partitioning of the solution space of Eq.(2.38) is depicted schematically in Figure 2.1.

In order to calculate the mode distributions correctly, the members of each of the sets indicated in Figure 2.1 must all be known (or at least knowable), which in turn requires consideration of the boundary conditions (2.22,2.23) and (2.30,2.31). These mathematical expressions can be translated into restrictions on the quantum numbers that correspond to nontrivial solutions to Eqs.(2.20,2.21). These restrictions will be described in detail in the following chapter where they are formalized into a set of criteria for properly discriminating between TM and TE modes.

CHAPTER 3. NUMERICAL EIGENMODE DISTRIBUTIONS

Several previous attempts to enumerate the eigenmodes in empty rectangular cavities by numerical computation have produced incorrect results. The purpose of this chapter is to correct these defective algorithms. A brief review of the physical principles involved in electromagnetic mode counting is given in the first section. A particular mode counting algorithm which yields the correct number of modes in a rectangular cavity is presented in the second section. Three different implementations of the algorithm are briefly described in the third section, followed in the next two sections by some important numerical results obtained from two of these programs. A discussion of the significance of these results is given in the last section.

3.1 Numerical Mode Counting

The spectral distribution of modes for a particular cavity may be presented graphically as a plot of the total number of modes with resonant frequencies not exceeding some upper frequency ω as a "function" of ω . Similarly, the spectral density of modes can be presented as a plot of the number of modes with resonant frequencies between some lower frequency ω and $\omega + \delta\omega$ as a "function" of ω . In either case, the computational problem essentially reduces to counting the number of allowable modes (eigenmodes) within a

specified frequency range. For rectangular cavities, these mode counts can easily be obtained using exhaustive substitution algorithms of the type described in the following sections. In fact, the results of similar computations have been reported in the form of tables [42,43,48] intended to aid designers in the choice of optimum cavity dimensions. However, the algorithms used by these authors do not account for the physical differences between TM and TE modes, and therefore do not yield the correct total number of modes.

The intrinsic eigenfrequencies of an ideal rectangular cavity are defined by Eq.(2.38) which, in the engineering literature, is usually written

$$f^2 = \frac{p_1^2 c^2}{4L_1^2} + \frac{p_2^2 c^2}{4L_2^2} + \frac{p_3^2 c^2}{4L_3^2} \quad (3.1)$$

where f is the more commonly used Hertzian frequency, c is the velocity of light, and the quantum numbers p_1, p_2, p_3 together comprise the so-called mode number (p_1, p_2, p_3) . If there were no restrictions on the mode number (except that it be nonnegative), then Eq.(3.1) could be used to generate the aforementioned plots by simply counting all of the possible mode numbers which define resonant frequencies within the appropriate range. This is, in fact, the approach used to compile the tables in [42,43].

As explained in the previous chapter, Eq.(3.1) results from the solution of the Helmholtz equation regardless of whether TM or TE modes are sought. Hence, in the hypothetical treatment described above, one might assume† that the total number of modes is just twice that determined for either species alone. Such a treatment presupposes that TM and TE modes have identical partial distributions, which they do not. That is, the TM wave function satisfies the Dirichlet condition on those portions of the boundary surface where the TE wave function satisfies the Neumann condition, and vice versa. As a result, if any one of the quantum numbers is zero, then one or the other wave type can exist, but not both. And if any two or three quantum numbers are zero, then neither wave type can exist.

Notwithstanding the above, certain mode numbers are ambiguous in that they can represent both a TM and a TE mode. Thus, any algorithm which is intended to count electromagnetic modes must include a facility for assigning multiplicities in order to account for this type of degeneracy. That is, if none of the quantum numbers are zero, then the mode number represents both a TM and a TE mode, and therefore can be said to have a multiplicity of two. Whereas, a single zero occurring in any position in the

†The instructions given in [42,43] are not explicit, but it is obvious from the context and the actual results that only one type has been considered, and no distinction between types is made clear in the discussion.

mode number will uniquely identify the mode as either TM or TE, which therefore has a multiplicity of one. The remaining case of two (or three) zeros in the mode number leads to the trivial solution where all of the eigenfunctions vanish, and so these modes are said to have a multiplicity of zero. These multiplicities are thus the same as those indicated in the diagram of Figure 2.1.

Due to the simplicity of the eigenvalue problem in rectangular geometry, the numerical analysis is straightforward (perhaps even elementary) once the physics is understood. Still, in order to establish a basis for comparing theory and experiment, it is worthwhile to examine a particular algorithm based on the above physical conditions.

3.2 A Mode Counting Algorithm

The algorithm consists of a simple "filtering" procedure for determining which of the possible mode numbers yield resonant frequencies in the desired range. And a "sorting" procedure for determining which of the filtered mode numbers correspond to valid cavity modes, and whether they can be TM, TE or both. The filtering procedure is essentially just an application of Eq.(3.1) and does not merit further consideration here. Hence, only the sorting procedure will be described in detail.

A thorough sorting procedure (i.e. one which can discriminate between TM and TE modes) requires a slight modification to the criteria briefly described in the last section. The actual criteria used in the present algorithm for sorting modes according to mode number, are the following:

(a) If more than one of the p_1, p_2, p_3 are zero, then the mode number represents neither a TM nor a TE mode (i.e. a longitudinal, or forbidden, mode).

(b) If only p_3 is zero, then the mode number represents a TM mode only.

(c) If either p_1 or p_2 (but not p_3) is zero, then the mode number represents a TE mode only.

(d) If none of the p_1, p_2, p_3 are zero, then the mode number represents both a TM and a TE mode.

The modification indicated by (b) and (c) follows directly from the complementarity of the boundary conditions.

Let P_1, P_2, P_3 be Boolean (input) variables which are true if p_1, p_2, p_3 respectively are nonzero, and false if they are zero. Also let E, H, B be Boolean (output) variables

which are true if a given set of input variables describes a TM (or E-type) mode, a TE (or H-type mode) or both respectively, and false otherwise. These definitions together with the criteria (a)-(d) can then be used to construct Table 3.1 which comprises all of the possible combinations of P_1, P_2, P_3 and the corresponding binary values of E, H, B.

In order to obtain an efficient algorithm, the minterm expansions for E, H and B are derived from the Karnaugh maps [54] as shown in Table 3.2, *viz.*

$$E = P_1 P_2 \quad (3.2)$$

$$H = P_1 P_3 + P_2 P_3 = (P_1 + P_2) P_3 \quad (3.3)$$

$$B = P_1 P_2 P_3 \quad (3.4)$$

which can then be used to test and validate (or invalidate) the mode number $(p_1 p_2 p_3)$. Similarly, a test for nonlongitudinal modes can be derived, *viz.*

$$N = P_1 P_3 + P_2 P_3 + P_1 P_2 \quad (3.5)$$

where the definition of N is analogous to those given for E, H, B. Note that N is just E+H as would be expected†.

†Perhaps all of the Eqs.(3.2-3.5) could have been written by inspection but, inasmuch as Karnaugh maps are a proven mathematical construct, the procedure described can, given Table 3.1, serve as a proof of these equations.

Table 3.1 Truth table for the Boolean output variables E,H,B,N which are true if the corresponding input combination describes a TM mode, a TE mode, or both, or a non-longitudinal mode respectively. The input variables P_1, P_2, P_3 are true if the quantum numbers p_1, p_2, p_3 respectively are non-zero.

P_1	P_2	P_3	E	H	B	N^a
0	0	0	0	0	0	0^b
0	0	1	0	0	0	0^b
0	1	0	0	0	0	0^b
0	1	1	0	1	0	1
1	0	0	0	0	0	0^b
1	0	1	0	1	0	1
1	1	0	1	0	0	1
1	1	1	1	1	1	1

^aThis column describes the algorithm used (implicitly) in [48] which yields different, though still incorrect, results from those reported in [42,43].

^bA slight simplification may seem possible if these are designated as "don't care" states, but a more complicated filtering procedure would then be required in order to eliminate these cases.

Table 3.2 Karnaugh maps for the Boolean output variables E, H, B, N. The resulting logic equations are written in minimum sum-of-product form as described in [54].

$P_1 P_2 \backslash P_3$	0	1
0 0	0	0
0 1	0	0
1 1	1	1
1 0	0	0

$$E = P_1 P_2$$

$P_1 P_2 \backslash P_3$	0	1
0 0	0	0
0 1	0	1
1 1	0	1
1 0	0	1

$$H = P_1 P_3 + P_2 P_3$$

$P_1 P_2 \backslash P_3$	0	1
0 0	0	0
0 1	0	0
1 1	0	1
1 0	0	0

$$B = P_1 P_2 P_3$$

$P_1 P_2 \backslash P_3$	0	1
0 0	0	0
0 1	0	1
1 1	1	1
1 0	0	1

$$N = P_1 P_3 + P_2 P_3 + P_1 P_2$$

Eqs.(3.4,3.5) can provide additional information if required, but Eqs.(3.2,3.3) are the essential core of the sorting procedure. The actual number of TM and TE modes, and therefore the total number of EM modes, can thus be counted during or after sorting. A flow chart which describes a likely implementation (and one used by the author) is presented in Figure 3.1. This algorithm was used to generate numerical data for a particular laboratory cavity for which experimental data could be obtained for comparison. These results are compared graphically in the next Chapter, for now let it suffice to say that the results are in close agreement.

3.3 Computer Aided Cavity Design

As expected, the above algorithm is not very complicated, and more efficient algorithms no doubt exist at least for some special cases†. But for practical cavity sizes and bandwidths, used in microwave heating applications, the computation time for any one cavity is reasonable (i.e. less than one minute, using interpreted BASIC on an 8 bit microcomputer; and less than one second, using Pascal or FORTRAN on a 32 bit mainframe). This algorithm has in fact been implemented, with satisfactory results, in a trilogy of interactive design/analysis

†For cubic cavities for example, which are inherently the most mode-dense, a much more efficient algorithm is described in [27].

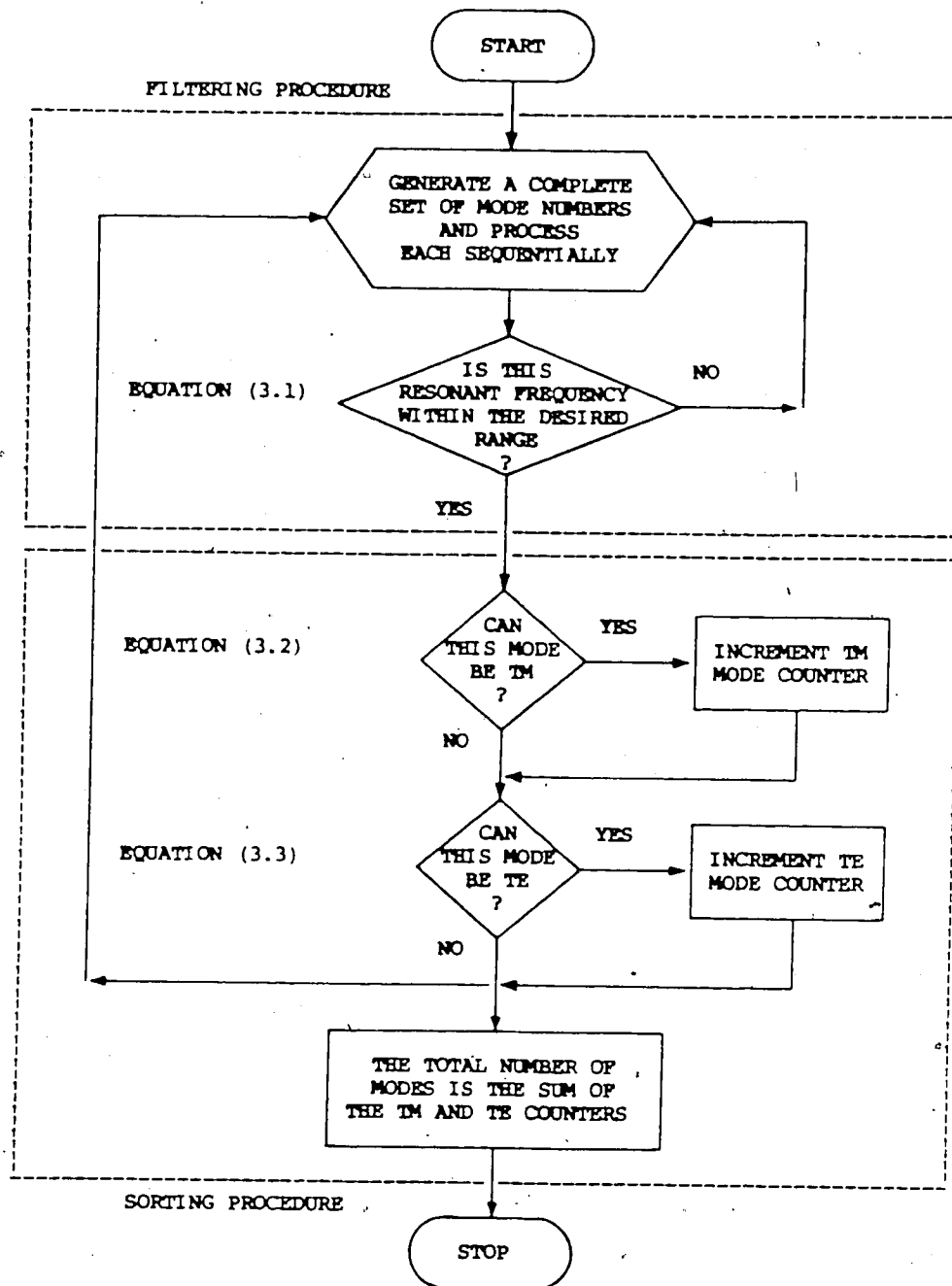


Figure 3.1 Flow chart representation of a mode counting algorithm for rectangular cavities. The applicable equations from the text are indicated beside the decision-making blocks.

programs used by the author.

In the program NEWCAV, the algorithm is used to find the most mode-dense cavities (over a given range of frequencies) in a set of cavities defined by varying, in a prescribed manner, a set of target dimensions. The program prints a listing of the eigenfrequencies, along with plots of the TM and TE line spectra, for each of the cavities found.

In the program MODIST, the algorithm is used (along with certain of the analytical formulae presented in Chapter 5) to generate mode distribution data with any required degree of resolution. The output data is written, in tabular form, to a file which can be viewed as is, or used as input to a plotting program.

In the program CARETAB, the algorithm is used to produce mode count reference tables for a set of cavities defined in a similar manner to that used in NEWCAV. The output of this program is described in Section 3.5.

Complete listings of each of the above programs and descriptions of the input/output are given in Appendix A.

A distinct limitation of these and similar CAD programs used in engineering is that the presence of the coupling

structure(s) and mode stirrer perturb the cavity enough that Eq.(3.1) is no longer useful. A considerable advantage would be gained if a numerical model could be devised which is sufficiently general to handle multiple antennae and arbitrary metallic structures within the interior of the cavity. It is beyond the scope of this thesis to consider this topic in detail, but some further thoughts on a possible approach are given in Appendix C.

3.4 Numerical Case Studies

The program MODIST described above can be used in conjunction with a graphics program to generate actual plots of the exact spectral distribution or spectral density of modes for any hypothetical cavity, for any finite range of frequencies. It is interesting to examine the results of such numerical case studies and some particularly instructive examples are presented here.

The cavity depicted in Figures 3.2,4,6,8 is cubic ($L_1=L_2=L_3=25$ cm) and therefore completely symmetric under an interchange of coordinate axes. This case gives rise to the maximum number of degenerate modes, and hence to the greatest step heights in the exact spectral distribution (see Figure 3.2). This in turn leads to the largest fluctuations in the spectral density plots (see Figures 3.4,6,8). The cavity of Figures 3.3,5,7,9 is slightly less

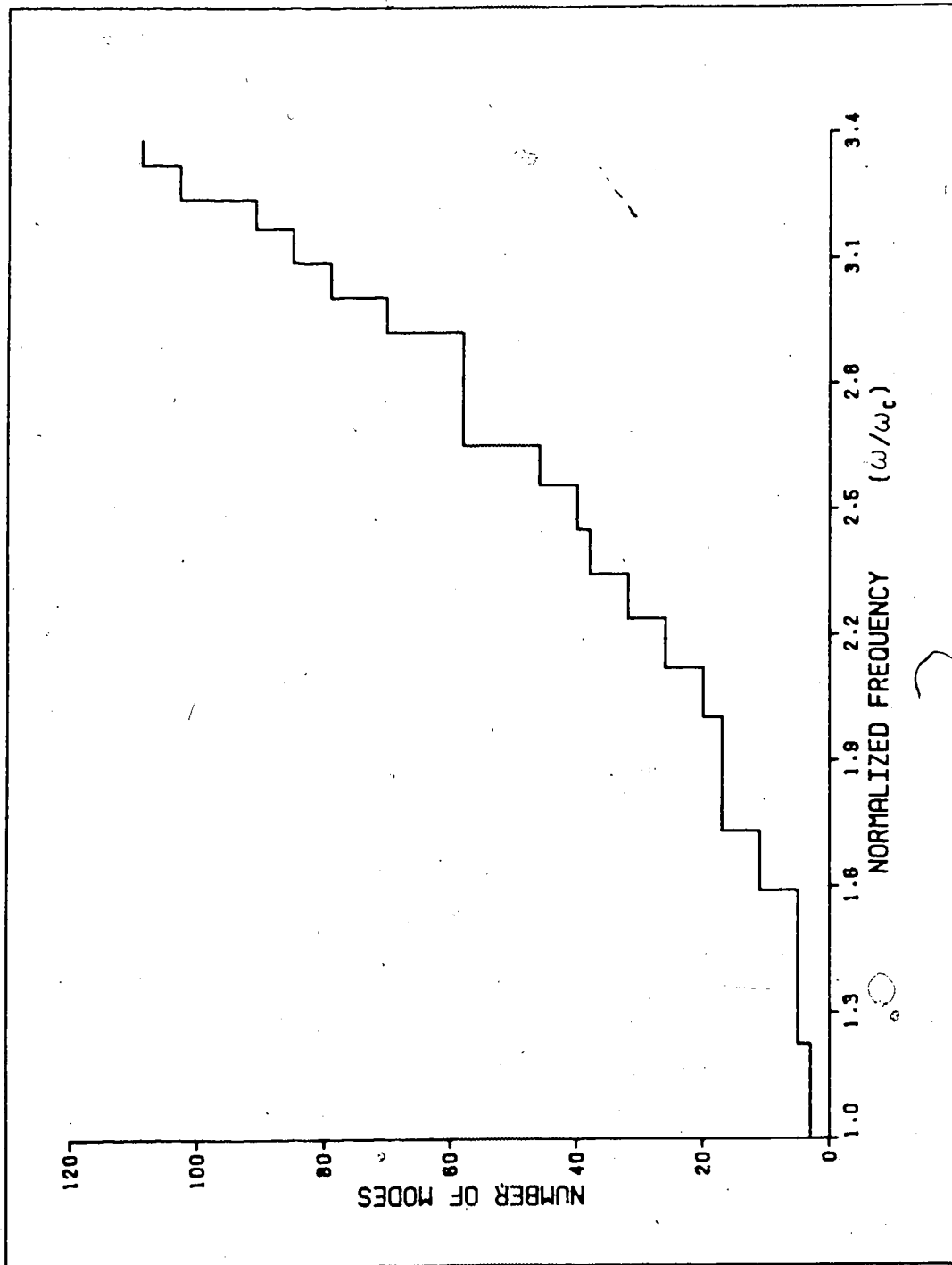


Figure 3.2 The theoretical spectral distribution of electromagnetic modes in an empty cubic cavity. The dimensions of the cavity are $L_1=L_2=L_3=25$ cm which give rise to a cutoff frequency $\omega_c/2\pi=848.5$ MHz.

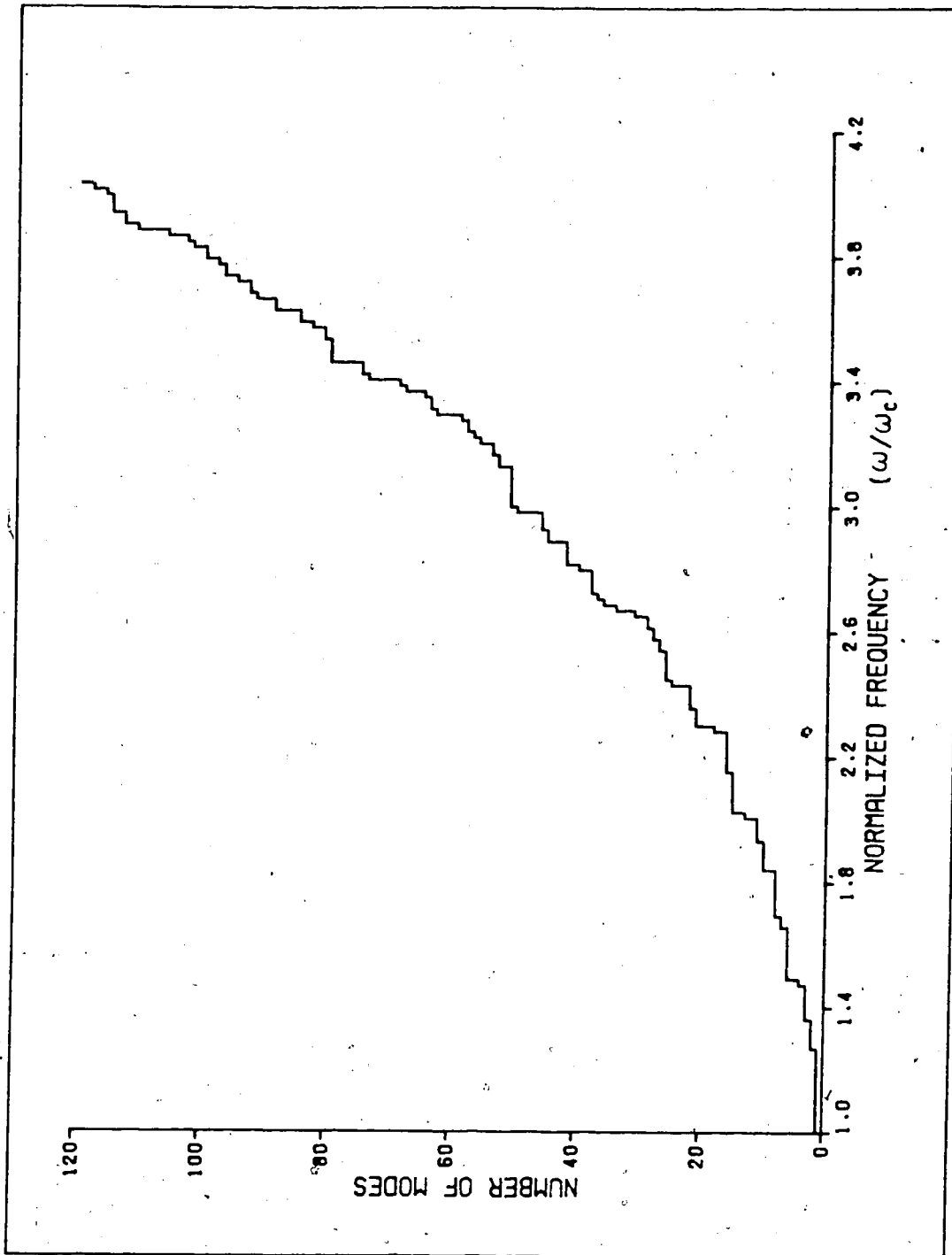


Figure 3.3 The theoretical spectral distribution of electromagnetic modes in an empty rectangular cavity. The dimensions of the cavity are $L_1=25$ cm, $L_2=35$ cm, $L_3=45$ cm which give rise to a cutoff frequency $\omega_c/2\pi=542.9$ MHz.

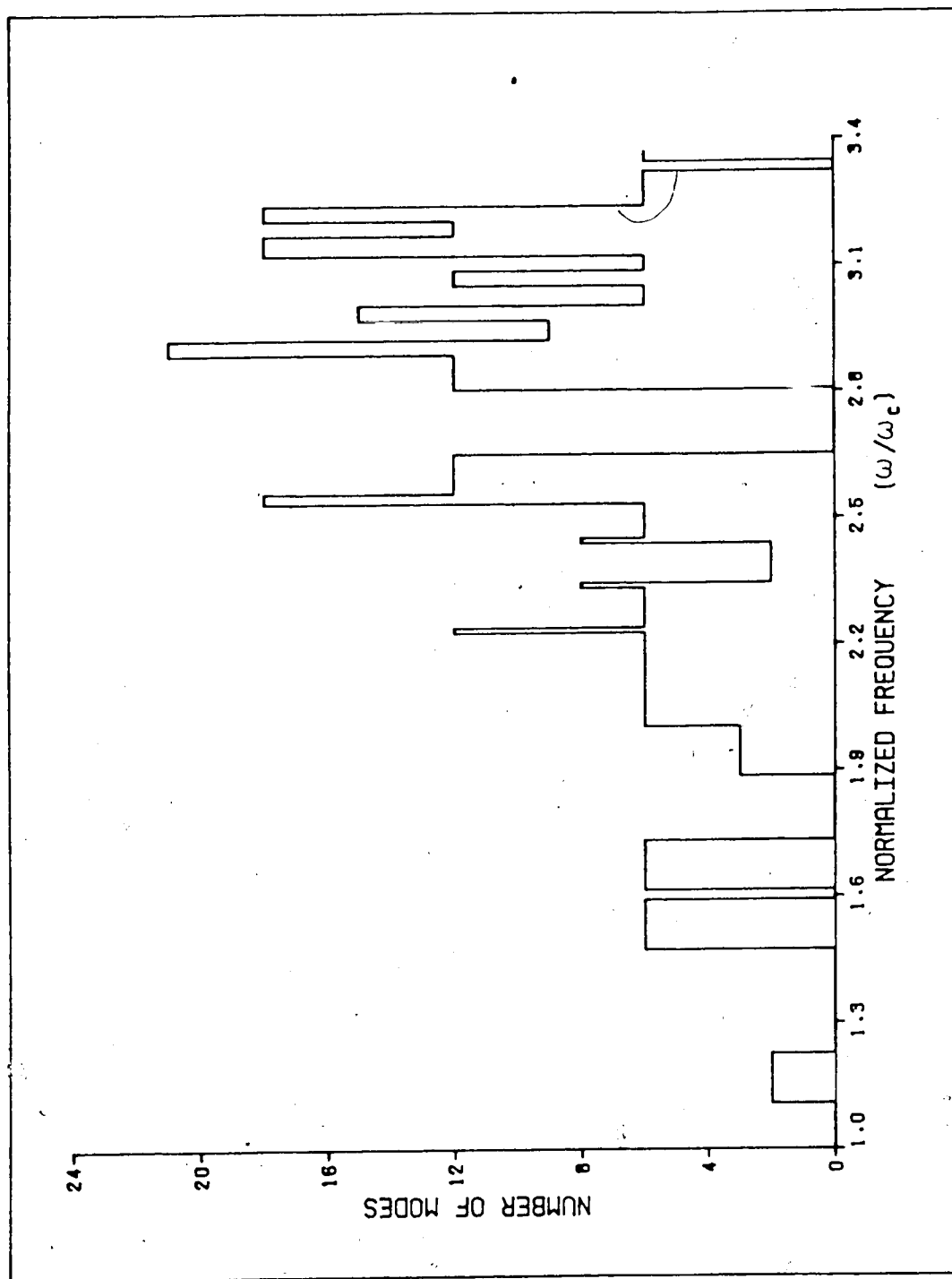


Figure 3.4 The theoretical spectral density of electromagnetic modes in an empty cubic cavity for a bandwidth of 100 MHz. The dimensions of the cavity are $L_1=L_2=L_3=25$ cm as in Figure 3.2.

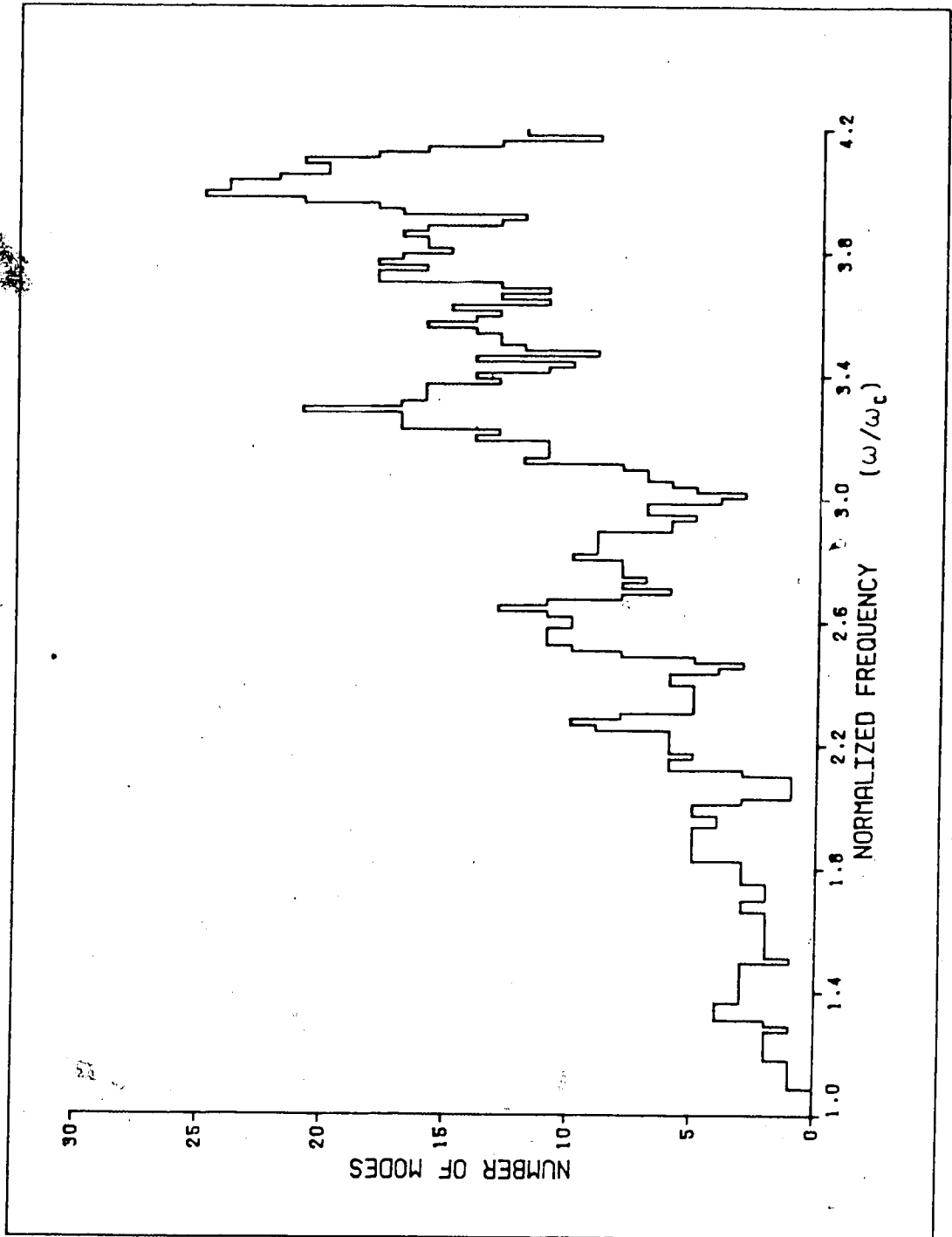


Figure 3.5 The theoretical spectral density of electromagnetic modes in an empty rectangular cavity for a bandwidth of 100 MHz. The dimensions of the cavity are $L_1=25$ cm, $L_2=35$ cm, $L_3=45$ cm as in Figure 3.3.

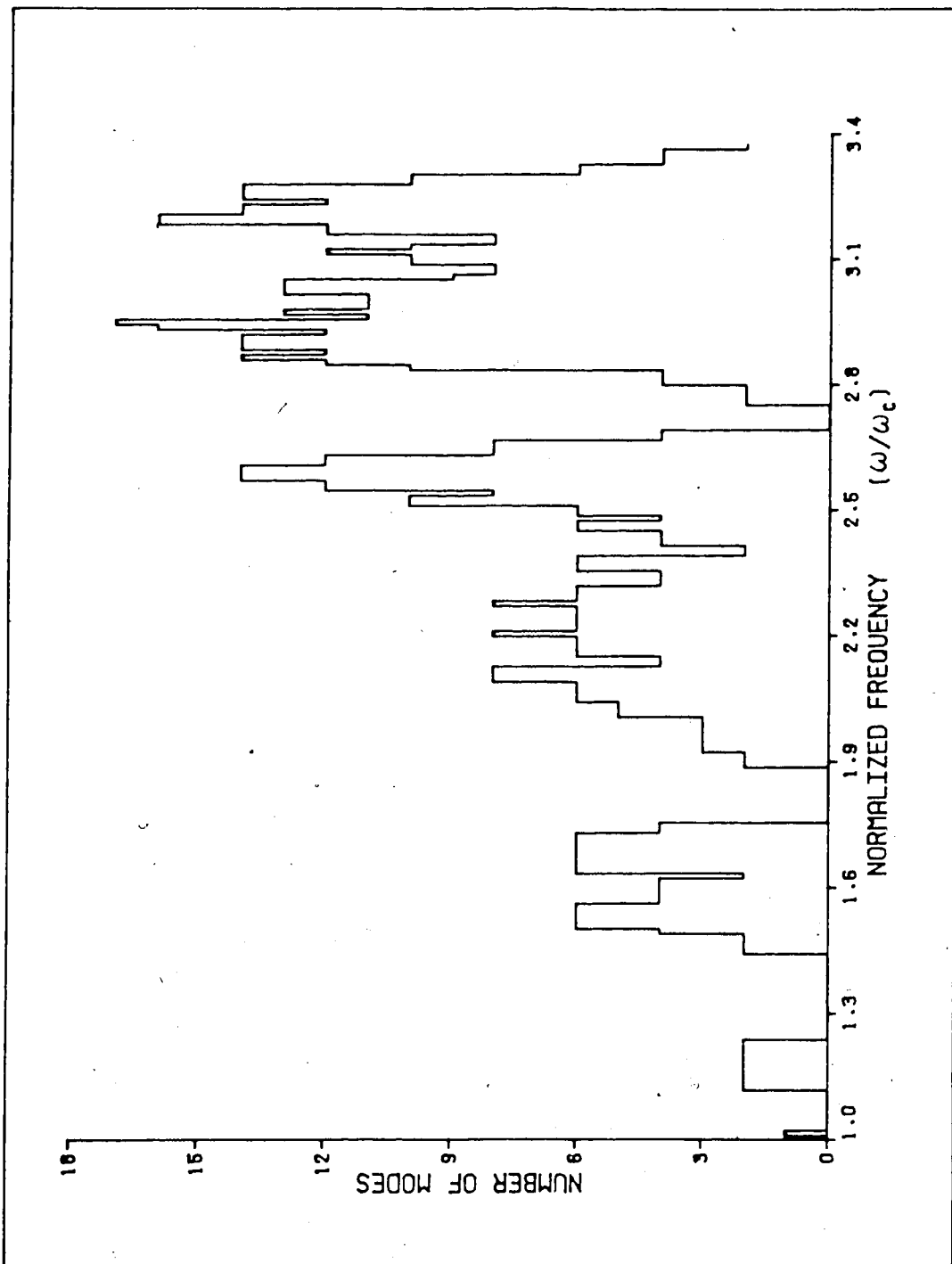


Figure 3.6 The theoretical spectral density of electromagnetic modes in an empty (nearly) cubic cavity for a bandwidth of 100 MHz. The dimensions of the cavity are $L_1=26$ cm, $L_2=L_3=25$ cm.

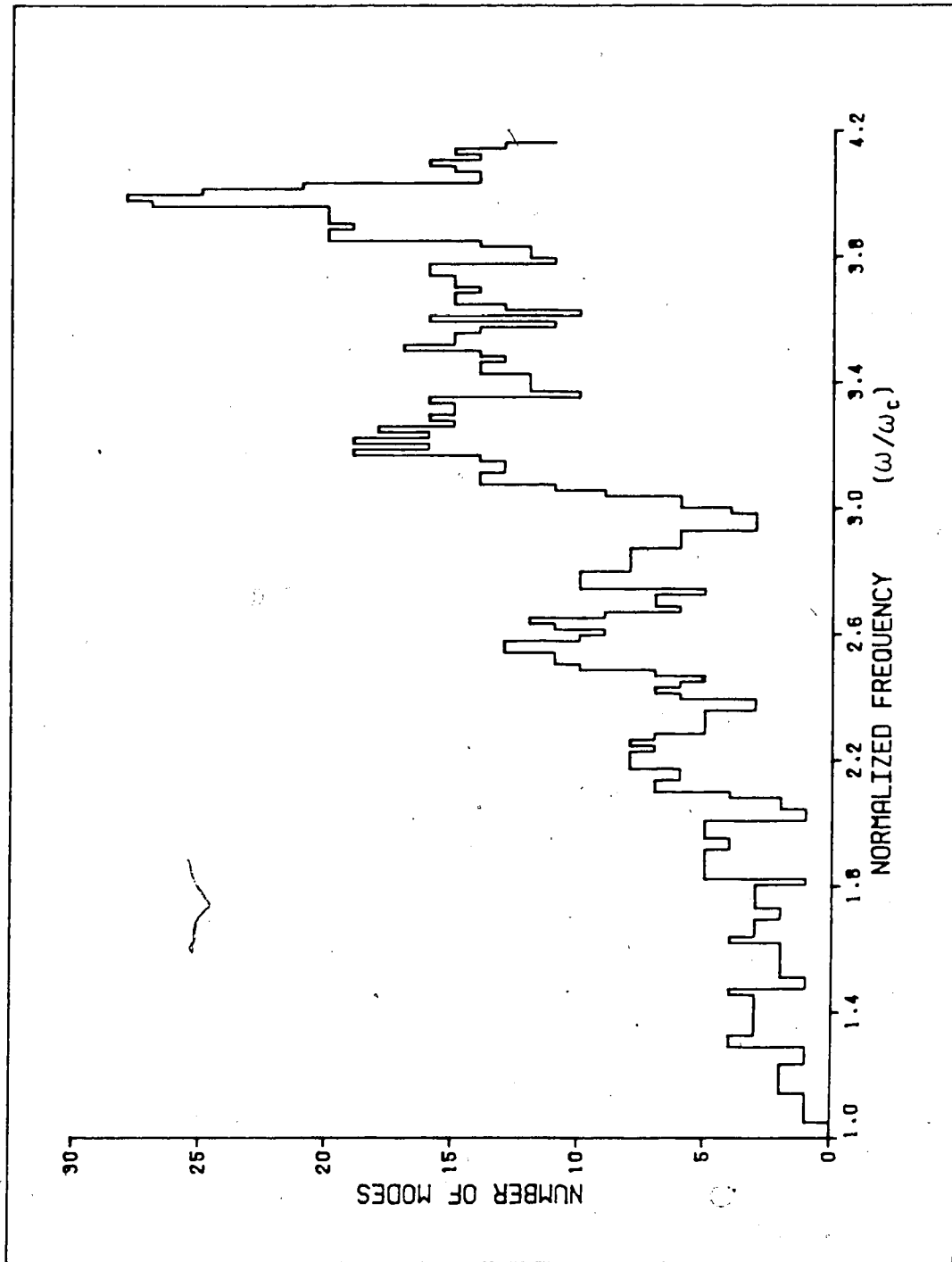


Figure 3.7 The theoretical spectral density of electromagnetic modes in an empty rectangular cavity for a bandwidth of 100 MHz. The dimensions of the cavity are $L_1=26$ cm, $L_2=35$ cm, $L_3=45$ cm.

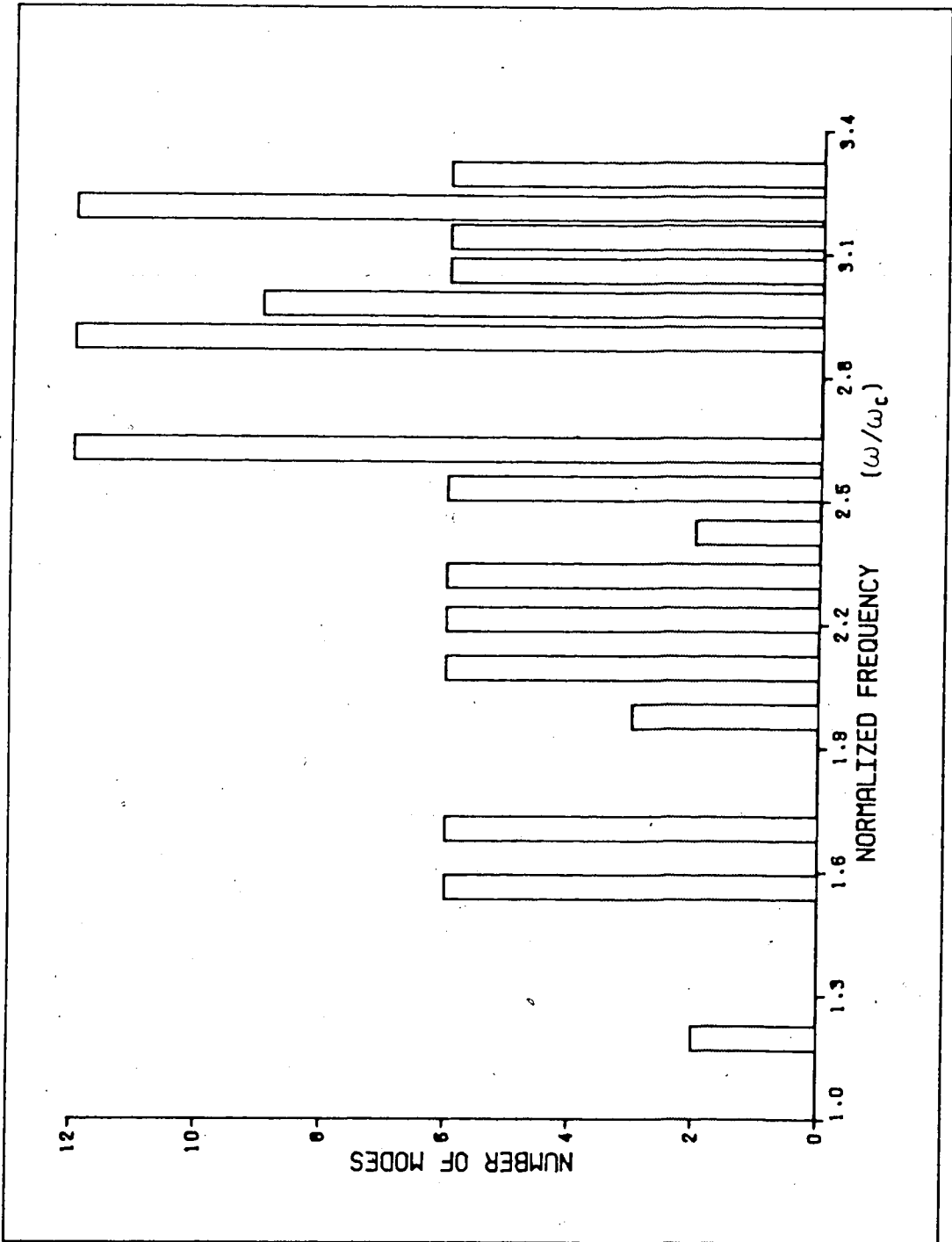


Figure 3.8 The theoretical spectral density of electromagnetic modes in an empty cubic cavity for a bandwidth of 50 MHz. The dimensions of the cavity are $L_1=L_2=L_3=25$ cm as in Figure 3.2.

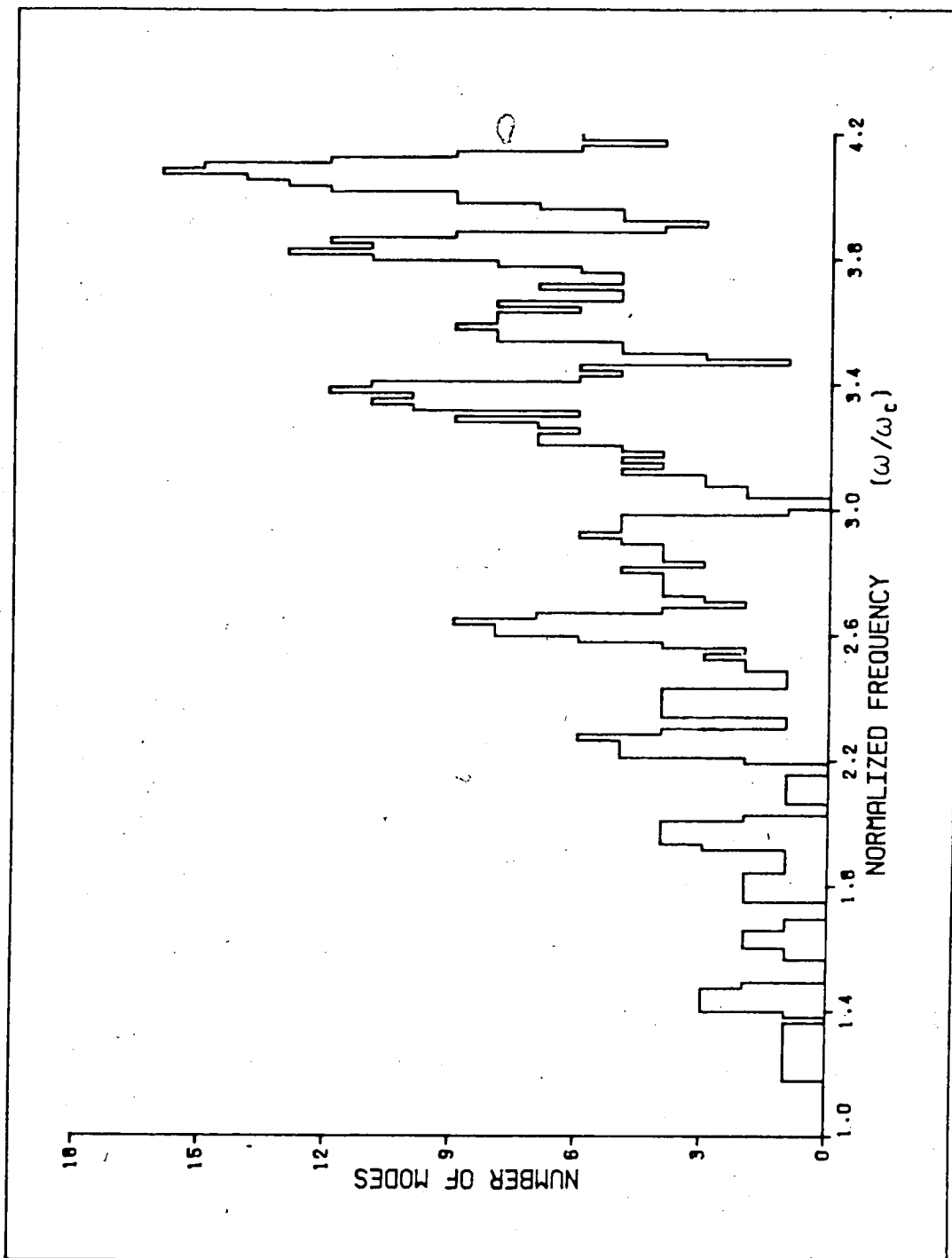


Figure 3.9 The theoretical spectral density of electromagnetic modes in an empty rectangular cavity for a bandwidth of 50 MHz. The dimensions of the cavity are $L_1=25$ cm, $L_2=35$ cm, $L_3=45$ cm as in Figure 3.3.

symmetric ($L_1=25$ cm, $L_2=35$ cm, $L_3=45$ cm) but the step heights in the spectral distribution (Figure 3.3) and the fluctuations in the spectral density (Figures 3.5,7,9) are substantially reduced. These figures clearly show the marked dependence of the mode distributions on the degree of symmetry of the cavity under consideration. Notice particularly the pronounced difference between Figures 3.4 and 3.6, and between Figures 3.5 and 3.7, where the only change in the parameters is that the L_1 dimension has been perturbed by 1 cm.

Figures 3.8 and 3.9 show another strong dependence (that is, on variations in bandwidth) which affects only the spectral densities. A visual comparison of Figures 3.8 and 3.9 with Figures 3.4 and 3.5 respectively, indicates the sensitivity of the fluctuations in the spectral density to a change in bandwidth (in this case, from 100 to 50 MHz).

3.5 Revised Cavity Design Tables

For the sake of comparison, example mode count data, obtained from the program CARETAB, is given in Table B.1 of Appendix B, in a form similar to the tables given in [42,43]. All entries pertain to the number of eigenvalues of the specified type within the (Hertzian) frequency range $2425 \leq f \leq 2475$ MHz. The column titled TS is the total number of mathematical solutions to Eq.(3.1), including

double-zero (longitudinal) modes. These are the values given in [42,43]. The column titled NL is the total number of nonlongitudinal modes (i.e. the same as TS but with the double-zero modes extracted). This is the method used in [48]. The remaining columns titled TE, TM and EM are the partial and total mode counts as determined by the present algorithm.

A similar set of data for the frequency range $900 \leq f \leq 930$ MHz are given in Table B.2 of Appendix B. Note that, due to the nature of the exact spectral distribution of modes, it is not possible to interpolate between cavity sizes given in Tables B.1 and B.2.

3.6 Discussion

It is not clear whether or not the authors of [42,43] intended users to double the values given in the tables. If they are doubled, then these results consistently overestimate the total number of modes. But if they are not doubled, then these tables would consistently underestimate the total number of modes, which may explain why the coupling to small cavities is often better than expected. In either case, the discrepancies are quite large. Note however, that these discrepancies may not have been possible to detect experimentally at the time of [42,43]. Since solid state microwave applicators will almost certainly

operate at lower frequencies initially (e.g. the 915 MHz ISM band), and with multiple sources, the coupling problems of small cavities are becoming increasingly more important.

It might seem that the existence of quasi-random fluctuations in the spectral distribution demonstrates the necessity for designers to have available extensive mode distribution data (or at least a facility to obtain such data) in order to optimize cavity dimensions. However, the sensitivity of these fluctuations to slight variations in shape and bandwidth raises some uncertainties regarding the interpretation of data obtained for ideal empty cavities. For example, construction tolerances and dynamic magnetron bandwidths cause unpredictable changes in the spectral density of modes in "real" cavities.

Furthermore, the resonances are quite sharp, even in a (lightly) loaded cavity, and sometimes widely spaced. Hence, in order to achieve satisfactory uniformity and efficiency in microwave applicators, mode stirrers and/or turn tables are usually employed. These drastically perturb the shape and symmetry of the cavity, which substantially changes the actual mode distribution. Thus, even if intrinsic mode distributions are accurately obtainable from numerical computations, one cannot necessarily expect to improve on empirical cavity designs. Some of these aspects are examined experimentally in the next chapter.

CHAPTER 4. EXPERIMENTAL EIGENMODE DISTRIBUTIONS

The algorithm described in the preceding chapter is based on principles which are strictly valid only for ideal empty cavities. The purpose of this chapter is to present the results of experimental measurements of the spectral distribution of modes for a "real" cavity at microwave frequencies. The laboratory cavity, the measurement system and the procedure are described in the first section. Experimentally obtained mode distributions for the empty cavity are compared in the next section with those obtained by numerical computation using the algorithm of Chapter 3. Additional measurements on the same cavity, equipped with a mode stirrer, are presented in the third section. These results are discussed in the last section.

4.1 Materials and Methods

The laboratory cavity is constructed of aluminum with interior dimensions $L_1=23$ cm, $L_2=50$ cm, $L_3=52$ cm, and can accommodate tunable probe type coupling structures on three orthogonal sides. Access to the interior of the cavity is provided via a securely fitting side door (23 cm x 52 cm), or through several small "ports" (1 cm dia.) which can be used to introduce perturbing instruments or additional probes. An aluminum mode stirrer, of the type used in Litton Menumaster® microwave ovens, could be installed in

the top wall and rotated manually from outside of the cavity. An aluminum bushing was used in order to maintain electrical contact between the mode stirrer and the cavity wall.

The distributions were measured by counting the number of minima in return loss vs. frequency traces obtained using a coaxial frequency-domain reflectometer system. A swept-frequency source (HP 8620C, HP 8621A, HP 8632A) capable of a continuous sweep from 0.1 to 4.0 GHz was used to excite the cavity. Incident and reflected power signals were sampled using ± 20 dB directional couplers, and the return loss in dB was displayed on a swept amplitude analyzer (HP 8755A). No attempt was made to match the impedance of the input circuit to the cavity in order to keep the loading effect of the external circuit as small as possible. A schematic diagram of the complete measurement system is shown in Figure 4.1.

Degenerate modes were resolved using perturbation methods [55]. In many cases the perturbing effect of the finite conductivity of the walls and the presence of the coupling probe† were sufficient to split degenerate modes just enough to make identification possible. From the case

†At least two probes (in at least two positions) were used in any given measurement run in order to excite all possible modes, but only one probe was excited at a time and the unused probes were removed from the cavity.

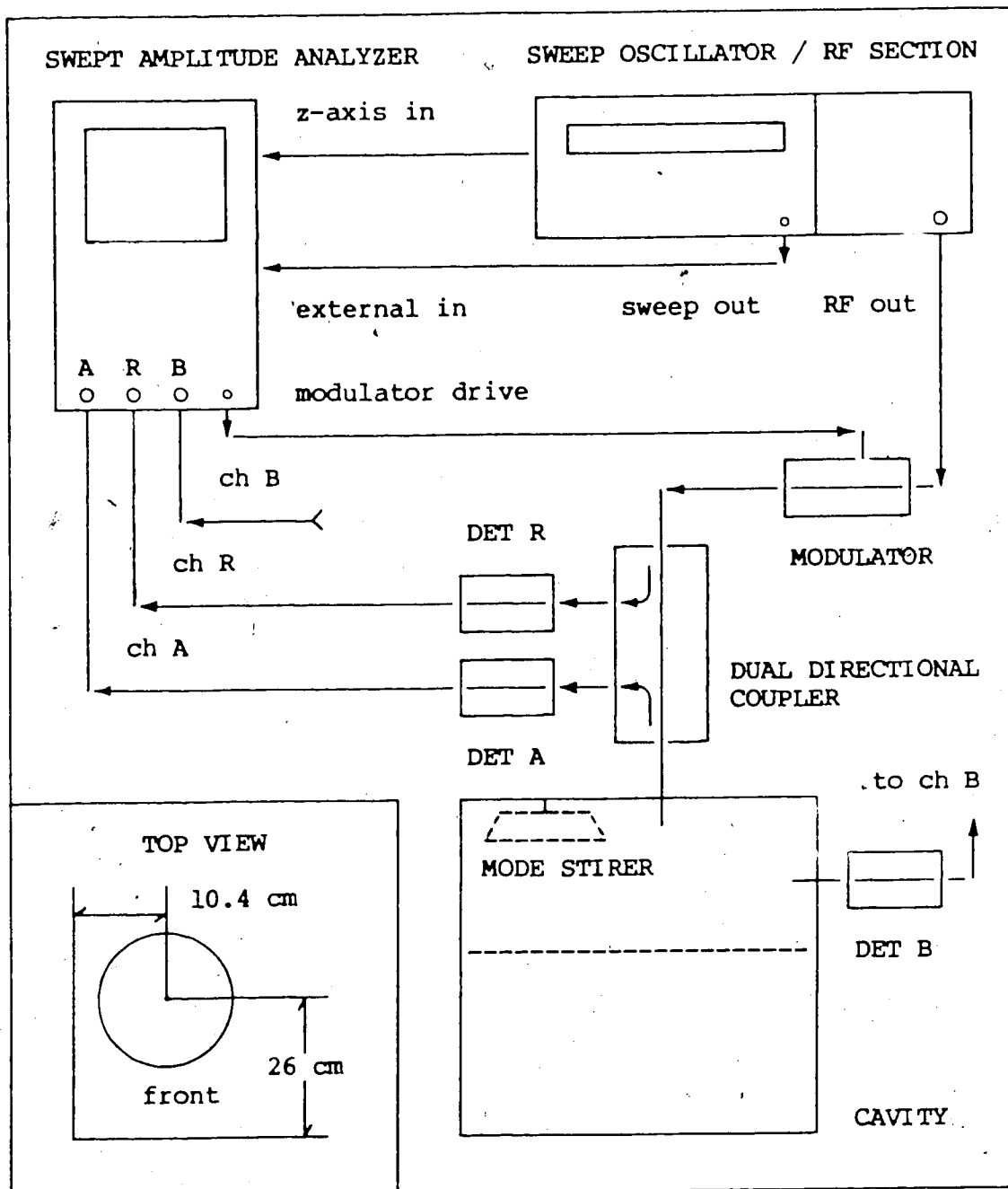


Figure 4.1 Schematic diagram of the measurement system used to obtain experimental mode distribution data. The inset shows the location of the mode stirrer used for the measurements reported in section 4.3.

studies discussed in the previous chapter, one would expect a higher sensitivity to probe perturbations in a more symmetric cavity. Some abbreviated measurements (not graphed) on a slightly more symmetric cavity (28 cm x 52 cm x 52 cm) did support this, as extremely short probes (<5 cm) were required in order to observe degenerate modes. However, the coupling from these short probes was extremely weak which made some degenerate modes very difficult to discern. Because the probes could be longer (<10 cm), this problem was less serious for the cavity used in the measurements reported here; although distinguishing weakly-coupled degenerate modes was still the probable cause of most of the error due to "missed modes".

Other sources of "miscount" error include the possible counting of artifacts in the return loss trace and recounting of modes that are excited by different probes. The artifacts could be identified in most cases by repetitive measurements and perturbation methods. The chances of recounting some modes could be lessened by exciting all probes simultaneously. However, cross-coupling between probes then introduces another source of error. Some (qualitative) observations of these effects are reported in Appendix C.

Errors in determining the resonant frequencies of nondegenerate modes and degenerate modes that required

manual intervention to split, were mainly due to the limited resolution of the scale (on the sweeper main-frame) used to obtain the frequency data. However, the resonant frequencies of modes that were split due to the perturbing effect of cavity walls and coupling probes could only be estimated. Fortunately, this type of error is small.

4.2 Results for the Empty Cavity

The experimentally measured mode distributions for the empty cavity are plotted in Figures 4.2 and 4.3 as the curves N^m and D^m . The abscissae are all normalized to the cutoff frequency (i.e. the lowest eigenfrequency) ω_c of the cavity. Superimposed on Figures 4.2 and 4.3 are the (numerically determined) theoretical distributions N^t and D^t respectively obtained using the algorithm presented in previous chapter.

The frequency resolution of the computed distributions was chosen to correspond with the resolution of the experimental measurements, which was estimated to be 10 MHz or approximately 0.023 on the normalized scale used in Figures 4.2 and 4.3. Within this resolution, there is close agreement between the computed and corresponding measured data. The deviation at higher frequencies is attributed to the experimental errors mentioned above. Note that the visual counting of modes becomes increasingly more difficult

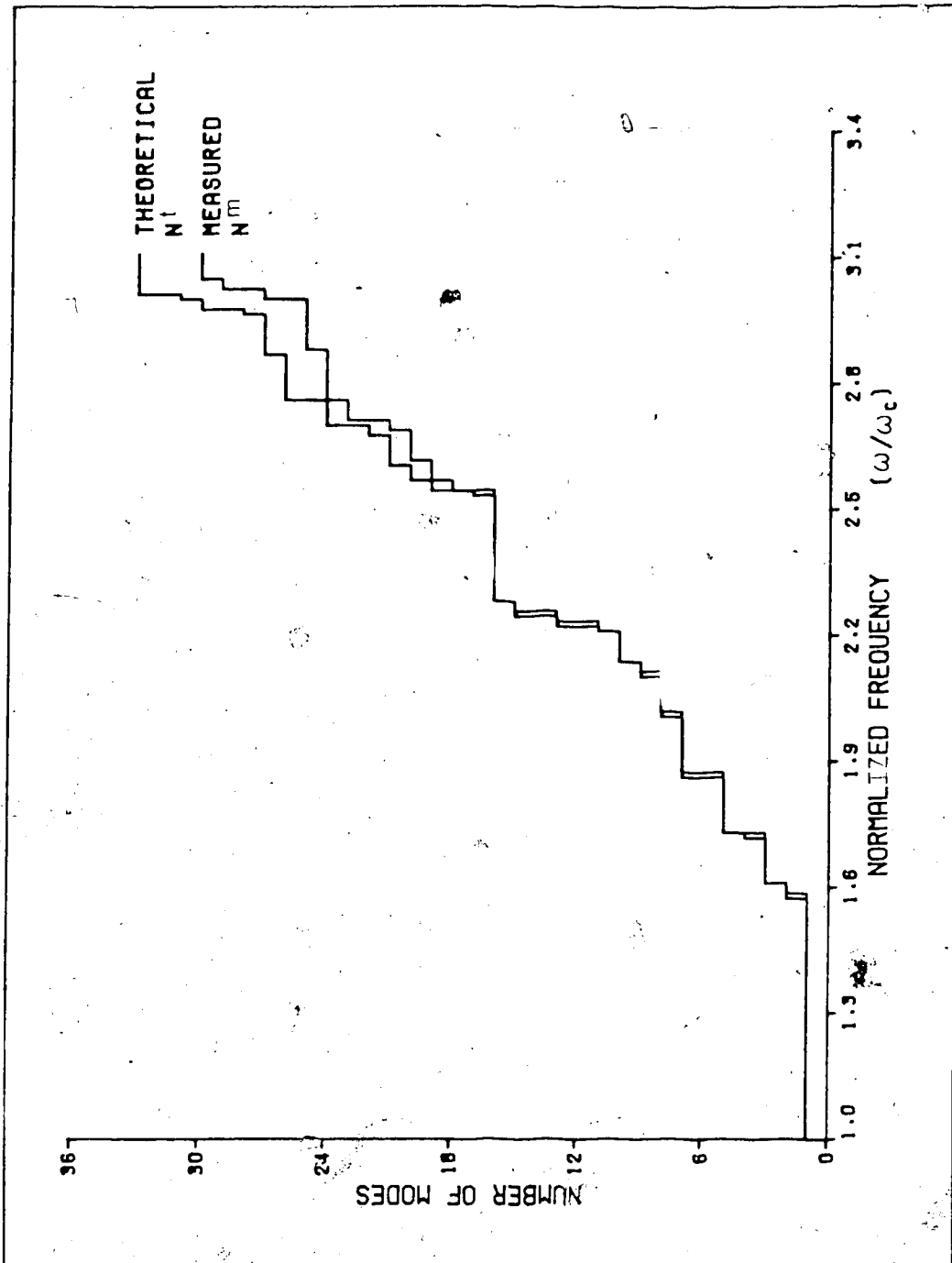


Figure 4.2 Comparison of the theoretical (N^t) and measured (N^m) spectral distribution of modes in an empty rectangular cavity. The interior dimensions of the cavity are $L_1=23$ cm, $L_2=50$ cm, $L_3=52$ cm which give rise to a cutoff frequency $\omega_c/2\pi=416.2$ MHz.

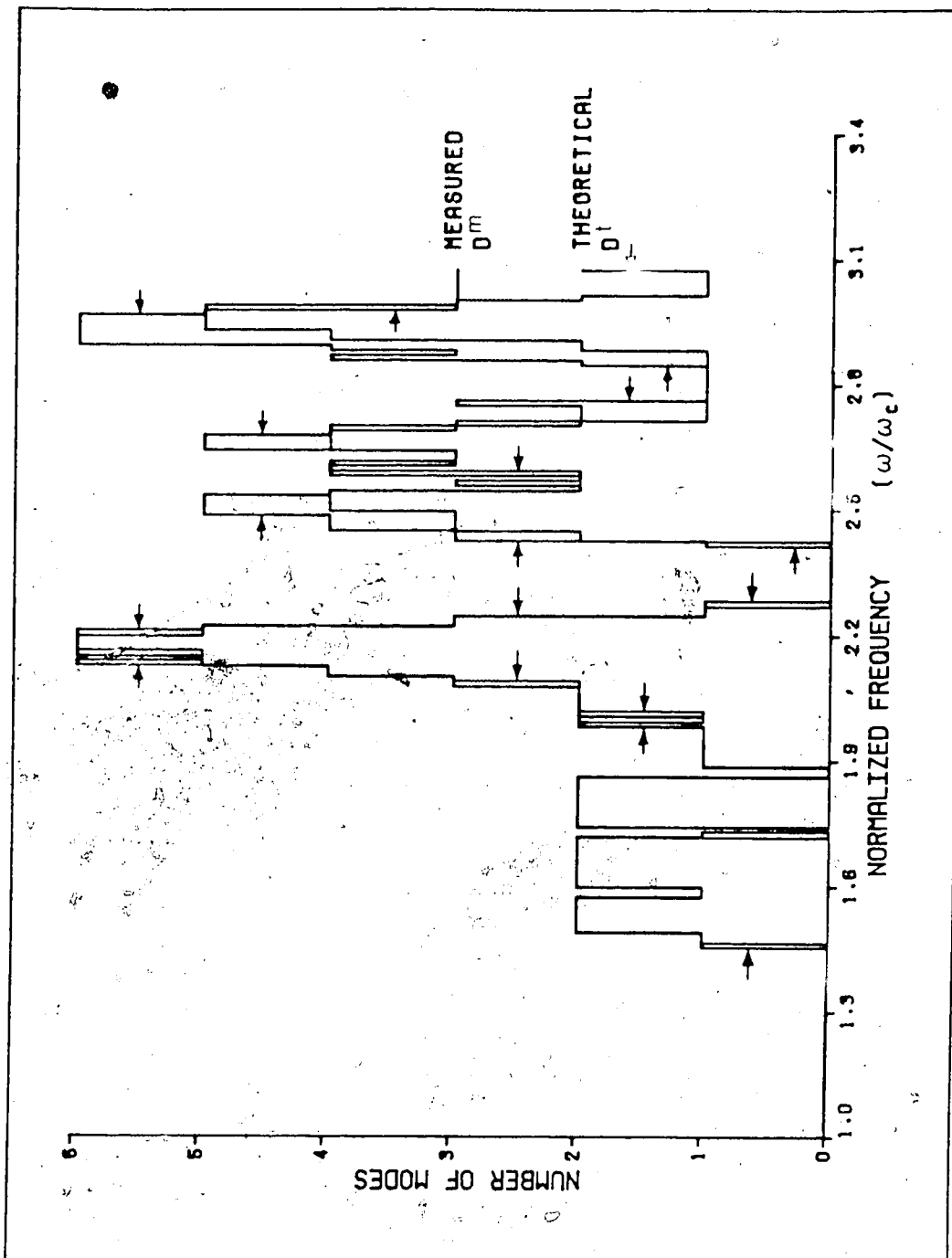


Figure 4.3 Comparison of the theoretical (D') and measured (D^m) spectral density of modes in an empty rectangular cavity for a bandwidth of 50 MHz. The interior dimensions of the cavity are $L_1=23$ cm, $L_2=50$ cm, $L_3=52$ cm as in Figure 4.2.

at higher mode densities and therefore the accuracy of the measurements deteriorates rapidly at frequencies beyond the range shown in the figures.

4.3 Results for the Cavity with a Mode Stirrer

The experimentally obtained spectral distribution of modes in the cavity fitted with a mode stirrer is plotted in figure 4.4 as the curve labelled N^m . The empty-cavity distribution N^m is redrawn on this figure for comparison.

The shaded portions of the curve indicate the range of resonant frequency shift due to changes in the angular displacement θ of the mode stirrer. There is a substantial degree of uncertainty in the determination of the endpoints of these ranges for some of the higher frequency modes. That is, the resonant frequencies of adjacent modes sometimes shifted to where they momentarily coincide; identification of the emerging modes was then difficult since the frequency shifting is not necessarily single-valued with respect to the angular position of the mode stirrer. Also, several of the modes exhibited drastic and abrupt fluctuations in coupling due to changes in θ . In fact, many modes which were strongly coupled at some values of θ could be made to completely vanish at others.

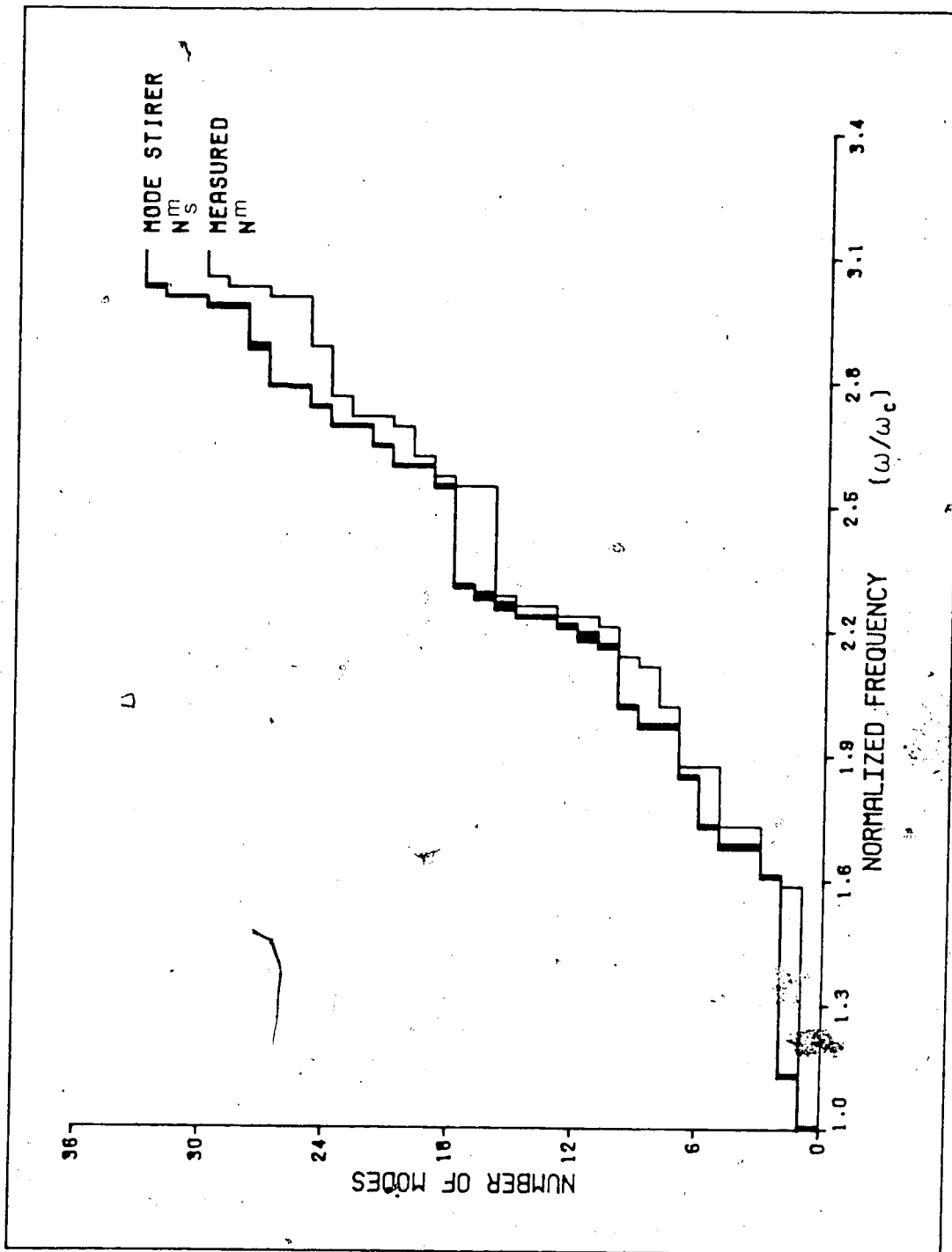


Figure 4.4 Comparison of measured spectral distribution of modes in a rectangular cavity with (N_s^m), and without (N^m), a mode stirrer. The interior dimensions of the cavity are $L_1=23$ cm, $L_2=50$ cm, $L_3=52$ cm as in Figure 4.2.

Note that the range of frequency shift was determined for each mode (or set of degenerate modes) separately, and hence the actual θ dependence of the ensemble distribution can not be determined from Figure 4.4. In this sense, N^m does not really depict the spectral distribution curve per se, but rather it depicts the envelope of possible spectral distribution curves within the frequency range shown. It is therefore pointless to attempt to extract any mode density information from Figure 4.4 as interpretation of such a "curve" would not be possible. Similar considerations apply to the experimental determination of the spectral density.

4.4 Discussion

The good agreement between the curves N^m and N^t and (hence) between the curves D^m and D^t constitutes a successful test of the algorithm presented in the previous chapter. This result is not surprising since the algorithm was derived from theoretically sound physical principles.

What is perhaps surprising is that the inclusion of a mode stirrer seems to have caused a slight negative shift of the entire spectral distribution curve (i.e. downward in frequency). Since the mode stirrer is located near the walls of the cavity, one might expect that magnetic fields would be perturbed more than electric fields which should

result in a net positive shift in the resonant frequencies [56]. However, the integral of the stored magnetic field energy does not exceed the integral of the stored electric field energy over a large enough region of the mode stirrer volume to result in a net positive frequency shift. Although, a slight positive shift could be obtained for most modes, for some angular positions of the mode stirrer.

The perturbing effect of the mode stirrer also caused a more thorough splitting of degenerate modes, thus reducing the amount of manual splitting required. Furthermore, the mode stirrer appeared to act somewhat like a short-circuited "dummy" antenna which received power from the exciting probe and reradiated it into modes normally inaccessible to the exciting probe. Thus, all of the modes could be excited from a single probe position which was advantageous from a measurement point of view. However, this effect would virtually eliminate at least one of the proposed methods [48] for reducing the cross-coupling between multiple source antennae—that of cross-polarized antennae.

An effect of the mode stirrer which is not conveyed by the curve in Figure 4.4 is the marked reduction in the Q of some of the modes even in the absence of other forms of loading. This effect may be attributed, at least partly, to the decrease in volume and the increase in surface area of the cavity due to the presence of the mode stirrer

(i.e. since Q is proportional to the ratio of V/S). Also, from an equivalent circuit point of view, the mode stirrer contributes a capacitance which is in series with the usual model capacitance, and since the Q is proportional to the total capacitance, a lower value results.

The experimental methods described here are not limited to measurements on rectangular cavities. In fact, some interesting effects have been observed in odd shaped (nonrectangular) acoustic cavities [55] which may be relevant to microwave heating applications of electromagnetic cavities. The authors of [55] present analyses of the statistical dispersion in the excitation amplitudes of neighbouring modes, which suggest that more uniform field patterns might be obtained with completely asymmetric cavities. Unfortunately, experimental results from these cavities are difficult to generalize, as very little theoretical analysis is possible. Presently, the only analytical aid for determining the mode distributions for these (nonrectangular) asymmetric cavities is offered by the shape-independent volume term in the asymptotic formulae discussed in the following chapter.

CHAPTER 5. ANALYTICAL EIGENMODE DISTRIBUTIONS

Asymptotic expansions of the eigenvalue distribution have been used in physics to approximate the exact spectral distribution of modes in several types of resonant cavities. Certain versions of these formulae have been incorrectly applied to microwave cavity problems in engineering. The purpose of this chapter is to correct these errors and to comment on the utility of the approximate formulae in engineering. A brief introduction describing the errors is given in the first section, followed in the next two sections by derivations of the correct electromagnetic formulae. In the fourth section, these formulae are compared with the numerical and experimental results presented in the last two chapters. In the fifth section, exact formulae for the spectral density of modes in rectangular and cubic cavities are given. In the last section, all of these formulae are discussed in terms of their role in the design and analysis of microwave heating cavities.

5.1 Asymptotic Eigenmode Distributions

Recall that the time independent behavior of oscillating fields in bounded domains is governed by the Helmholtz equation, *viz.*

$$\nabla^2\psi + k^2\psi = 0 \quad (5.1)$$

where the wave function ψ may be either scalar or vector depending on the type of wave phenomenon under consideration. For example, the scalar form of Eq.(5.1) applies to (gas phase) acoustic waves and the vector form applies to electromagnetic waves, as discussed in Chapter 2. In either case†, the eigenvalues of Eq.(5.1) satisfy

$$k^2 = \frac{\omega^2}{c^2} = \frac{p_1^2 \pi^2}{L_1^2} + \frac{p_2^2 \pi^2}{L_2^2} + \frac{p_3^2 \pi^2}{L_3^2} \quad (5.2)$$

where the valid combinations of p_1, p_2, p_3 depend on the boundary conditions.

The previous two chapters both dealt with methods of determining the exact eigenvalue distributions as defined in Chapter 2. Such methods can only give qualitative information about the general behavior of eigenvalue spectra. However, analytical functions of frequency can be derived which fit the curves of N, D empirically, at least for asymptotically large frequencies. These functions have been used by physicists, for example, to elucidate certain properties of blackbody radiation in finite cavities [27,28,30,31,33-37].

From prior discussions, it should be expected that several forms of asymptotic formulae must exist in order to

†Note that not all problems involving Eq.(5.1) lead to Eq.(5.2). A case in point is that of acoustic modes in solid-filled cavities due to a nonisotropic phase velocity.

handle different sets of boundary conditions, geometries, etc. For example, the leading terms of an asymptotic expansion of the eigenvalue distribution valid for the scalar form of Eq.(5.1) in a rectangular parallelepiped domain is

$$N_{\text{scalar}}(\omega) = \frac{V}{6\pi^2} \frac{\omega^3}{c^3} \pm \frac{S}{16\pi} \frac{\omega^2}{c^2} + \frac{(L_1+L_2+L_3)}{4\pi} \frac{\omega}{c} \pm \frac{1}{8} \quad (5.3)$$

where V is the volume of the cavity and S is the interior surface area. The plus signs in Eq.(5.3) apply to Neumann problems and the minus signs apply to Dirichlet problems. The constant term may be viewed as being necessary to properly account for the 000 mode, but its contribution to the total number of modes is usually minor enough to be omitted. The appropriate form of Eq.(5.3) valid for acoustic modes (in a gas-filled cavity) is

$$N_{\text{acous.}}(\omega) = \frac{V}{6\pi^2} \frac{\omega^3}{c^3} + \frac{S}{16\pi} \frac{\omega^2}{c^2} + \frac{(L_1+L_2+L_3)}{4\pi} \frac{\omega}{c} - \frac{7}{8} \quad (5.4)$$

which is the form derived in [40]. Since Eq.(5.2) applies to both the scalar and electromagnetic problems, it was (apparently) assumed that Eq.(5.4) also applies to the electromagnetic problems. The form suggested in [43-45], is

$$N(\omega) = \frac{V}{3\pi^2} \frac{\omega^3}{c^3} + \frac{S}{8\pi} \frac{\omega^2}{c^2} + \frac{(L_1+L_2+L_3)}{2\pi} \frac{\omega}{c} \quad (5.5)$$

where the ω dependent terms in Eq.(5.4) have simply been doubled to account for both TM and TE mode types—a procedure which is correct only for the volume term. The

problem being that, while the scalar problems admit solutions which are oscillatory in one dimension only (i.e. longitudinal), electromagnetic problems do not. Furthermore, although the solution spaces of TM and TE modes do overlap, there are solutions which are unique to each set.

Although electromagnetic waves are governed by the vector form of Eq.(5.1), the (vector) wave functions can be obtained in terms of two scalar wave potentials representing TM (E-type) and TE (H-type) modes respectively. This formulation enables the TM and TE modes to be dealt with in separate (scalar) problems, each subject to a different, albeit complementary, set of mixed boundary conditions. This complementarity leads to the cancellation of the surface area dependent term in the electromagnetic distribution. That is, the terms proportional to ω^2 for each mode type have equal but opposite signs; and hence, when the partial solutions are superimposed, the surface term vanishes. The first rigorous treatment where TM and TE modes are considered separately was given in [27]. The important results are derived here by a method similar to that used by Maa.

5.2 Asymptotic Spectral Distribution of EM Modes

Eq.(5.2) can be interpreted as describing the boundary of an ellipsoid in the space of the quantum numbers p_1, p_2, p_3 †. Hence, any point in p-space having integral coordinates that lie interior to the ellipsoid will represent a mode with eigenfrequency less than ω . There will be, on the average, one of these characteristic points per unit volume in p-space. The number of TM or TE modes with resonant frequencies less than ω , to a first approximation, is then simply the volume in the first octant enclosed by the ellipsoid, viz.

$$\frac{1}{8} \frac{4\pi}{3} \left[\frac{L_1}{\pi} \frac{\omega}{c} \frac{L_2}{\pi} \frac{\omega}{c} \frac{L_3}{\pi} \frac{\omega}{c} \right] = \frac{V}{6\pi^2} \frac{\omega^3}{c^3} \equiv N(\omega) \quad (5.6)$$

where the subscript 0 indicates that Eq.(5.6) is applicable to both TM and TE modes. Eq.(5.6) is the familiar Rayleigh formula and it (or a multiple of it) is the dominant term which describes all eigenvalue spectra in the limit of infinitely high frequencies or infinitely large cavities.

Note that the mode numbers comprised only of nonzero quantum numbers have been fully counted in Eq.(5.6).

†The hypothetical surface described by Eq.(5.2) is ellipsoidal due to the simple rectangular geometry of x-space. Clearly, more complicated surfaces would result for any other shaped cavity.

However, only partial† consideration has been given to those points which lie in the coordinate planes separating the first octant from the rest of p-space. Obviously, a significant number of points—those with zeros in their mode numbers—will be miscounted if Eq.(5.6) is not modified. Since these points represent the "unambiguous" mode numbers (i.e. those with multiplicities less than two), a bifurcation of Eq.(5.6) is necessary in order to properly count both TM and TE modes.

By considering only the first octant of p-space, the off-axes points on the coordinate planes have effectively been cut into halves, and the points on the coordinate axes have been cut into fourths. Following this line of reasoning, the modified forms of Eq.(5.6) are obtained as follows:

The first quadrants of the ellipses formed by the intersection of the coordinate planes and the ellipsoid (5.2) have areas

$$\frac{L_1 L_2}{4\pi} \frac{\omega^2}{c^2}, \frac{L_2 L_3}{4\pi} \frac{\omega^2}{c^2}, \frac{L_1 L_3}{4\pi} \frac{\omega^2}{c^2} \quad (5.7)$$

†In this volumetric representation of characteristic points, it is understood that a point has not been fully counted until an entire equivalent unit volume, which can be associated with it, has been accounted for. It is in this sense that "portions" of a lattice point can be counted separately.

and the line segments formed by the intersection of the coordinate axes and the ellipsoid (5.2) have lengths

$$\frac{L_1}{\pi} \frac{\omega}{c}, \frac{L_2}{\pi} \frac{\omega}{c}, \frac{L_3}{\pi} \frac{\omega}{c} \quad (5.8)$$

in the first octant. The terms (5.7,5.8) can be converted to volume terms by multiplying by a simple numerical fraction representing the portion of volume required. Now the set of TE modes include those represented by characteristic points in the p_1p_3 and p_2p_3 planes, but excludes those represented by characteristic points in the p_1p_2 plane; and conversely for the set of TM modes. The characteristic points on the coordinate axes represent longitudinal modes which are excluded from both TM and TE sets. Thus

$$N_{TM}'(\omega) = N_0(\omega) - \frac{(S_{1,2}-S_3)}{16\pi} \frac{\omega^2}{c^2} - \frac{(L_1+L_2-L_3)}{4\pi} \frac{\omega}{c} \quad (5.9)$$

$$N_{TE}'(\omega) = N_0(\omega) + \frac{(S_{1,2}-S_3)}{16\pi} \frac{\omega^2}{c^2} - \frac{(L_1+L_2+3L_3)}{4\pi} \frac{\omega}{c} \quad (5.10)$$

where $S_{1,2}=2L_1L_3+2L_2L_3$ and $S_3=2L_1L_2$. The plus/minus signs on the RH sides are required in order to correct $N_0(\omega)$ for the undercounting/overcounting of the characteristic points described above.

One further modification term in each of Eqs.(5.9,5.10) is required in order to properly account for the 000 mode at the origin of p-space. That is, each of the terms on the RH sides of Eqs.(5.9,5.10) contribute a positive or negative

fraction of the 000 characteristic point to their respective "subtotals". The sums of these contributions in each case are

$$+\frac{1}{8} + \frac{1}{8} + \frac{1}{8} - \frac{1}{8} - \frac{1}{8} - \frac{1}{8} - \frac{3}{8} = -\frac{3}{8} \quad (5.11)$$

due to $N_{TM}^+(\omega)$, and

$$+\frac{1}{8} - \frac{1}{8} - \frac{1}{8} + \frac{1}{8} - \frac{1}{8} - \frac{1}{8} + \frac{1}{8} = -\frac{1}{8} \quad (5.12)$$

due to $N_{TE}^+(\omega)$, and these must be subtracted from Eqs.(5.9,5.10) respectively. Hence the partial asymptotic spectral distributions of TM and TE modes respectively in a rectangular cavity are

$$N_{TM}(\omega) = N_0(\omega) - \frac{(S_{1,2}-S_3)}{16\pi} \frac{\omega^2}{c^2} - \frac{(L_1+L_2-L_3)}{4\pi} \frac{\omega}{c} + \frac{3}{8} \quad (5.13)$$

$$N_{TE}(\omega) = N_0(\omega) + \frac{(S_{1,2}-S_3)}{16\pi} \frac{\omega^2}{c^2} - \frac{(L_1+L_2+L_3)}{4\pi} \frac{\omega}{c} + \frac{1}{8} \quad (5.14)$$

and therefore the total asymptotic distribution of electromagnetic modes is

$$N_{EM}(\omega) = 2N_0(\omega) - \frac{(L_1+L_2+L_3)}{2\pi} \frac{\omega}{c} + \frac{1}{2} \quad (5.15)$$

which is equivalent to the form (in terms of k) derived by Baltes *et al.* [27,28], and very close to the form anticipated by Pathria [23] in 1966.

From the partial distribution functions (5.13,5.14), it is clear that any calculation of N —either analytical or

numerical—that presumes TM and TE modes to have the same distributions, will be in error.

5.3 Asymptotic Spectral Density of EM Modes

Applying the same reasoning which led to Eq.(2.51), the number of electromagnetic modes with resonant frequencies between ω and $\omega + \delta\omega$ is

$$D_{EM}(\omega)\delta\omega = N_{EM}(\omega + \delta\omega) - N_{EM}(\omega) \quad (5.16)$$

which, in terms of the p-space model, corresponds to the number of characteristic points within an ellipsoidal shell which is not, in general, of uniform thickness. Substituting Eqs.(5.6, 5.15) into Eq.(5.16) and performing the subtraction yields

$$D_{EM}(\omega)\delta\omega = \frac{V}{3\pi^2} \frac{1}{c^3} [(\omega + \delta\omega)^3 - \omega^3] - \frac{(L_1 + L_2 + L_3)}{2\pi} \frac{1}{c} [(\omega + \delta\omega) - \omega] \quad (5.17)$$

or

$$D_{EM}(\omega)\delta\omega = \frac{V}{3\pi^2} \frac{1}{c^3} [3\omega^2\delta\omega + 3\omega(\delta\omega)^2 + (\delta\omega)^3] - \frac{(L_1 + L_2 + L_3)}{2\pi} \frac{1}{c} \delta\omega \quad (5.18)$$

which, as $\delta\omega$ approaches an infinitesimal, reduces to

$$D_{EM}(\omega)\delta\omega = 2D_0(\omega)\delta\omega - \frac{(L_1 + L_2 + L_3)}{2\pi} \frac{1}{c} \delta\omega \quad (5.19)$$

where $D_0(\omega) = dN_0(\omega)/d\omega$. The asymptotic spectral density function for electromagnetic modes in rectangular cavities is therefore

$$D_{EM}(\omega) = 2D_0(\omega) - \frac{(L_1 + L_2 + L_3)}{2\pi} \frac{1}{c} \quad (5.20)$$

which, as anticipated in Chapter 2, is just the derivative of Eq.(5.15) with respect to ω .

The asymptotic forms for the component partial spectral densities can be derived in exactly the same manner as Eq.(5.20) above. The resulting formulae are

$$D_{TM}(\omega) = D_0(\omega) - \frac{(S_{1,2} - S_3)}{8\pi} \frac{\omega}{c^2} - \frac{(L_1 + L_2 + L_3)}{4\pi} \frac{1}{c} \quad (5.21)$$

$$D_{TE}(\omega) = D_0(\omega) + \frac{(S_{1,2} - S_3)}{8\pi} \frac{\omega}{c^2} - \frac{(L_1 + L_2 + 3L_3)}{4\pi} \frac{1}{c} \quad (5.22)$$

which are the derivatives of Eqs.(5.13, 5.14) respectively.

5.4 Verification of the Asymptotic Formulae

Only the first term in each of the asymptotic formulae survives in the limit $\omega V \rightarrow \infty$, which is to be expected if Eq 5.20) to be consistent with the familiar black body radiation laws. These laws are well-tested experimentally and as such the asymptotic formulae are verified in the high frequency limit. However, at lower frequencies when the contributions of the second (and third) terms become important, Eqs.(5.15, 5.20) have yet to be verified

experimentally.

The accuracy of the asymptotic formulae at lower frequencies was investigated by comparing the numerically and experimentally determined mode distributions of Chapter 4 with the corresponding results predicted by the asymptotic formulae. This comparison is illustrated in Figure 5.1 for the spectral distribution of modes and in Figure 5.2 for the spectral density of modes. Also plotted on Figures 5.1, 5.2 are the incorrect distributions predicted by Eq. (5.5) and its derivative respectively.

A visual inspection of the curves in Figures 5.1, 5.2 is quite convincing, but in order to provide some quantitative measure of the accuracy of the asymptotic approximations, an average error is quoted for each of the asymptotic curves. The figure E is defined for either N or D type (N, D) distributions by

$$E_{N,D} \equiv \frac{1}{P} \sum_{i=1}^P (N', D') | \omega_i - N, D(\omega_i) \delta \omega_i \quad (5.23)$$

where P is the total number of points calculated. The average error is useful for comparing the "fit" of different approximations, but does not give any indication of the amplitude of fluctuations in the exact curve, about the approximate curve. A slightly different figure—the average absolute error—is defined for either N or D type

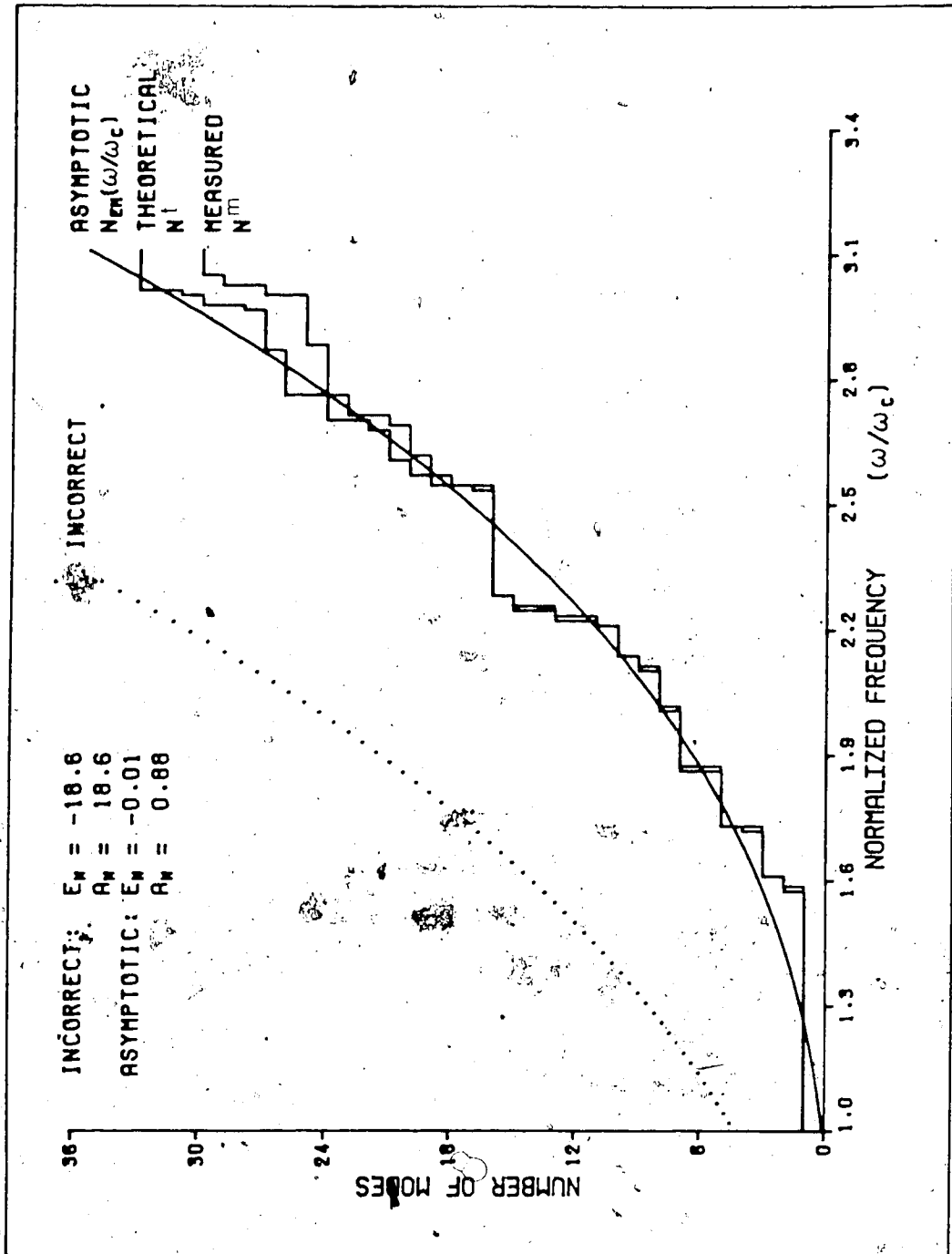


Figure 5.1 Comparison of the exact and approximate spectral distribution of EM modes for a particular rectangular cavity. The interior dimensions of the cavity are $L_1=23$ cm, $L_2=50$ cm, $L_3=52$ cm. The dotted curve is the erroneous distribution predicted by Eq.(5.5).

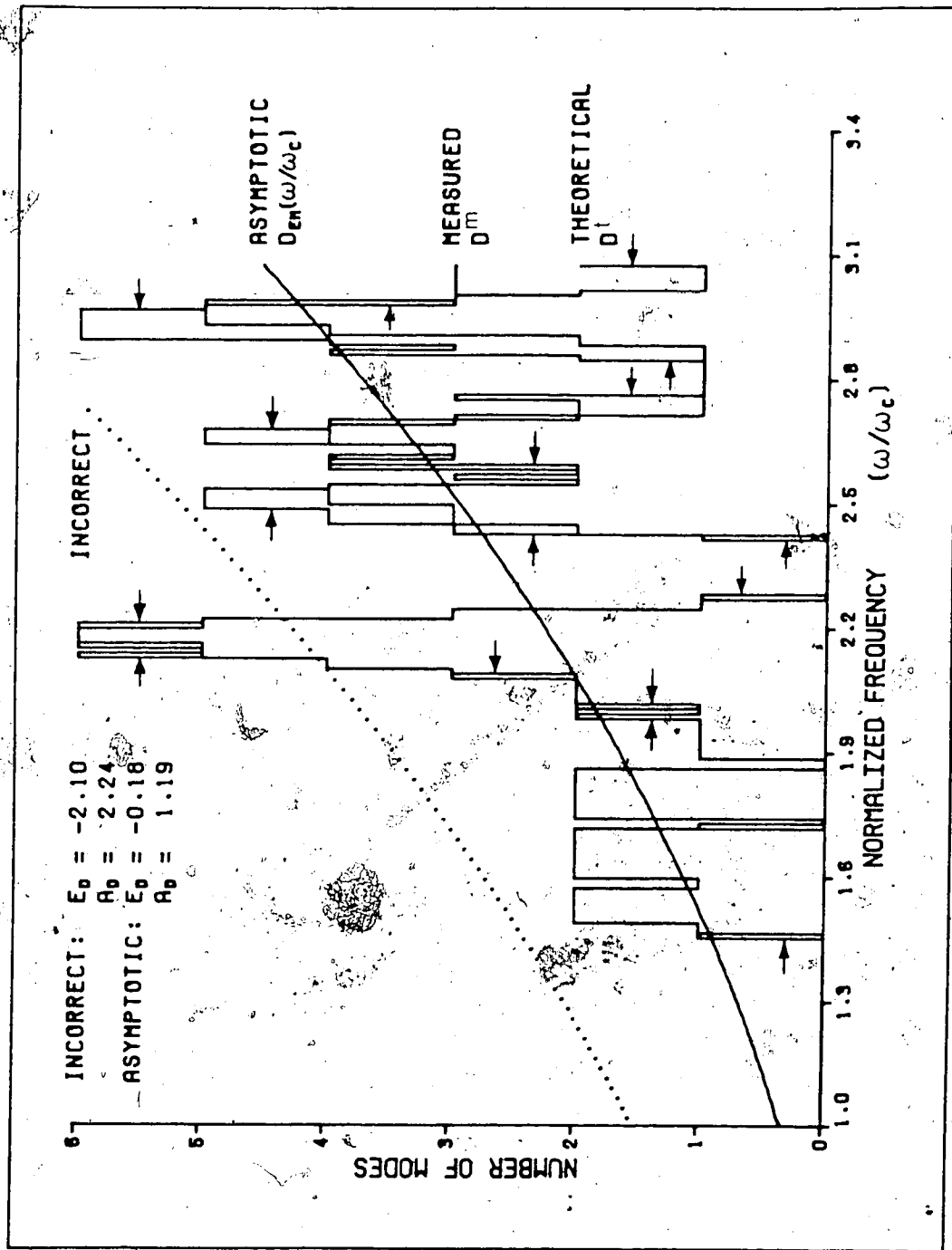


Figure 5.2 Comparison of the exact and approximate spectral density of EM modes for a particular rectangular cavity for a bandwidth of 50 MHz. The cavity dimensions are the same as for Figure 5.1. The dotted curve is the erroneous distribution predicted by the derivative of Eq.(5.5).

distributions by

$$A_{N',D'} \equiv \frac{1}{P} \sum_{i=1}^P |(N', D')(\omega_i) - N, D(\omega_i)| \delta\omega \quad (5.24)$$

and can be used to provide this extra information.

The singular case presented in Figures 5.1, 5.2 does not clearly show the effects of cavity shape and symmetry on the accuracy of the asymptotic formulae. In order to get an indication of these effects, Eqs. (5.5, 5.19) were used to generate the approximate mode distributions for each of the hypothetical cavities discussed in Chapter 3. These results were not graphed, but the figures E, A for each case are compared in Table 5.1.

5.5 Exact Spectral Density of EM Modes

Eqs. (5.20-5.22) are smooth, continuous, monotonic functions of frequency and as such are only approximations for finite (if not too small) frequencies. However, if the bandwidth and/or the cavity is very small, then the exact distribution D' can exhibit large fluctuations about the asymptote $D(\omega)$ due to the step discontinuities in the exact distribution N' . Of course the accuracy of Eqs. (5.20-5.22) is seriously degraded under these conditions. The exact spectral density of modes is, however, known analytically for rectangular domains and is given in [31] as

Table 5.1 Comparison of the figures E and A for the asymptotic formulae applied to the hypothetical cavities discussed in Chapter 3. The first figure of each pair is E as defined by Eq. (5.23) and the second figure is A as defined by Eq. (5.24).

VERSION OF APPROXIMATE FORMULA	E AND A FOR CURVES OF N vs ω/ω_c	E AND A FOR CURVES OF D vs ω/ω_c		
		BW=50 MHz	BW=100 MHz	$L_1=L_1+1\text{cm}^a$
CUBIC CAVITY ($L_1=L_2=L_3=L=25\text{cm}$)				
CORRECT EM ^b	0.00; 2.19	-0.14; 2.70	-0.12; 3.14	-0.03; 2.67
ACOUSTICx2 ^c	-34.1; 34.1	-1.66; 3.27	-3.19; 4.39	-3.18; 3.66
RAYLEIGHx2 ^d	-4.30; 4.43	-0.27; 2.74	-0.37; 3.46	-0.29; 2.67
RECTANGULAR CAVITY ($L_1=25\text{cm}, L_2=35\text{cm}, L_3=45\text{cm}$)				
CORRECT EM ^b	0.02; 1.63	-0.01; 2.08	-0.03; 2.50	-0.04; 2.95
ACOUSTICx2 ^c	-55.6; 55.6	-2.60; 3.18	-5.25; 5.38	-5.37; 5.66
RAYLEIGHx2 ^d	-5.68; 5.68	-0.19; 2.09	-0.38; 2.53	-0.39; 2.98

^aThe bandwidth associated with this column of figures is 100 MHz.

^bThese values were obtained using data generated from the correct asymptotic formulae for electromagnetic modes, Eqs. (5.15, 5.19).

^cThese values were obtained using data generated from the incorrect formula, Eq. (5.5), and its derivative.

^dThese values were obtained using data generated from just the first terms of Eqs. (5.15, 5.19).

$$\begin{aligned} \tilde{D}_{EM}(k) = & \frac{V k^2}{\pi^2} \left[1 + \sum'_{f_1, f_2, f_3 = -\infty}^{+\infty} \frac{\sin(2\mu k)}{2\mu k} \right] \\ & - \frac{1}{2\pi} \sum_{i=1}^3 L_i \left[1 + \sum'_{m=-\infty}^{+\infty} \cos(2mL_i k) \right] + \frac{1}{2} \delta(k) \quad (5.25) \end{aligned}$$

where $f_i = p_i c / 4L_i$, $\mu^2 = f_1^2 L_1^2 + f_2^2 L_2^2 + f_3^2 L_3^2$; and the primes on the Σ signs indicate that the $f_i = 0$ and $m = 0$ terms are to be omitted from the sum. If $L_1 = L_2 = L_3 = L$ (i.e. a cube shaped cavity), then Eq.(5.25) reduces [31,32] to

$$\begin{aligned} \tilde{D}_{EM}(k) = & \frac{V k^2}{\pi^2} \left[1 + \sum'_{f_1, f_2, f_3 = -\infty}^{+\infty} \frac{\sin(2fkL)}{2fkL} \right] \\ & - \frac{3L}{2\pi} \left[1 + \sum'_{m=-\infty}^{+\infty} \cos(2mLk) \right] + \frac{1}{2} \delta(k). \quad (5.26) \end{aligned}$$

where $f^2 = f_1^2 + f_2^2 + f_3^2$ and the primes have the same meaning as above.

Note that Eqs.(5.25,5.26) describe distributions in the mathematical sense, rather than distribution functions per se, and as such are valid only in integral form. Thus, the convolution

$$\int_0^\infty \tilde{D}(k') W(k-k') dk' \quad (5.27)$$

yields the number of modes within the bandwidth described by the window function W . A thorough and rigorous treatment of the mode density fluctuations is given in [25].

5.6 Discussion

The utility, at least for rectangular cavity design purposes, of the asymptotic formulae is apparently questionable at best since they clearly do not provide realistic descriptions of the exact mode distributions. The domain of Figures 5.1, 5.2 is of course far from the asymptotic regime, and hence one could only expect "best fit" representations of the exact distributions. This may be adequate for large cavities or large bandwidths where the computation of the exact N, D is not feasible. However, for a large class of microwave cavity problems, the lower frequency range is the most interesting [42-49] and accurate knowledge of the spectral density of modes is desirable, especially if bandwidth is limited. The approximate distribution functions would seem to be of limited value in these applications. Yet, the approximate formulae (albeit incorrect versions of them) have been mentioned several times in the engineering literature, without qualification, in the context of microwave cavity design. But quite unexpected results could be obtained if Eq.(5.15), or especially Eq.(5.20) were used naively in design calculations.

For nonrectangular cavity design, however, the approximate formulae may be very useful. As mentioned in the last chapter, there may be advantages to using

odd-shaped nonrectangular cavities for some microwave heating applications. In such cases, it can be extremely difficult, if not impossible, to calculate the exact mode distribution; and hence the asymptotic formulae yield valuable information, even for low frequencies. Furthermore, the accuracy of the approximations would be better for the case of irregular cavity shapes because of the absence of degeneracies due to geometric symmetry.

CHAPTER 6. SUMMARY AND CONCLUSIONS

The purpose of this chapter is to briefly summarize the contributions made by this work to the field of Electrical Engineering.

6.1 Regarding Calculated Mode Distributions

A numerical algorithm has been presented which correctly enumerates the TM and TE modes within a finite bandwidth for an empty rectangular cavity. Three computer programs which utilize this algorithm for the design/analysis of microwave heating cavities were also presented. These programs are useful for analysis purposes and also for obtaining target cavity dimensions (i.e. a starting point for the design process) which yield favourable mode distributions for a particular application.

One of the programs was used to generate theoretical (exact) mode distribution data for several hypothetical cavities. The results revealed certain characteristics—in particular the marked sensitivity to cavity shape and bandwidth—which suggest that, due to practical considerations, intrinsic mode density calculations are potentially misleading from a design point of view. However, these calculations are still valuable for reference purposes, and additional numerical results were compiled in

reference tables which are intended to replace (and augment) previously published incorrect data [59]. The discrepancies between the correct and incorrect mode counts were shown to be on the order of 50-100% and hence it is extremely important to use the correct algorithm, especially when small cavities (or low frequencies) are being considered.

Correct asymptotic mode distribution functions for rectangular cavities have been derived in a heuristic manner which can be understood by engineers without a graduate-level background in mathematics. These derivations emphasize the origin and nature of the physical differences between TM and TE modes which must be understood if these functions are to be used for research (or design) purposes. The formulae quoted here appear for the first time, in their correct forms, in the microwave engineering literature. Several factors affecting the utility of these analytical formulae were evident from comparisons with results obtained numerically and experimentally. These were discussed.

Only rectangular cavities have been considered in detail here. However, it is understood that the physical principles which apply to mode counting in rectangular cavities also carry over to other geometries. For example, the fact that TM and TE modes have different distributions and therefore must be counted separately in order to obtain the correct number of modes in a cavity, holds true for any

regular geometry (i.e. where the distinction between TM and TE modes makes sense). Also, conclusions regarding factors which affect the mode distributions (e.g. shape, bandwidth) in rectangular cavities can probably be generalized, at least qualitatively, to other cavity shapes.

6.2 Regarding Measured Mode Distributions

The low frequency spectral distribution of electromagnetic modes in an empty, rectangular, laboratory cavity has been determined experimentally. These measurements constitute the first experimental verification of the electromagnetic mode counting theory [60]. The straightforward measurement technique described here is applicable to microwave cavities of arbitrary shape and is therefore useful in investigations of nonrectangular cavities and cavities with mode stirrers, turntables, etc.

The effect of the presence of a mode stirrer on the spectral distribution of modes in the laboratory cavity was investigated experimentally. The results indicate that a mode stirrer causes more thorough splitting of degenerate modes, where the actual resonant frequencies depend strongly on the angular position (and, of course, the geometry and location) of the mode stirrer. Lower Qs and a very strong dependence of the coupling on angular position (etc.) were also observed. All of these effects can be used to

advantage in the design of microwave applicators. However, more theoretical and experimental work is required in order to exploit these effects optimally.

6.3 Some Topics for Further Research

In achieving the objectives set forth in Chapter 1, several interesting research topics have been uncovered which are unfortunately beyond the scope of this thesis. For example: mode distribution and field pattern measurements on nonrectangular (e.g. trapezoidal) cavities; experimental (and theoretical) investigations of cavity perturbations due to mode stirrers; more thorough and rigorous investigations of the cross-coupling between multiple source antennae; corrections to $N(\omega)$ to account for the presence of a mode stirrer; improvements to CAD programs for cavity design. These are some of the topics which will soon become very important in the area of small, low power applicator design (e.g. solid state microwave ovens).

6.4 Concluding Remarks

At this stage, only a qualitative interpretation can be given to the intrinsic mode distributions for a given cavity. Hence, it would seem that less (but not zero) emphasis should be placed on mode counting as a design aid, at least for cavities intended for use as microwave power

applicators. However, as research (or diagnostic?) tools, mode distribution measurements and calculations may be very valuable. Understanding these distributions is an essential first step in the investigation of shape and symmetry effects, and arbitrary loading in small cavities.

Furthermore, as electrical engineers become more involved in work which requires a knowledge of thermodynamics and radiation physics (as in the space program, fusion research, solid state electronics, etc.), it will be necessary to understand and apply the basic laws of Planck, Wien, Stefan-Boltzmann, Einstein, etc. The asymptotic spectral density formula is involved in all of these laws and the classical texts do not consider the corrections which become important at lower frequencies (i.e. <infrared). With a correct understanding of the theory of mode counting, it is less difficult to determine the limitations of the classical theory, and therefore avoid the kind of errors which currently exist in the microwave engineering literature.

The last text on microwave power engineering has certainly not been written, and every new text will undoubtedly deal with the subject of mode counting in some form or another. It is hoped that this work will serve, not only to correct the current literature, but also to provide future authors and researchers with adequate reference

material to prevent further errors from occurring. It is also hoped that this thesis will inspire further research in this area, especially on the topics given above.

BIBLIOGRAPHY AND REFERENCES

- [1] F. Pockels, "Über die partielle Differentialgleichung $\Delta u + k^2 u = 0$ und deren Auftreten in der mathematischen Physik", (B.G. Teubner Verlag, Leipzig), 1891. Cited in [10,28].
- [2] J.W. Strutt (Lord Rayleigh), "On the passage of electric waves through tubes or the vibrations of dielectric cylinders", Phil. Mag., ser. 5, no. 43, pp. 125-128, 1897.
- [3] J.W. Strutt (Lord Rayleigh), "The dynamical theory of gases and of radiation", Nature, vol. 72, no. 1855, pp. 54,55, 1905. (See also "The constant of radiation as calculated from molecular data", Ibid., no. 1863, pp. 243,244.)
- [4] J.H. Jeans, "On the partition of energy between matter and æther", Phil. Mag., ser. 6, no. 55, pp. 91-98, 1905.
- [5] H. Weyl, "Über die asymptotische Verteilung der Eigenwerte", Akademie der Wissenschaften, Göttingen Nachr., Geschäftliche Mitteilungen, pp. 110-117, 1911.
- [6] H. Weyl, "Das asymptotische Verteilungsgesetz der

- Eigenwerte linearer partieller Differentialgleichungen (mit einer Anwendung auf die theorie der Hohlraumstrahlung)", *Mathematische Annalen*, vol. 71, pp. 441-479, 1911.
- [7] H. Weyl, "Über das Spektrum der Hohlraumstrahlung", *J. f. reine u. angewandte Mathematik*, vol. 141, pp. 163-181, 1912.
- [8] H. Weyl, "Über die Randwertaufgabe der Strahlungstheorie und asymptotische Spektralgesetze", *J. f. reine u. angewandte Mathematik*, vol. 143, pp. 177-202, 1913.
- [9] R. Courant, "Über die Eigenwerte bei den Differentialgleichungen der mathematischen Physik", *Math. Z.*, vol. 7, pp. 1-57, 1920.
- [10] R. Courant and D. Hilbert, Methoden der Mathematischen Physik, vol. 1, Chs. 5,6, Julius Springer (Berlin), 1924. (See also: Methods of Mathematical Physics, 1st ed., translated and revised from the German original, Interscience Publishers (New York), 1953.)
- [11] T. Carleman, "Über die asymptotische Verteilung der Eigenwerte partieller Differentialgleichungen", *Ber. der Sächs. Akad. d. Wissenschaften, Leipzig*, vol. 88,

pp. 119-132, 1936.

[12] A. Pleijel, "Propriétés asymptotique des fonctions et valeurs propres de certaines problèmes de vibrations", Ark. Mat. Astr. Fys., vol. 27~~A~~, no. 13, pp. 1-101, 1940.

[13] A. Pleijel, "On the problem of improving Weyl's law for the asymptotic eigenvalue distribution", Convagno Internazionale sulle Equazioni Lineari alle Derivate Partiali, Trieste, 1954. Edizioni Cremonese, Rome, pp. 69-75, 1955. Cited in [18,28].

[14] F.H. Brownell, "An extension of Weyl's asymptotic law for eigenvalues", Pacific J. Math., vol. 5, pp. 483-499, 1955.

[15] F.H. Brownell, "Extended asymptotic eigenvalue distributions for bounded domains in n -space", J. Math. Mech., vol. 6, no. 1, pp. 119-166, 1957.

[16] S. Agmon, "On the eigenfunctions and on the eigenvalues of general elliptic boundary value problems", Comm. Pure. Appl. Math., vol. 15, pp. 119-147, 1962.

[17] S. Agmon, Lectures on Elliptic Boundary Value Problems, Van Nostrand (Princeton), 1965. Cited in [18,28].

- [18] C. Clark, "The asymptotic distribution of eigenvalues and eigenfunctions for elliptic boundary value problems", *SIAM Rev.*, vol. 9, no. 4, pp. 627-646, 1967.
- [19] C. Müller, Grandprobleme der Mathematischen Theorie Elektromagnetischer Schwingungen, Springer (Berlin, Göttingen, Heidelberg), 1957. Cited in [20,28].
- [20] C. Müller and H. Niemyer, "Greensche Tensoren und asymptotische Gesetze der elektromagnetischen Hohlraumschwingungen", *Arch. Rat. Mech. Anal.*, vol. 7, pp. 305-348, 1961..
- [21] H. Niemyer, "On electromagnetic eigenfunctions in closed cavities", *New York University Inst. Math. Sci., Div. of Electromag. Res., Research Report BR-34*, 1960.
- [22] H. Niemyer, "Eine Verschärfung der asymptotischen Gesetze elektromagnetischer Hohlraumschwingungen", *Arch. Rat. Mech. Anal.*, vol. 7, pp. 412-433, 1961.
- [23] R.K. Pathria, "Influence of boundary conditions on the distribution of quantum states", *Supplemento al Nuovo Cimento*, vol. 4, pp. 276-290, 1966.
- [24] K.M. Case and S.C. Chiu, "Electromagnetic fluctuations in a cavity", *Phys. Rev.*, vol. A1, no. 4,

pp. 1170-1174, 1970.

- [25] R. Balian and C. Bloch, "Distribution of eigenfrequencies for the wave equation in a finite domain—part III: eigenfrequency density oscillations", *Ann. Phys. (New York)*, vol. 69, pp. 76-160, 1972. (See also parts I and II, *Ibid.*, vol. 60, pp. 401-447, 1970, and vol. 64, pp. 271-307, 1971 respectively.)
- [26] R. Balian and B. Duplantier, "Electromagnetic waves near perfect conductors—part I: Multiple scattering expansions. Distribution of modes", *Ann. Phys. (New York)*, vol. 104, pp. 300-335, 1977. (See also part II, *Ibid.*, vol. 112, pp. 165-208, 1978.)
- [27] H.P. Baltes and F.K. Kneubühl, "Thermal radiation in finite cavities", Dissertation Nr. 4776, ETH Zurich, Switzerland, *Helv. Phys. Acta*, vol. 45, pp. 481-529, 1972. (180 refs.)
- [28] H.P. Baltes and E.R. Hilf, Spectra of Finite Systems, Bibliographisches Institut AG, Zurich, Switzerland, 1976. (217 refs.)
- [29] H.P. Baltes, "Asymptotic eigenvalue distributions for the wave equation in a cylinder of arbitrary cross section", *Phys. Rev.*, vol. A6, pp. 2252-2257, 1972.

- [30] H.P. Baltes, "Coherence and the radiation laws", Appl. Phys., vol. 12, sect. 2, pp. 221-244, 1977. (256 refs.)
- [31] B. Steinle and H.P. Baltes, "Oscillatory spectral density and partial coherence of blackbody radiation in cuboidal cavities", Infrared Phys., vol. 16, pp. 25-27, 1976.
- [32] H.P. Baltes and B. Steinle, "Eigenfrequency density oscillations and Walfisz lattice sums", J. Math. Phys., vol. 18, no. 6, pp. 1275-1276, 1977.
- [33] H.P. Baltes, "Deviations from the Stefan-Boltzmann law at low temperatures", Appl. Phys., vol. 1, pp. 39-43, 1973.
- [34] W. Eckhardt, "Corrections to the Stefan-Boltzmann radiation law in cavities with walls of finite conductivity", Optics Comm., vol. 14, no. 1, pp. 95-98, 1975.
- [35] B. Steinle, H.P. Baltes and M. Pabst, "Asymptotic expansion for the temporal coherence functions of a finite blackbody", Phys. Rev., vol. A12, pp. 1519-1524, 1975.

- [36] H.P. Baltes, B. Steinle and M. Pabst, "Poincaré cycles and coherence of bounded thermal radiation fields", Phys. Rev., vol. A13, pp. 1866-1873, 1976.
- [37] H.P. Baltes, "Planck's radiation law for finite cavities and related problems", Infrared Phys., vol. 16, pp. 1-8, 1976.
- [38] H.P. Baltes and E. Simánek, "Physics of microparticles", Topics in Current Physics: Aerosol microphysics II, vol. 29, edited by W.H. Marlow, Springer-Verlag (Berlin, Heidelberg), pp. 7-53, 1982. (177 refs.)
- [39] R.H. Bolt, "Frequency distribution of eigentones in a three dimensional continuum", J. Acoust. Soc. Am., vol. 10, pp. 228-234, 1939.
- [40] Dah-you Maa, "Distribution of eigentones in a rectangular chamber at low frequency range", J. Acoust. Soc. Am., vol 10, pp. 235-238, 1939.
- [41] P.M. Morse, Vibration and Sound, 1st ed., Ch. 8, McGraw-Hill (New York), 1936. (See also 2nd ed., 1948)
- [42] Philips Electron Tube Division, Philips Continuous-Wave Magnetrons for the Heating of Food in Microwave Ranges,

Philips Research Laboratories (Eindhoven), 1960.

- [43] H. Püschner, Heating With Microwaves, Philips Inc., Technical Library, pp. 177-179, Springer-Verlag (New York), 1966.
- [44] C.R. James, W.R. Tinga and W.A.G. Voss, "Some factors affecting energy conversion in multimode cavities", J. Microwave Power, vol. 1, no. 3, pp. 97-107, 1966.
- [45] C.R. James, W.R. Tinga and W.A.G. Voss, "Energy conversion in closed microwave cavities", Microwave Power Engineering, ed. by E.C. Okress, vol. 2, pp. 28-37, Academic Press (New York), 1968.
- [46] A.C. Metaxas and R.J. Meredith, Industrial Microwave Heating, IEE Power Engineering Series 4, ch. 6, Peter Peregrinus (London), 1983.
- [47] D.A. Copson and R.V. Decareau, "Ovens", Microwave Power Engineering, ed. by E.C. Okress, vol. 2, pp. 6-27, Academic Press (New York), 1968.
- [48] A. Mackay B, "Experimental study on microwave oven design", Ph.D. Dissertation, University of Alberta, 1977.

- [49] Chen Han-kui, Shen Zhi-yuan, Fu Chen-seng and Wu Ding, "The development of microwave power applications in China", *J. Microwave Power*, vol. 17, no. 1, pp. 11-15, 1982.
- [50] Chen Han-kui, "The calculation of resonant modes in a rectangular microwave heating cavity", *Nature (Ziran Zazhi)*, vol. 2, no. 3, p. 3, 1979.
- [51] J.D. Jackson, Classical Electrodynamics, 2nd ed., ch. 8, John Wiley & Sons (New York), 1975.
- [52] S. Ramo, J.R. Whinnery and T. Van Duzer, Fields and Waves in Communication Electronics, chs. 7, 10, John Wiley & Sons (New York), 1965.
- [53] J.R. Reitz, F.J. Milford and R.W. Christy, Foundations of Electromagnetic Theory, 3rd ed., chs. 16, 18, Addison-Wesley (Massachusetts), 1979.
- [54] C.H. Roth Jr., Fundamentals of Logic Design, 2nd ed., ch. 6, West (St. Paul), 1979.
- [55] J.M. van Nieuwland and C. Weber, "Eigenmodes in non-rectangular reverberation rooms", paper C2, presented at The 9th International Congress on Acoustics, Madrid, July 4-9, 1977.

- [56] E.L. Ginzton, Microwave Measurements, Ch. 10, McGraw-Hill (New York), 1957.
- [57] F.K. Richtmyer and E.H. Kennard, Introduction to Modern Physics, 4th ed., Ch. 5, McGraw-Hill (New York), 1947.
- [58] J.C. Slater, Microwave Electronics, Bell Telephone Lab Series, ch. 4, D. Van Nostrand (Princeton), 1950.
- [59] R.F.B. Turner, W.A.G. Voss, W.R. Tinga and H.P. Baltes, "On the counting of modes in rectangular cavities", J. Microwave Power, vol. 19, no. 3, 1984. In press.
- [60] R.F.B. Turner, W.A.G. Voss, W.R. Tinga and H.P. Baltes, "Eigenfrequency distributions in multimode rectangular cavities", To be published.

APPENDIX A. COMPUTER PROGRAM LISTINGS

A.1 NEWCAV

```

1  $RUN *WATFIV T=10 P=99 5=*MSOURCE* 6=*MSIN* 7=-OUT(*L) PAR=SIZE=20
2  /COMPILE T=10 NOWARN NOEXT NOLIST
3  C
4  C
5  C   Located in MTS file: NEWCAV           Revised: 29 September 84
6  C
7  C
8  C
9  C   MAIN PROGRAM
10 C
11 C
12 C
13 C   AA - base dimension along the X axis (cm)
14 C   AS - step size for the increments of dimension A (cm)
15 C   AN - number of steps taken in the direction of A
16 C   BB - base dimension along the Y axis (cm)
17 C   BS - step size for the increments of dimension B (cm)
18 C   BN - number of steps taken in the direction of B
19 C   DD - base dimension along the Z axis (cm)
20 C   DS - step size for the increments of dimension D (cm)
21 C   DN - number of steps taken in the direction of D
22 C   F1 - minimum frequency in the band of interest (MHz)
23 C   F2 - maximum frequency in the band of interest (MHz)
24 C   RE - response to indicate whether or not to rerun
25 C   LR - last chance to prevent termination of program
26 C   SR - response to indicate whether or not to save results
27 C   LS - last chance to save results of current run
28 C   RC - response to indicate whether or not to change data
29 C
30 C
31 C
32 C   DD - indicates what output device is currently in effect
33 C   EF - indicates that input errors have been detected
34 C   FR - remains TRUE only until the end of the first run
35 C   BC - counts the number of unsuccessful runs
36 C   SW - switch to indicate whether or not to reset BC
37 C   UC - counts the number of elements in CAV
38 C   VC - counts the total number of TE and TM modes
39 C   HCP - contains TM mode totals for each element of CAV
40 C   ECP - contains TE mode totals for each element of CAV
41 C   PMX - contains the maximum values of the input parameters
42 C   OKP - indicates whether or not input parameters are ok
43 C   CA - contains dimensions of the most mode-dense cavities
44 C   MTL - contains indices of the TE modes supported by above
45 C   MTY - contains indices of the TM modes supported by above
46 C   FTE - contains resonant frequencies of each mode in MTE
47 C   FTM - contains resonant frequencies of each mode in MTM
48 C   PTE - characters required to construct TE mode spectrum
49 C   PTM - characters required to construct TM mode spectrum
50 C   LBL - contains mid-band frequencies for labelling spectra
51 C
52 C
53 C   REAL*4 AA,AS,BB,BS,DD,DS,F1,F2,
54 C   +   CAV(10,3),FTE(10,50),FTM(10,50),
55 C   +   PMX(7)/2*1E3,1E2,1E5,1E4,1E3,1E2/
56 C   INTEGER*2 E,I,J,K,L,M,N,P,Q,R,S,U,V,
57 C   +   AN,BN,DN,BC,UC,VC,EC,HC,SW,XI,LE,ME,
58 C   +   LBL(11),MTE(10,50,3),MTM(10,50,3),ECP(10),HCP(10)
59 C   INTEGER*4 OD
60 C   LOGICAL*1 EF,FR/.TRUE./,DKP(6)

```

NEWCAV Cont'd.

```

61 CHARACTER*1 PTE(10,10,71),PTM(10,10,71)
62 CHARACTER*4 RE,LR,SR,LS,RC
63 COMMON /REAL/ AA,AS,BB,BS,DD,DS,F1,F2
64 COMMON /INTGR/ AN,BN,DN
65 ON ERROR GOTO 22
66 C
67 C
68 C An introduction to the program is displayed at the start
69 C of every session.
70 C
71 C
72 C WRITE(6,611)
73 C
74 C
75 C BC is set to 0 initially and following a successful run.
76 C
77 C
78 11 BC=0
79 SW=1
80 C
81 C
82 C Current values of AA,BB,DD are displayed (if not first
83 C run) and user is asked whether changes are required and
84 C if so is prompted for the new values.
85 C
86 C
87 12 IF(.NOT.FR)THEN DO
88 WRITE(6,621) 'AA',AA
89 WRITE(6,621) 'BB',BB
90 WRITE(6,621) 'DD',DD
91 WRITE(6,624)
92 READ(5,511,END=22,ERR=22) RC
93 IF((RC.EQ.'NO').OR.(RC.EQ.'no').OR.(RC.EQ.'N')
94 + .OR.(RC.EQ.'n').OR.(RC.EQ.'0'))GO TO 13
95 END IF
96 WRITE(6,612) PMX(1)
97 READ(5,*,END=22,ERR=22) AA,BB,DD
98 C
99 C
100 C Current values of AS,BS,DS are displayed (if not first
101 C run) and user is asked whether changes are required and
102 C if so is prompted for the new values.
103 C
104 C
105 13 IF(.NOT.FR)THEN DO
106 WRITE(6,621) 'AS',AS
107 WRITE(6,621) 'BS',BS
108 WRITE(6,621) 'DS',DS
109 WRITE(6,624)
110 READ(5,511,END=22,ERR=22) RC
111 IF((RC.EQ.'NO').OR.(RC.EQ.'no').OR.(RC.EQ.'N')
112 + .OR.(RC.EQ.'n').OR.(RC.EQ.'0'))GO TO 14
113 END IF
114 WRITE(6,613) PMY(2)
115 READ(5,*,END=22,ERR=22) AS,BS,DS
116 C
117 C
118 C Current values of AN,BN,DN are displayed (if not first
119 C run) and user is asked whether changes are required and
120 C if so is prompted for the new values.

```


NEWCAV Cont'd.

```

121 C |
122 C
123 14 IF (.NOT.FR) THEN DO
124     WRITE(6,622) 'AN',AN
125     WRITE(6,622) 'BN',BN
126     WRITE(6,622) 'DN',DN
127     WRITE(6,624)
128     READ(5,511,END=22,ERR=22) RC
129     IF ((RC.EQ.'NO') .OR. (RC.EQ.'no') .OR. (RC.EQ.'N')
130 +     .OR. (RC.EQ.'n') .OR. (RC.EQ.'0')) GO TO 15
131     END IF
132     XI=PMX(3)
133     WRITE(6,614) XI
134     READ(5,*,END=22,ERR=22) 'AN,B',DN

```

Current values of F1,F2 are displayed (if not first run) and user is asked whether changes are required and if so is prompted for the new values.

```

141 C
142 C
143 15 IF (.NOT.FR) THEN DO
144     WRITE(6,623) 'F1',F1
145     WRITE(6,623) 'F2',F2
146     WRITE(6,624)
147     READ(5,511,END=22,ERR=22) RC
148     IF ((RC.EQ.'NO') .OR. (RC.EQ.'no') .OR. (RC.EQ.'N')
149 +     .OR. (RC.EQ.'n') .OR. (RC.EQ.'0')) GO TO 16
150     END IF
151     WRITE(6,615) PMX(4),PMX(5)
152     READ(5,*,END=22,ERR=22) F1,F2

```

Input parameters are passed to subroutine PARCHK which sets certain elements of OKP=.FALSE. if incompatibilities are detected. The elements of OKP are then checked and appropriate error messages are displayed corresponding to elements of OKP which are .FALSE. The user is allowed 3 attempts at a successful run before execution terminates.

```

161 C
162 C
163 16 CALL PARCHK(PMX,OKP)
164     EF=.FALSE.
165     DO 17 E=1,6
166     IF (.NOT.OKP(E)) EF=.TRUE.
167 17 CONTINUE
168     IF (EF) THEN DO
169         BC=BC+1
170         IF (BC.EQ.3) THEN DO
171             WRITE(6,821)
172             GO TO 99
173         END IF
174         WRITE(6,811)
175         IF (.NOT.OKP(1)) WRITE(6,812)
176         IF (.NOT.OKP(2)) WRITE(6,813)
177         IF (.NOT.OKP(3)) WRITE(6,814)
178         IF (.NOT.OKP(4)) WRITE(6,815)
179         IF (.NOT.OKP(5)) WRITE(6,816)
180         IF (.NOT.OKP(6)) WRITE(6,817)

```

NEWCAV Cont'd.

```

181      END IF
182      C
183      C
184      C
185      C
186      C
187      C
188      C
189      C
190      C
191      C
192      C
193      C
194      CALL DISPRS(CAV,MTE,MTM,FTE,FTM,UC,HCP,ECP,VC)
195      IF(UC.EQ.0)THEN DO
196          WRITE(6,818)
197          GO TO 21
198      END IF
199      C
200      C
201      C
202      C
203      C
204      C
205      C
206      C
207      C
208      C
209      CALL LINSPP(CAV,MTE,MTM,FTE,FTM,UC,HCP,ECP,PTE,PTM,LBL)
210      C
211      C
212      C
213      C
214      C
215      C
216      C
217      C
218      C
219      C
220      DD=6
221      -18 WRITE(OD,711) AA,BB,DD,AS,BS,DS,AN,BN,DN,F1,F2
222      WRITE(OD,712)
223      DO 19 I=1,UC
224      HC=HCP(I)
225      EC=ECP(I)
226      WRITE(OD,713)
227      IF(HC.NE.0)THEN DO
228          WRITE(OD,714) (CAV(I,J),J=1,3),(MTE(I,1,K),K=1,3),FTE(I,1)
229          IF(HC.GT.1)WRITE(OD,715)
230          + ((MTE(I,L,M),M=1,3),FTE(I,L),L=2,HC)
231          IF(HC.EQ.50)WRITE(OD,819)
232          WRITE(OD,716) HC, 'TE'
233          IF(EC.NE.0)THEN DO
234              WRITE(OD,715) (MTM(I,LE,ME),ME=1,3),FTM(I,LE),LE=1,EC)
235              IF(EC.EQ.50)WRITE(OD,819)
236          END IF
237          WRITE(OD,716) EC, 'TM'
238      ELSE DO
239          WRITE(OD,714) (CAV(I,J),J=1,3),(MTM(I,1,K),K=1,3),FTM(I,1)
240          IF(EC.GT.1)WRITE(OD,715)

```

NEWCAV Cont'd.

```

241 + ((MTM(I,L,M),M=1,3),FTM(I,L),L=2,EC)
242 IF(EC.EQ.50)WRITE(OD,819)
243 WRITE(OD,716) EC, TM
244 WRITE(OD,716) HC, TE
245 END IF
246 IF(HC.NE.0)THEN DO
247 WRITE(OD,717)
248 WRITE(OD,718) ((PTE(I,N,P),P=1,71),N=1,10)
249 WRITE(OD,719)
250 WRITE(OD,720)
251 WRITE(OD,721) (LBL(Q),Q=1,11)
252 END IF
253 IF(EC.NE.0)THEN DO
254 WRITE(OD,722)
255 WRITE(OD,718) ((PTM(I,R,S),S=1,71),R=1,10)
256 WRITE(OD,719)
257 WRITE(OD,720)
258 WRITE(OD,721) (LBL(V),V=1,11)
259 END IF
260 19 CONTINUE
261 IF(UC.EQ.10)WRITE(OD,820)

```

C
C
C
C
C
C
C

The user is asked whether or not a duplicate copy of the printed output is required and if so the copy is appended to the bottom of the temporary file -OUT.

```

262 IF(OD.EQ.7)WRITE(6,619)
270 20 IF(OD.EQ.6)THEN DO
271 WRITE(6,618)
272 READ(5,511,END=22,ERR=22) SR
273 IF((SR.EQ.'YES').OR.(SR.EQ.'yes').OR.(SR.EQ.'Y')
274 + .OR.(SR.EQ.'y').OR.(SR.EQ.'OK').OR.(SR.EQ.'ok')
275 + .OR.(SR.EQ.'1'))THEN DO
276 OD=7
277 GO TO 18
278 END IF
279 IF((SR.NE.'NO').AND.(SR.NE.'no').AND.(SR.NE.'N')
280 + .AND.(SR.NE.'n').AND.(SR.NE.'0'))THEN DO
281 WRITE(6,617) SR
282 READ(5,511,END=22,ERR=22) LS
283 IF((LS.EQ.'NO').OR.(LS.EQ.'no').OR.(LS.EQ.'N')
284 + .OR.(LS.EQ.'n').OR.(LS.EQ.'0'))GO TO 20
285 END IF
286 WRITE(6,620)
287 END IF

```

C
C
C
C
C

Multiple reruns may be requested. The number of reruns is limited only by the maximum allotted CPU time.

```

294 SW=2
295 21 WRITE(6,616)
296 READ(5,511,END=22,ERR=22) RE
297 IF((RE.EQ.'YES').OR.(RE.EQ.'yes').OR.(RE.EQ.'Y')
298 + .OR.(RE.EQ.'y').OR.(RE.EQ.'OK').OR.(RE.EQ.'ok')
299 + .OR.(RE.EQ.'1'))THEN DO
300 FR=.FALSE.

```

NEWCAV Cont'd.

```

301          GO TO (12,11),SW
302      END IF
303      IF((RE.NE.'NO').AND.(RE.NE.'no').AND.(RE.NE.'N')
304      +.AND.(RE.NE.'n').AND.(RE.NE.'O'))THEN DO
305          WRITE(6,617) RE
306          READ(5,511,END=22,ERR=22) LR
307          IF((LR.EQ.'NO').OR.(LR.EQ.'no').OR.(LR.EQ.'N')
308      +.OR.(LR.EQ.'n').OR.(LR.EQ.'O'))GO TO 21
309      GO TO 99
310      ELSE DO
311          GO TO 99
312      END IF
313      22 WRITE(6,822)
314
315      C
316      C
317      C
318      C
319      C
320      C
321      C
322      511 FORMAT(A4)
323      611 FORMAT(//////////,'O',10X,
324      + 'This program helps the user to design ',
325      + 'a rectangular multimode'//'.5X,'cavity with the ',
326      + 'highest possible mode density given a particular set ',
327      + 'of input parameters. These parameters ',
328      + 'consist of: a set of starting'//'.5X,'dimensions ',
329      + '(AA,BB,DD) and corresponding step sizes (AS,BS,DS)',
330      + 'and'//'.5X,'step numbers (AN,BN,DN); and a pair ',
331      + 'of frequencies (F1,F2) to define'//'.5X,'the ',
332      + 'bandwidth of interest. The program then calculates ',
333      + 'all the modes'//'.5X,'supported by each cavity ',
334      + 'formed by varying the starting dimensions.',
335      + '//'.5X,'Line spectra are displayed for the cavities ',
336      + 'which yield the highest'//'.5X,'number of modes.')
337      612 FORMAT(//'O',16X,'ENTER BASE (STARTING) DIMENSIONS IN ',
338      + 'CENTIMETERS'//'.24X,'ALONG X,Y,Z AXES RESPECTIVELY'//
339      + '.3X,'| the allowable range (of real numbers) ',
340      + 'is: 0 < AA,BB,DD < ',F7.2,' cm ]'//)
341      613 FORMAT(//'O',8X,'ENTER STEP SIZE IN CENTIMETERS IN X,Y,Z ',
342      + 'DIRECTIONS RESPECTIVELY'//'.4X,'| the allowable ',
343      + 'range (of real numbers) is: 0 < AS,BS,DS < ',
344      + 'F7.2,' cm ]'//)
345      614 FORMAT(//'O',12X,'ENTER NUMBER OF STEPS IN X,Y,Z DIRECTIONS ',
346      + 'RESPECTIVELY'//'.8X,'| the allowable range (of ',
347      + 'integers) is: 0 < AN,BN,DN < ',I4,' ]'//)
348      615 FORMAT(//'O',8X,'DEFINE BANDWIDTH BY ENTERING START,STOP ',
349      + 'FREQUENCIES RESPECTIVELY'//'.34X,'IN MEGAHERTZ'//
350      + '.4X,'| the allowable range (of real numbers) ',
351      + 'is: 0 < F1 < F2 < ',F9.2,' MHz'//'.28X,'
352      + 'and F2-F1 < ',F8.2,' MHz ]'//)
353      616 FORMAT(//'O',26X,'DO YOU REQUIRE ANOTHER RUN?')
354      617 FORMAT(//'O',26X,'OK TO ASSUME ',A4,' MEANS NO?')
355      618 FORMAT(//'O',9X,'DO YOU WISH TO SAVE THE RESULTS OF THIS ',
356      + 'RUN IN THE FILE -OUT?')
357      619 FORMAT(//'O',33X,'RESULTS SAVED')
358      620 FORMAT(//'O',31X,'RESULTS DISCARDED')
359      621 FORMAT('O',21X,'THE CURRENT VALUE OF ',A2,' IS',F8.2,' cm')
360      622 FORMAT('O',21X,'THE CURRENT VALUE OF ',A2,' IS',I5)

```

FORMAT STATEMENTS

500 - 599	formatted input	700 - 799	program output
600 - 699	instructions	800 - 899	error messages

NEWCAV Cont'd.

```

361 623 FORMAT('0',21X,'THE CURRENT VALUE OF ',A2,' IS',F12.4,' MHZ')
362 624 FORMAT(' ',23X,'DO YOU WISH TO MAKE ANY CHANGES?')
363 711 FORMAT('1',20X,'THE INPUT PARAMETERS USED IN THIS RUN ARE:')
364 + // '0',32X,'AA =',F8.2,' cm / ',32X,'BB =',F6.2,' cm'
365 + // ' ',32X,'DD =',F8.2,' cm / ',32X,'AS =',F8.2,' cm'
366 + // ' ',32X,'BS =',F8.2,' cm / ',32X,'DS =',F8.2,' cm'
367 + // ' ',32X,'AN =',15./',32X,'BN =',15./',32X,'DN =',15
368 + // ' ',32X,'F1 =',F12.4,' MHZ'
369 + // ' ',32X,'F2 =',F12.4,' MHZ')
370 712 FORMAT(' ',10X,'THE MOST MODE-DENSE CAVITIES ARE:')
371 713 FORMAT(' ',5X,64(' ')/'0',8X,'A (cm)',6X,'B (cm)',6X,'D (cm)',
372 + 5X,' ',2X,'m',2X,'n',7X,'F (MHZ)')
373 714 FORMAT('0',5X,3(F8.2,4X),3I3,2X,F12.4)
374 715 FORMAT('0',41X,3I3,2X,F12.4)
375 716 FORMAT('0',5X,64(' ')/'0',6X,'TOTAL: ',13.1X,A2.1X,'MODE(S)')
376 + // '0',5X,64(' '))
377 717 FORMAT(' ',10X,'NORMALIZED ELECTRIC FIELD LINE SPECTRUM FOR ',
378 + 'TE MODES: '// '0',)
379 718 FORMAT(' ',5X,71A1)
380 719 FORMAT(' ',5X,' ',10(' '))
381 720 FORMAT(' ',5X,' ',10(' '))
382 721 FORMAT(' ',2X,11(15.2X)('// '0',)
383 722 FORMAT(' ',10X,'NORMALIZED ELECTRIC FIELD LINE SPECTRUM FOR ',
384 + 'TM MODES: '// '0',)
385 811 FORMAT('0',15X,'***** ENCOUNTERED IMPROPER OR INVALID ',
386 + 'DATA *****'/' ',10X,'***** MAKE CORRECTIONS TO ',
387 + 'DATA FILE BEFORE RERUNNING *****')
388 812 FORMAT('0',10X,'***** ONE OR MORE "STARTING DIMENSIONS" ',
389 + 'OUT OF RANGE *****')
390 813 FORMAT('0',11X,'***** ONE OR MORE "STEP SIZE" ENTRIES ',
391 + 'OUT OF RANGE *****')
392 814 FORMAT('0',8X,'***** ONE OR MORE "NUMBER OF STEPS" ',
393 + 'ENTRIES OUT OF RANGE *****')
394 815 FORMAT('0',8X,'***** ONE OR MORE "START,STOP FREQUENCIES" ',
395 + 'OUT OF RANGE *****')
396 816 FORMAT('0',10X,'***** TOO MANY COMPUTATIONS REQUIRED TO ',
397 + 'COMPLETE RUN *****')
398 817 FORMAT('0',,'***** DIMENSIONS TOO SMALL TO ',
399 + 'SUSTAIN OSCILLATION WITHIN GIVEN BANDWIDTH *****')
400 818 FORMAT('0',10X,'***** NO MODES WERE FOUND TO EXIST WITHIN ',
401 + 'THE BANDWIDTH GIVEN *****')
402 819 FORMAT('0',10X,'***** TOO MANY MODES EXIST WITHIN THE ',
403 + 'BANDWIDTH GIVEN *****'/' ',23X,'***** OUTPUT LIST ',
404 + 'TRUNCATED *****')
405 820 FORMAT('0',13X,'***** TOO MANY CAVITIES ARE EQUALLY ',
406 + 'MODE-DENSE *****'/' ',23X,'***** OUTPUT LIST ',
407 + 'TRUNCATED *****')
408 821 FORMAT('// '0',10X,'***** PLEASE FAMILIARIZE YOURSELF WITH ',
409 + 'INPUT REQUIREMENTS *****'/' ',21X,'***** BEFORE ',
410 + 'ATTEMPTING ANOTHER RUN *****')
411 822 FORMAT('// '0',2X,'***** UNRECOVERABLE ERROR WILL TERMINATE ',
412 + 'THIS RUN - PLEASE TRY AGAIN *****')
413
414
415 C
416 C
417 C
418 C
419 C
420 C

```

SUBROUTINE PARCHK

Subroutine PARCHK provides some rudimentary error
checking by performing a series of simple tests on all

NEWCAV Cont'd.

```

421 C | of the parameters (en mass) before allowing them to be
422 C | used in any computation.
423 C |
424 C |
425 C |
426 C | AAM - maximum allowable value of parameter AA (cm)
427 C | ASM - maximum allowable value of parameter AS (cm)
428 C | ANM - maximum allowable value of parameter AN
429 C | BBM - maximum allowable value of parameter BS (cm)
430 C | BSM - maximum allowable value of parameter BS (cm)
431 C | BNM - maximum allowable value of parameter BN
432 C | DDM - maximum allowable value of parameter DD (cm)
433 C | DSM - maximum allowable value of parameter DS (cm)
434 C | DNM - maximum allowable value of parameter DN
435 C | F2M - maximum allowable value of parameter F2 (MHz)
436 C | BWM - maximum allowable value of bandwidth (MHz)
437 C | NCM - maximum allowable number of cavities
438 C | MNM - maximum allowable value of any L,M,N
439 C |
440 C |
441 C |
442 C | OK - indicates whether or not input parameters are ok
443 C | AL - becomes TRUE if AA is less than one half wavelength
444 C | BL - becomes TRUE if BB is less than one half wavelength
445 C | DL - becomes TRUE if DD is less than one half wavelength
446 C | OKP - elements become FALSE if corresponding tests failed
447 C |
448 C |
449 C | SUBROUTINE PARCHK(PMX,OKP)
450 C | REAL*4 AAM,ASM,BBM,BSM,DDM,DSM,F2M,BWM,PMX(7),
451 C | + AA,AS,BB,BS,DD,DS,F1,F2
452 C | INTEGER*2 ANM,BNM,DNM,NCM,MNM,AN,BN,DN,I
453 C | LOGICAL*1 AL,BL,DL,OKP(6)
454 C | COMMON /REAL/ AA,AS,BB,BS,DD,DS,F1,F2
455 C | COMMON /INTGR/ AN,BN,DN
456 C |
457 C |
458 C | All elements of OKP are initialized to .TRUE. and local
459 C | maxima are set according to values passed in array PMX.
460 C |
461 C |
462 C | DO 11, I=1,6
463 C | 11: OKP(I)=.TRUE.
464 C | AAM=BBM=DDM=PMX(1)
465 C | ASM=BSM=DSM=PMX(2)
466 C | ANM=BNM=DNM=PMX(3)
467 C | F2M=PMX(4)
468 C | BWM=PMX(5)
469 C | NCM=PMX(6)
470 C | MNM=PMX(7)
471 C |
472 C |
473 C | All input parameters must be equal to or greater than
474 C | zero.
475 C |
476 C |
477 C | IF((AA.LE.0).OR.(BB.LE.0).OR.(DD.LE.0))OKP(1)=.FALSE.
478 C | IF((AS.LT.0).OR.(BS.LT.0).OR.(DS.LT.0))OKP(2)=.FALSE.
479 C | IF((AN.LT.0).OR.(BN.LT.0).OR.(DN.LT.0))OKP(3)=.FALSE.
480 C | IF((F1.LE.0).OR.(F2.LE.0))OKP(4)=.FALSE.

```

NEWCAV Cont'd.

```

481 C
482 C
483 C
484 C
485 C
486 C
487 C
488 C
489 C
490 C
491 C
492 C
493 C
494 C
495 C
496 C
497 C
498 C
499 C
500 C
501 C
502 C
503 C
504 C
505 C
506 C
507 C
508 C
509 C
510 C
511 C
512 C
513 C
514 C
515 C
516 C
517 C
518 C
519 C
520 C
521 C
522 C
523 C
524 C
525 C
526 C
527 C
528 C
529 C
530 C
531 C
532 C
533 C
534 C
535 C
536 C
537 C
538 C
539 C
540 C

```

All input parameters must be equal to or less than their respective maximum allowable values and must not combine in such a way as to cause an error.

```

IF((AA.GT.AAM).OR.(BB.GT.BBM).OR.(DD.GT.DDM))OKP(1)=.FALSE.
IF((AS.GT.ASM).OR.(BS.GT.BSM).OR.(DS.GT.DSM))OKP(2)=.FALSE.
IF((AN.GT.ANM).OR.(BN.GT.BNM).OR.(DN.GT.DNM))OKP(3)=.FALSE.
IF((F2.GT.F2M).OR.(F1.GT.F2).OR.(F2-F1.GT.BWM))OKP(4)=.FALSE.
IF((AN*BN.GT.NCM).OR.(BN*DN.GT.NCM).OR.(DN*AN.GT.NCM).OR.
+ (AN*BN*DN.GT.NCM))OKP(5)=.FALSE.
IF(((AA+(AS*AN))*2*F2*1E6/3E10.GT.MNM))OKP(5)=.FALSE.
IF(((BB+(BS*BN))*2*F2*1E6/3E10.GT.MNM))OKP(5)=.FALSE.
IF(((DD+(DS*DN))*2*F2*1E6/3E10.GT.MNM))OKP(5)=.FALSE.

```

The initial dimensions must be large enough to sustain at least one mode.

```

IF(ABS(F2).LT.1E-10)THEN DD
  OKP(6)=.FALSE.
  GO TO 99
END IF
AL=BL=DL=.FALSE.
IF(AA+(AS*AN).LT.3E10/(2*F2*1E6))AL=.TRUE.
IF(BB+(BS*BN).LT.3E10/(2*F2*1E6))BL=.TRUE.
IF(DD+(DS*DN).LT.3E10/(2*F2*1E6))DL=.TRUE.
IF((AL.AND.BL).OR.(BL.AND.DL).OR.(DL.AND.AL))OKP(6)=.FALSE.

```

If any elements of OKP become .FALSE. the user will be instructed (by MAIN PROGRAM) to examine the data file for improper entries.

```

99 RETURN
END

```

SUBROUTINE DISPRS

Subroutine DISPRS searches for those modes with resonant frequencies within the specified bandwidth - all possible combinations of l,m,n within a calculated range are substituted into the dispersion relation for all possible sets of dimensions.

See MAIN PROGRAM for a complete list of input parameters

UC - counts the number of elements in the array CAV
VC - counts the total number of valid TE and TM modes
AC - current value of dimension 'A' used in computations
BC - current value of dimension 'B' used in computations

NEWCAV Cont'd.

```

541 C DC - current value of dimension 'D' used in computations
542 C RF - resonant frequency calculated from dispersion rel.
543 C CAV - contains dimensions of most mode-dense cavities
544 C MTE - contains indices of the TE modes supported by above
545 C MTM - contains indices of the TM modes supported by above
546 C FTE - contains resonant frequencies of each TE mode in CAV
547 C FTM - contains resonant frequencies of each TM mode in CAV
548 C TTE - stores current values of L,M,N,RF for valid TE modes
549 C TTM - stores current values of L,M,N,RF for valid TM modes
550 C
551 C
552 SUBROUTINE DISPRS(CAV,MTE,MTM,FTE,FTM,UC,HCP,ECP,VC)
553 REAL*4 AA,AS,BB,BS,DD,DS,F1,F2,AC,BC,DC,RF,A1,A2,
554 + TTE(50,4),TTM(50,4),FTE(10,50),FTM(10,50),CAV(10,3)
555 INTEGER*2 I,J,K,L,M,N,P,Q,R,AN,BN,DN,A3,AE,BE,DE,RE,PE,QE,
556 + UC,HC,EC,VC,VE,VH,VT,EX,EY,HX,HY,
557 + MTE(10,50,3),MTM(10,50,3),ECP(10),HCP(10)
558 COMMON /REAL/ AA,AS,BB,BS,DD,DS,F1,F2
559 COMMON /INTGR/ AN,BN,DN
560 UC=0
561 VC=0
562 MAXIND(A1,A2,A3)=((A1+(A2*A3))*2+F2*1E6/3E10)+1
563 AE=AN+1
564 BE=BN+1
565 DE=DN+1
566 PE=MAXIND(AA,AS,AN)
567 QE=MAXIND(BE,BS,BN)
568 RE=MAXIND(DD,DS,DN)
569 C
570 C
571 C AC,BC,DC comprise the current set of dimensions.
572 C
573 C
574 DO 19 I=1,AE
575 AC=AA+((I-1)*AS)
576 DO 19 J=1,BE
577 BC=BB+((J-1)*BS)
578 DO 19 K=1,DE
579 DC=DD+((K-1)*DS)
580 C
581 C
582 C L,M,N comprise the current set of mode indices.
583 C
584 C
585 VH=0
586 VE=0
587 DO 11 P=1,PE
588 L=P-1
589 DO 11 Q=1,QE
590 M=Q-1
591 DO 11 R=1,RE
592 N=R-1
593 C
594 C
595 C AC,BC,DC,L,M,N are all substituted into the dispersion
596 C relation and if the resulting resonant frequency RF is
597 C within the specified bandwidth then L,M,N,RF are either
598 C stored (temporarily) in TTE,TTM or rejected depending on
599 C whether the mode is TE or TM or neither.
600 C

```


NEWCAV Cont'd.

```

601      C
602      RF=SQRT(((L/AC)**2)+((M/BC)**2)+((N/DC)**2))*(3E10/2)
603      IF(RF.LT.(F1*1E6))GO TO 11
604      IF(RF.GT.(F2*1E6))GO TO 11
605      IF(((L.GT.0).OR.(M.GT.0)).AND.(N.GT.0))THEN DO
606          VH=VH+1
607          TTE(VH,1)=L
608          TTE(VH,2)=M
609          TTE(VH,3)=N
610          TTE(VH,4)=RF/1E6
611          IF(VH.EQ.50)GO TO 12
612      END IF
613      IF((L.GT.0).AND.(M.GT.0))THEN DO
614          VE=VE+1
615          TTM(VE,1)=L
616          TTM(VE,2)=M
617          TTM(VE,3)=N
618          TTM(VE,4)=RF/1E6
619          IF(VE.EQ.50)GO TO 12
620      END IF
621      11 CONTINUE
622      C
623      C
624      C
625      C
626      C
627      C
628      C
629      C
630      12 VT=VH+VE
631      IF(VT.EQ.0)GO TO 19
632      IF(VT-VC)19,14,13
633      13 UC=0
634      14 UC=UC+1
635          VC=VT
636          HC=VH
637          EC=VE
638          HCP(UC)=HC
639          IF(HC.EQ.0)THEN DO
640              FTE(UC,1)=0
641              MTE(UC,1,1)=0
642              GO TO 16
643          END IF
644          DO 15 HY=1,HC
645              FTE(UC,HY)=TTE(HY,4)
646          DO 15 HX=1,3
647              15 MTE(UC,HY,HX)=TTE(HY,HX)
648      16 ECP(UC)=EC
649          IF(EC.EQ.0)THEN DO
650              FTM(UC,1)=0
651              MTM(UC,1,1)=0
652              GO TO 18
653          END IF
654          DO 17 EY=1,EC
655              FTM(UC,EY)=TTM(EY,4)
656          DO 17 EX=1,3
657              17 MTM(UC,EY,EX)=TTM(EY,EX)
658      18 CAV(UC,1)=AC
659          CAV(UC,2)=BC
660          CAV(UC,3)=DC

```

Dimensions of the most mode-dense cavities are saved in the array CAV and the corresponding mode numbers and resonant frequencies are saved in the arrays MTE,MTM and FTE,FTM respectively.

NEWCAV Cont'd.

```

661          IF(UC.EQ.10)GO TO 99
662          19 CONTINUE
663          99 RETURN
664          END
665          C
666          C
667          C
668          C
669          C
670          C
671          C
672          C
673          C
674          C
675          C
676          C
677          C
678          C
679          C
680          C
681          C
682          C
683          C
684          C
685          C
686          C
687          C
688          C
689          C
690          C
691          C
692          C
693          C
694          C
695          C
696          C
697          C
698          C
699          C
700          C
701          C
702          C
703          C
704          C
705          C
706          C
707          C
708          C
709          C
710          C
711          C
712          C
713          C
714          C
715          C
716          C
717          C
718          C
719          C
720          C

```

SUBROUTINE LINSPPM

Subroutine LINSPPM generates two (crude) normalized line spectra for each cavity described by the elements of CAV.

UC - counts the number of elements in the array CAV
HCP - contains the TE mode counts for each cavity in CAV
ECP - contains the TM mode counts for each cavity in CAV
CAV - contains dimensions of the most mode-dense cavities
MTE - contains indices of the TE modes supported by above
MTM - contains indices of the TM modes supported by above
FTE - contains resonant frequencies of each mode in MTE
FTM - contains resonant frequencies of each mode in MTM

see MAIN PROGRAM for a complete list of input parameters

WC - counts number of modes with same X axis position
XTE - contains the X axis positions of each TE mode
XTM - contains the X axis positions of each TM mode
WTE - contains the multiplicities of each TE mode
WTM - contains the multiplicities of each TM mode
TEU - contains unnormalized E field magnitudes of TE modes
TMU - contains unnormalized E field magnitudes of TM modes
TEN - contains normalized E field magnitudes of TE modes
TMN - contains normalized E field magnitudes of TM modes
PTE - characters required to construct TE field spectrum
PTM - characters required to construct TM field spectrum
LBL - contains mid-band frequencies for labelling spectra

```

SUBROUTINE LINSPPM(CAV,MTE,MTM,FTE,FTM,UC,HCP,ECP,PTE,PTM,LBL,
REAL*4 AA,AS,BB,BS,DD,DS,F1,F2,FF,QA,QB,QD,HF,EF,
+ CAV(10,3),FTE(10,50),FTM(10,50),TEU(50),TMU(50),
INTEGER*2 I,I1,I2,I3,JE,JH,KE,KH,M,N,P,W,PL,PM,PN,
+ AN,BN,DN,Y1,Y2,YF,YP,VE,VH,SE,SH,
+ HL,HM,HN,EL,EM,EN,UC,WC,EC,HC,
+ MTE(10,50,3),MTM(10,50,3),XTE(50),XTM(50),LBL(11),
+ WTE(71),WTM(71),ECP(10),HCP(10),TEN(50),TMN(50)
CHARACTER*1 PTE(10,10,71),PTM(10,10,71)
COMMON /REAL/ AA,AS,BB,BS,DD,DS,F1,F2
COMMON /INTGR/ AN,BN,DN

```

The character arrays PTE and PTM are initialized with blanks throughout. The entire bandwidth defined by F1 and F2 is resolved into 71 discrete X axis positions.

NEWCAV Cont'd.

```

721      DO 11 I1=1,10
722      DO 11 I2=1,10
723      DO 11 I3=1,71
724      PTE(I1,I2,I3)=1
725      PTM(I1,I2,I3)=1
726      11 CONTINUE
727      C
728      C
729      C
730      C
731      C
732      C
733      C
734      C
735      DO 21 I=1,UC
736      HC=HCP(I)
737      IF(HC.EQ.0)GO TO 14
738      DO 13 JH=1,HC
739      XTE(JH)=(((FTE(I,JH)-(F1))/(F2-F1))*70)+1
740      WC=0
741      DO 12 KH=1,JH
742      IF(XTE(KH).EQ.XTE(JH))WC=WC+1
743      W=XTE(JH)
744      WTE(W)=WC
745      12 CONTINUE
746      C
747      C
748      C
749      C
750      C
751      C
752      HL=MTE(I,JH,1)
753      HM=MTE(I,JH,2)
754      HN=MTE(I,JH,3)
755      HF=FTE(I,JH)
756      QA=CAV(I,1)
757      QB=CAV(I,2)
758      QD=CAV(I,3)
759      TEU(JH)=TEFMAG(HL,HM,HF,QA,QB)
760      13 CONTINUE
761      C
762      C
763      C
764      C
765      C
766      C
767      C
768      C
769      14 EC=ECP(I)
770      IF(EC.EQ.0)GO TO 17
771      DO 16 JE=1,EC
772      XTM(JE)=(((FTM(I,JE)-(F1))/(F2-F1))*70)+1
773      WC=0
774      DO 15 KE=1,JE
775      IF(XTM(KE).EQ.XTM(JE))WC=WC+1
776      W=XTM(JE)
777      WTM(W)=WC
778      15 CONTINUE
779      C
780      C

```

The relative position along the X axis of each TE mode is located with respect to its resonant frequency. The number of modes found to occupy the same X axis position are counted by WC and stored in WTE.

The magnitudes of the TE modes are calculated for each mode and stored (temporarily) in TEU.

The relative position along the X axis of each TM mode is located with respect to its resonant frequency. The number of modes found to occupy the same X axis position are counted by WC and stored in WTM.

NEWCAV Cont'd.

```

781 C   The magnitudes of the TM modes are calculated for each
782 C   mode and stored (temporarily) in TMU. TEU, TMU are then
783 C   passed to the subroutine MAGNRM which returns the
784 C   normalized magnitudes in the arrays TEN, TMN respectively.
785 C
786 C
787       EL=MTM(I,JE,1)
788       EM=MTM(I,JE,2)
789       EN=MTM(I,JE,3)
790       EF=FTM(I,JE)
791       QA=CAV(I,1)
792       QB=CAV(I,2)
793       QD=CAV(I,3)
794       TMU(JE)=TMFMAG(EL,EM,EN,EF,QA,QB,QD)
795 16 CONTINUE
796 17 IF(HC.NE.0)CALL MAGNRM(TEU,HC,TEN)
797    IF(EC.NE.0)CALL MAGNRM(TMU,EC,TMN)
798
799 C
800 C   The spectra PTE and PTM are formed by writing over the
801 C   appropriate blank characters with a plotting symbol so
802 C   that the resulting pattern resembles a plot of magnitude
803 C   versus frequency.
804 C
805 C
806       IF(HC.EQ.0)GO TO 19
807       DO 18 M=1,HC
808         SH=TEN(M)
809         VH=XTE(M)
810         DO 18 Y1=1,SH
811           YF=10-Y1+1
812           IF(WTE(VH).EQ.1)PTE(I,YF,VH)='1'
813           IF(WTE(VH).EQ.2)PTE(I,YF,VH)='2'
814           IF(WTE(VH).EQ.3)PTE(I,YF,VH)='3'
815           IF(WTE(VH).EQ.4)PTE(I,YF,VH)='4'
816           IF(WTE(VH).EQ.5)PTE(I,YF,VH)='5'
817           IF(WTE(VH).EQ.6)PTE(I,YF,VH)='6'
818           IF(WTE(VH).EQ.7)PTE(I,YF,VH)='7'
819           IF(WTE(VH).EQ.8)PTE(I,YF,VH)='8'
820           IF(WTE(VH).EQ.9)PTE(I,YF,VH)='9'
821 18 IF(WTE+VH).GT.9)PTE(I,YF,VH)='*'
822 19 CONTINUE
823       IF(EC.EQ.0)GO TO 21
824       DO 20 N=1,EC
825         SE=TMN(N)
826         VE=XTM(N)
827         DO 20 Y2=1,SE
828           YP=10-Y2+1
829           IF(WTM(VE).EQ.1)PTM(I,YP,VE)='1'
830           IF(WTM(VE).EQ.2)PTM(I,YP,VE)='2'
831           IF(WTM(VE).EQ.3)PTM(I,YP,VE)='3'
832           IF(WTM(VE).EQ.4)PTM(I,YP,VE)='4'
833           IF(WTM(VE).EQ.5)PTM(I,YP,VE)='5'
834           IF(WTM(VE).EQ.6)PTM(I,YP,VE)='6'
835           IF(WTM(VE).EQ.7)PTM(I,YP,VE)='7'
836           IF(WTM(VE).EQ.8)PTM(I,YP,VE)='8'
837           IF(WTM(VE).EQ.9)PTM(I,YP,VE)='9'
838 20 IF(WTM(VE).GT.9)PTM(I,YP,VE)='*'
839 21 CONTINUE
840       DO 22 P=1,11

```

NEWCAV Cont'd.

```

841      22 LBL(P)=F1+((P-1)*(F2-F1)/10)
842      99 RETURN
843      END
844      C
845      C
846      C      FUNCTION SUBPROGRAM TEFMAG
847      C
848      C      Subprogram TEFMAG calculates the magnitude of the total
849      C      electric field (to within an arbitrary constant) for a
850      C      given TE mode.
851      C
852      C
853      C      REAL FUNCTION TEFMAG(L,M,F,A,B)
854      C      REAL*4 F,A,B,KC,EX,EY
855      C      INTEGER*2 L,M
856      C      KC=((L/A)**2)+((M/B)**2)
857      C      EX=(F*M)/(KC*B)
858      C      EY=(F*L)/(KC*A)
859      C      TEFMAG=SQRT((EX**2)+(EY**2))
860      C      99 RETURN
861      C      END
862      C
863      C
864      C      FUNCTION SUBPROGRAM TMFMAG
865      C
866      C      Subprogram TMFMAG calculates the magnitude of the total
867      C      electric field (to within an arbitrary constant) for a
868      C      given TM mode.
869      C
870      C
871      C      REAL FUNCTION TMFMAG(L,M,N,F,A,B,D)
872      C      REAL*4 F,A,B,D,KC,EX,EY
873      C      INTEGER*2 L,M,N
874      C      KC=((L/A)**2)+((M/B)**2)
875      C      EX=(L/A)*(N/D)/KC
876      C      EY=(M/B)*(N/D)/KC
877      C      TMFMAG=SQRT((EX**2)+(EY**2)+1)
878      C      99 RETURN
879      C      END
880      C
881      C
882      C      SUBROUTINE MAGNRM
883      C
884      C      Subroutine MAGNRM normalizes an array YYU to the largest
885      C      element in that array and copies the result to an integer
886      C      array YYN whose elements have a maximum value of 10 and a
887      C      minimum value of 1.
888      C
889      C
890      C      SUBROUTINE MAGNRM(YYU,N,YYN)
891      C      REAL*4 LV,YYU(50)
892      C      INTEGER*2 I,J,N,YYN(50)
893      C      LV=0
894      C      DO 11 I=1,N
895      C      IF(YYU(I).GT.LV)LV=YYU(I)
896      C      11 CONTINUE
897      C      IF(LV.EQ.0)LV=1
898      C      DO 12 J=1,N
899      C      YYN(J)=(YYU(J)/LV)*10
900      C      IF(YYN(J).EQ.0)YYN(J)=1

```

NEWCAV Cont'd.

```
901      12 CONTINUE
902      99 RETURN
903      END
904      /EXECUTE
905      /BTCHEND
End of file
```

A.2 MODIST

```

1  $RUN *PascalW T=25 P=50 SPRINT=-OUT(*1+1) PAR=NOLIST
2  {
3  {
4  { Located in MTS file:  MODIST.NEW          Revised:  09 August 84
5  {
6  {
7  PROGRAM ModeDistribution(input,output); {$ S 1000000}
8  {
9  {
10 { Generates N or D vs. frequency data using the asymptotic mode
11 { distribution functions and compares the result with the exact
12 { values obtained from the dispersion relation.
13 {
14 {
15 CONST pi=3.141592654; {computational value of pi}
16      c=2.9979256E8; {speed of light in free space}
17      Tilt=1.0E-20; {smallest allowed denominator}
18
19 VAR Lx,Ly,Lz: real; {cavity dimensions}
20     fMin,fMax: real; {range of distribution}
21     StepSize: integer; {resolution of distribution}
22     bandwidth: real; {determines type of distribution}
23     V,Sx,Sy,Sz,L,R: real; {geometric properties of cavity}
24
25 PROCEDURE ComputeVSL;
26 {
27 {
28 { Assigns values to the (global) variables V,Sx,Sy,Sz,L.
29 {
30 {
31 BEGIN {ComputeVSL}
32     V:=Lx*Ly*Lz; {volume}
33     Sx:=2*Ly*Lz; {surface area of walls normal to x axis}
34     Sy:=2*Lx*Lz; {surface area of walls normal to y axis}
35     Sz:=2*Lx*Ly; {surface area of walls normal to z axis}
36     L:=Lx+Ly+Lz; {sum of linear dimensions}
37 END; {ComputeVSL}
38
39 PROCEDURE GenerateData;
40 {
41 {
42 { Generates exact and approximate N vs. f or D vs. f data
43 { (and associated discrepancies) depending on the value of
44 { bandwidth.
45 {
46 {
47 VAR fOne,fTwo: real; {defines valid range for exact formula}
48     fPrime: real; {moveable dummy abscissa}
49     ErrorTE,ErrorTM,ErrorEM: real; {signed errors}
50     ErrSumTE,ErrSumTM,ErrSumEM: real; {integrated errors}
51     AbsErrSumTE,AbsErrSumTM,AbsErrSumEM: real; {int abs err}
52     TE,TM,EM: integer; {exact number of modes}
53     i,j,k: integer; {dummy indices}
54
55 PROCEDURE CountModes(fOne,fTwo: real);
56 {
57 {
58 { Determines the number of allowable modes with resonant
59 { frequencies between fOne and fTwo.
60 {

```

MODIST Cont'd.

```

61
62   VAR px,py,pz: integer; {test mode numbers}
63
64   FUNCTION MaxIndex(dimension,frequency: real): integer;
65   {
66   {
67   { Calculates the maximum value of a mode index.
68   {
69   }
70   }
71   VAR HalfWaves: real; {dimension in terms of half waves}
72
73   BEGIN {MaxIndex}
74     HalfWaves:=2*dimension*frequency/c;
75     MaxIndex:=trunc(HalfWaves)
76   END; {MaxIndex}
77
78   PROCEDURE TestMode(px,py,pz: integer);
79   {
80   {
81   { Tests whether or not (px,py,pz) specifies an allowed
82   { mode and if so increments the appropriate counter(s).
83   {
84   }
85   }
86   VAR RF: real; {resonant frequency}
87
88   BEGIN {TestMode}
89     RF:=sqrt((sqrt(px/Lx)+sqrt(py/Ly)+sqrt(pz/Lz))*c/2;
90     IF ((RF>=fOne)AND(RF<=fTwo)) THEN
91       BEGIN {IF}
92         IF ((px>0)OR(py>0))AND(pz>0) THEN TE:=TE+1;
93         IF (px>0)AND(py>0) THEN TM:=TM+1;
94         EM:=TE+TM
95       END; {IF}
96     END; {TestMode}
97
98   BEGIN {CountModes}
99     FOR px:=0 TO MaxIndex(Lx,fTwo)+1 DO
100
101     BEGIN {FOR #1}
102       FOR py:=0 TO MaxIndex(Ly,fTwo)+1 DO
103
104       BEGIN {FOR #2}
105         FOR pz:=0 TO MaxIndex(Lz,fTwo)+1 DO
106
107         BEGIN {FOR #3}
108           TestMode(px,py,pz)
109         END; {FOR #3}
110
111       END; {FOR #2}
112
113     END; {FOR #1}
114
115   END; {CountModes}
116
117   FUNCTION NTE(frequency: real): real;
118   {
119   {
120   { Calculates NTE from the asymptotic (partial) formula.

```


MODIST Cont'd.

```

121      { | _____ | }
122
123      VAR Arg3,Arg2,Arg1: real; {reduced frequencies}
124
125      BEGIN {NTE}
126          Arg3:=exp(3*ln(frequency/c));
127          Arg2:=sqr(frequency/c);
128          Arg1:=frequency/c;
129          NTE:=(4*pi*V*Arg3/3)+(pi*(Sx+Sy-Sz)*Arg2/4)-
130              ((Lx+Ly+(3*Lz))*Arg1/2)+(3/8);
131      END; {NTE}
132
133      FUNCTION DTE(frequency,bandwidth: real): real;
134      {
135      { _____ }
136      { Calculates DTE from the asymptotic (partial) formula. }
137      { _____ }
138
139      VAR dArg3,dArg2,
140          dArg1: real; {derivatives of reduced frequencies}
141
142      BEGIN {DTE}
143          dArg3:=3*sqr(frequency/c)/c;
144          dArg2:=2*frequency/sqr(c);
145          dArg1:=1/c;
146          DTE:=((4*pi*V*dArg3/3)+(pi*(Sx+Sy-Sz)*dArg2/4)-
147              ((Lx+Ly+(3*Lz))*dArg1/2))*bandwidth;
148      END; {DTE}
149
150      FUNCTION NTM(frequency: real): real;
151      {
152      { _____ }
153      { Calculates NTM from the asymptotic (partial) formula. }
154      { _____ }
155
156      VAR Arg3,Arg2,Arg1: real; {reduced frequency}
157
158      BEGIN {NTM}
159          Arg3:=exp(3*ln(frequency/c));
160          Arg2:=sqr(frequency/c);
161          Arg1:=frequency/c;
162          NTM:=(4*pi*V*Arg3/3)-(pi*(Sx+Sy-Sz)*Arg2/4)-
163              ((Lx+Ly-Lz)*Arg1/2)+(1/8);
164      END; {NTM}
165
166      FUNCTION DTM(frequency,bandwidth: real): real;
167      {
168      { _____ }
169      { Calculates DTM from the asymptotic (partial) formula. }
170      { _____ }
171
172      VAR dArg3,dArg2,
173          dArg1: real; {derivatives of reduced frequencies}
174
175      BEGIN {DTM}
176          dArg3:=3*sqr(frequency/c)/c;
177          dArg2:=2*frequency/sqr(c);
178          dArg1:=1/c;
179          DTM:=((4*pi*V*dArg3/3)-(pi*(Sx+Sy-Sz)*dArg2/4)-
180              ((Lx+Ly-Lz)*dArg1/2))*bandwidth;

```

MODIST Cont'd.

```

181      END; {DTM}
182
183      FUNCTION NEM(frequency: real): real;
184      {
185      { Calculates NEM from the asymptotic formula,
186      {
187      {
188      {
189      VAR Arg3,Arg1: real; {reduced frequencies}
190
191      BEGIN {NEM}
192      Arg3:=exp(3*ln(frequency/c));
193      Arg1:=frequency/c;
194      NEM:=(8*pi*V*Arg3/3)-(L*Arg1)+(1/2);
195      END; {NEM}
196
197      FUNCTION DEM(frequency,bandwidth: real): real;
198      {
199      {
200      { Calculates DEM from the asymptotic formula.
201      {
202      {
203      {
204      VAR dArg3,dArg1: real; {derivative of reduced frequencies}
205
206      BEGIN {DEM}
207      dArg3:=3*sqrt(frequency/c)/c;
208      dArg1:=1/c;
209      DEM:=(8*pi*V*dArg3/3)-(L*dArg1)*bandwidth;
210      END; {DEM}
211
212      PROCEDURE OutputNvsf;
213      {
214      { Tabulates the values of N computed from the approximate
215      { formulae and the deviations of each from the exact
216      { value of N.
217      {
218      {
219      {
220      {
221      {
222      { Prints column headers for table.
223      {
224      {
225      BEGIN {PrintTitles}
226      Writeln ('      N versus Frequency Data:');
227      Writeln;
228      Writeln ('      _____');
229      Writeln ('      _____');
230      Writeln ('      _____');
231      Writeln ('      _____');
232      Writeln ('      | :12, | :27, | :27, | :27);
233      Writeln ('      FREQUENCY
234      NUMBER OF TE MODES
235      NUMBER OF TM MODES
236      NUMBER OF EM MODES | ');
237      Writeln ('      _____');
238      Writeln ('      _____');
239      Writeln ('      _____');
240      Writeln ('      _____');

```

MODIST Cont'd.

```

241      Writeln ('      (HERTZ)      |      |      |      |
242      |      :9. |      :9. |      :9. |
243      |      :9. |      :9. |      :9. |
244      |      :9. |      :9. |      :9. |
245      Writeln ('
246      |      EXACT |      APPROX |      ERROR |
247      |      EXACT |      APPROX |      ERROR |
248      |      EXACT |      APPROX |      ERROR |');
249      Writeln ('
250      |      |      |      |
251      |      |      |      |
252      |      |      |      |');
253      Writeln ('      :12. |      :27. |      :27. |      :27. |');
254      END; {PrintTitles}
255
256      PROCEDURE PrintResults;
257      {
258      {-----}
259      { Computes the total number of modes with resonant }
260      { frequencies less than fTwo. }
261      {-----}
262      }
263      BEGIN {PrintResults}
264      ErrorTE:=TE-NTE(fTwo);
265      ErrorTM:=TM-NTM(fTwo);
266      ErrorEM:=EM-NEM(fTwo);
267      Write ('      fTwo:10. ');
268      Write ('      TE:5.      NTE(fTwo):5:2. ');
269      Write ('      ErrorTE:7:2. ');
270      Write ('      TM:5.      NTM(fTwo):5:2. ');
271      Write ('      ErrorTM:7:2. ');
272      Write ('      EM:5.      NEM(fTwo):5:2. ');
273      Write ('      ErrorEM:7:2. ');
274      Writeln;
275      ErrSumTE:=ErrSumTE+ErrorTE; {integrate errors}
276      AbsErrSumTE:=AbsErrSumTE+abs(ErrorTE); {int abs err}
277      ErrSumTM:=ErrSumTM+ErrorTM;
278      AbsErrSumTM:=AbsErrSumTM+abs(ErrorTM);
279      ErrSumEM:=ErrSumEM+ErrorEM;
280      AbsErrSumEM:=AbsErrSumEM+abs(ErrorEM);
281      j:=j+1; {count the number of output lines}
282      END; {PrintResults}
283
284      BEGIN {OutputNvsf}
285      IF (fPrime=fMin) THEN
286
287      BEGIN {IF}
288      PrintTitles;
289      ErrSumTE:=0; {initialize integrated errors}
290      ErrSumTM:=0;
291      ErrSumEM:=0;
292      AbsErrSumTE:=0; {initialize absolute int errors}
293      AbsErrSumTM:=0;
294      AbsErrSumEM:=0;
295      j:=0; {initialize output line counter}
296      END; {IF}
297
298      PrintResults;
299      IF (fPrime=fMax-StepSize) THEN
300

```

MODIST Cont'd.

```

301 BEGIN {IF}
302   Writeln (' _____
303            |_____
304            |_____
305            |_____');
306   Writeln;
307   Writeln (' AVERAGE ERRORS: ',
308            (ErrSumTE/j):21:2,
309            (ErrSumTM/j):27:2,
310            (ErrSumEM/j):27:2);
311   Writeln (' AVERAGE ABSOLUTE ERRORS: ',
312            (AbsErrSumTE/j):12:2,
313            (AbsErrSumTM/j):27:2,
314            (AbsErrSumEM/j):27:2);
315 END; {IF}
316
317 END; {OutputNvsf}
318
319 PROCEDURE OutputDvsf(Method: 1..2);
320 {
321 { Tabulates the number of modes aluated spectral density
322 { the approximate formulae and from the differential form
323 { of the approximate formulae.
324 {
325 {
326 {
327 VAR deltaTE,deltaTM,deltaEM: real; {values of D}
328
329 PROCEDURE PrintTitles;
330 {
331 { Prints column headers for table.
332 {
333 {
334 {
335 BEGIN (PrintTitles)
336   Writeln (' _____
337            |_____
338            |_____
339            |_____');
340   Writeln (' :12, :27, :27, :27);
341   Writeln (' FREQUENCY
342            NUMBER OF TE MODES
343            NUMBER OF TM MODES
344            NUMBER OF EM MODES | ');
345   Writeln (' _____
346            |_____
347            |_____
348            |_____');
349   Writeln (' :9, :9, :9,
350            :9, :9, :9,
351            :9, :9, :9);
352   Writeln (' (HERTZ)
353            EXACT APPROX ERROR
354            EXACT APPROX ERROR
355            EXACT APPROX ERROR | ');
356   Writeln (' _____
357            |_____
358            |_____
359            |_____
360            |_____');

```

MODIST Cont'd.

```

361       Writeln ('|', '|':12, '|':27, '|':27, '|':27);
362       END; {PrintTitles}
363
364     PROCEDURE PrintDifferences;
365     {
366     {-----}
367     { Uses the difference relations to compute deltaN.
368     {-----}
369     }
370     BEGIN {PrintDifferences}
371       deltaTE:=NTE(fTwo)-NTE(fOne);
372       deltaTM:=NTM(fTwo)-NTM(fOne);
373       deltaEM:=NEM(fTwo)-NEM(fOne);
374       ErrorTE:=TE-deltaTE;
375       ErrorTM:=TM-deltaTM;
376       ErrorEM:=EM-deltaEM;
377       Write ('|', fOne:10, '|');
378       Write ('|', TE:5, '|', deltaTE:5:2, '|');
379       Write ('|', ErrorTE:7:2, '|');
380       Write ('|', TM:5, '|', deltaTM:5:2, '|');
381       Write ('|', ErrorTM:7:2, '|');
382       Write ('|', EM:5, '|', deltaEM:5:2, '|');
383       Write ('|', ErrorEM:7:2, '|');
384       Writeln;
385       ErrSumTE:=ErrSumTE+ErrorTE;
386       AbsErrSumTE:=AbsErrSumTE+abs(ErrorTE);
387       ErrSumTM:=ErrSumTM+ErrorTM;
388       AbsErrSumTM:=AbsErrSumTM+abs(ErrorTM);
389       ErrSumEM:=ErrSumEM+ErrorEM;
390       AbsErrSumEM:=AbsErrSumEM+abs(ErrorEM);
391       k:=k+1;
392     END; {PrintDifferences}
393
394     PROCEDURE PrintDifferentials;
395     {
396     {-----}
397     { Uses the differential relations to compute D.
398     {-----}
399     }
400     BEGIN {PrintDifferentials}
401       deltaTE:=DTE(fOne,bandwidth);
402       deltaTM:=DTM(fOne,bandwidth);
403       deltaEM:=DEM(fOne,bandwidth);
404       ErrorTE:=TE-deltaTE;
405       ErrorTM:=TM-deltaTM;
406       ErrorEM:=EM-deltaEM;
407       Write ('|', fOne:10, '|');
408       Write ('|', TE:5, '|', deltaTE:5:2, '|');
409       Write ('|', ErrorTE:7:2, '|');
410       Write ('|', TM:5, '|', deltaTM:5:2, '|');
411       Write ('|', ErrorTM:7:2, '|');
412       Write ('|', EM:5, '|', deltaEM:5:2, '|');
413       Write ('|', ErrorEM:7:2, '|');
414       Writeln;
415       ErrSumTE:=ErrSumTE+ErrorTE;
416       AbsErrSumTE:=AbsErrSumTE+abs(ErrorTE);
417       ErrSumTM:=ErrSumTM+ErrorTM;
418       AbsErrSumTM:=AbsErrSumTM+abs(ErrorTM);
419       ErrSumEM:=ErrSumEM+ErrorEM;
420       AbsErrSumEM:=AbsErrSumEM+abs(ErrorEM);

```

MODIST Cont'd.

```

421         k:=k+1;
422         END; {PrintDifferentials}
423
424     BEGIN {OutputDvsf}
425     IF (fPrime=fMin) THEN
426
427         BEGIN {IF}
428         IF (Method=1) THEN
429
430             BEGIN {IF}
431             Writeln ('          D versus Frequency Data ');
432             Writeln ('          (Calculated from Differences:');
433             Writeln;
434             END {IF}
435
436         ELSE
437
438             BEGIN {IF}
439             Writeln ('          D versus Frequency Data ');
440             Writeln ('          (Calculated from Differentials:');
441             Writeln;
442             END; {IF}
443
444             PrintTitles;
445             ErrSumTE:=0; {initialize integrated errors}
446             ErrSumTM:=0;
447             ErrSumEM:=0;
448             AbsErrSumTE:=0; {initialize absolute int errors}
449             AbsErrSumTM:=0;
450             AbsErrSumEM:=0;
451             k:=0; {initialize output line counter}
452         END; {IF}
453
454     IF (Method=1) THEN PrintDifferences
455     ELSE PrintDifferentials;
456     IF (fPrime=fMax-StepSize) THEN
457
458         BEGIN {IF}
459         Writeln ('
460
461
462
463
464
465
466
467
468
469
470
471
472
473
474
475
476
477
478
479
480

```

MODIST Cont'd.

```

481         fPrime:=fMin; {initialize fPrime}
482     REPEAT
483         fOne:=0; {set 1st marker}
484         fTwo:=fPrime+StepSize; {set 2nd marker}
485         TE:=0; {initialize TE mode counter}
486         TM:=0; {initialize TM mode counter}
487         EM:=0; {initialize total mode counter}
488         CountModes(fOne,fTwo); {find N}
489         OutputNvsf; {print values in a table}
490         fPrime:=fPrime+StepSize; {increment fPrime}
491     UNTIL fPrime>=fMax
492 END {IF}
493
494 ELSE FOR i:=1 TO 2 DO
495
496     BEGIN {FOR}
497         fPrime:=fMin; {initialize fPrime}
498     REPEAT
499         fOne:=fPrime; {set 1st marker}
500         fTwo:=fPrime+bandwidth; {set 2nd marker}
501         TE:=0; {initialize TE mode counter}
502         TM:=0; {initialize TM mode counter}
503         EM:=0; {initialize N}
504         CountModes(fOne,fTwo); {find N}
505         OutputDvsf(i); {print values in a table}
506         fPrime:=fPrime+StepSize; {increment fPrime}
507     UNTIL fPrime>=fMax
508 END; {FOR}
509
510     END; {GenerateData}
511
512 BEGIN
513     Readln(Lx,Ly,Lz,fMin,fMax,StepSize,bandwidth);
514     Writeln('The input parameters used in this run are:');
515     Writeln:
516     Writeln('Lx,Ly,Lz = ',42,Lx:5,' m, ',Ly:5,' m, ',Lz:5,' m');
517     Writeln('fMin,fMax = ',42,fMin:5,' Hz, ',fMax:5,' Hz');
518     Writeln('StepSize = ',42,StepSize:5,' Hz');
519     Writeln('bandwidth = ',42,bandwidth:5,' Hz');
520     Writeln:
521     ComputeVSL;
522     GenerateData
523 END; {ModeDistribution}
524 $ENTRY
525 0.23
526 0.50
527 0.52
528 4.0E8
529 1.3E9
530 5000000
531 50000000

```

End of file

A.3 CARETAB

```

10 REM =====
20 REM          PROGRAM: CARETAB      VERSION: 1.1      REVISED: AUGUST 08, 1984
30 REM =====
40 REM
50 REM          PURPOSE: To calculate the conceivable number of TE, TM and EM
60 REM                    modes in a (computed) series of rectangular cavities
70 REM                    within a given bandwidth.
80 REM          NOTES: The mode count results are sorted into four types:
90 REM                    1. TS, the total number of (mathematical) solutions
100 REM                       to the dispersion relation.
110 REM                    2. NL, the total number of non-longitudinal solutions
120 REM                       only (as given by MacKay, et.al.).
130 REM                    3. TE, the true number of Transverse Electric modes.
140 REM                    4. TM, the true number of Transverse Magnetic modes.
150 REM                    Run with DOS Version 1.1 using the advanced interpreter.
160 REM                    Allocate 32 Kbytes of RAM to the flashdisk.
170 REM =====
180 REM
190 REM          Definitions and Dimensions (constants, variables, arrays)
200 REM =====
210 DEFSTR A 'character string (esp. user responses entered from keyboard)
220 DEFSNG B,C,D,F,H,U,V,W,X,Y,Z 'single precision (real variables)
230 DEFINT E,G,I,J,K,L,M,N,O,P,Q,R,S,T 'integer (counters, integer variables)
240 DIM CAVS(500,3) 'contains dimensions of each cavity tested
250 DIM MODS(500,5) 'contains results of the various mode counts
260 DIM MAXTE(100) 'contains indices of CAVS and MODS (max. no. of TE modes)
270 DIM MAXTM(100) 'contains indices of CAVS and MODS (max. no. of TM modes)
280 DIM MAXEM(100) 'contains indices of CAVS and MODS (max. no. of EM modes)
290 LET HZ=1000000! 'MHz to Hz conversion factor
300 LET C=3E+10 'speed of light in free space (cm/s)
310 REM =====
320 REM          Initialization (counters, array indices, files, pointers)
330 REM =====
340 P=1: Q=1 'indices used in arrays CAVS and MODS (for storing and printing)
350 S=1: T=0 'output device number and number of lines printed to that file
360 PL=0: RL=0 'logical variables used to direct program flow
370 TEM=0: TMM=0: EMM=0 'reference mode counts used in MAXTE, MAXTM, MAXEM
380 TEC=0: TMC=0: EMC=0 'counters and indices used in MAXTE, MAXTM, MAXEM
390 OPEN "SCRN:" FOR OUTPUT AS #1 'establish CRT screen as output device
400 OPEN "C:TEMP" FOR APPEND AS #2 'establish flash disk as output device
410 OPEN "C:TEMP" FOR INPUT AS #3 'establish flash disk as input device
420 OPEN "COM1:300,N,8" AS #4 'establish printer as output device via COM1
430 ON KEY(1) GOSUB 1380 'interrupts program after completing current cavity
440 REM =====
450 REM          Entry of Input Parameters From Keyboard
460 REM =====
470 KEY OFF: BEEP: CLS 'erase soft key definitions and clear screen
480 READ X1,X2,XS,Y1,Y2,YS,Z1,Z2,ZS,F1,F2 'read default data
490 DATA 20,23,1,20,23,1,20,23,1,900,930, 'short-execution demo data
500 DATA 48.5,51.5,0.5,38.5,41.5,0.5,38.5,41.5,0.5,2425,2475, 'Puschner's data
510 INPUT "New data? ", A1: IF NOT(LEFT$(A1,1)="y") THEN 700 'or default data
520 PRINT: PRINT TAB(20) "NOTE: Large bandwidths and/or ranges for X,Y,Z"
530 PRINT TAB(28) "will lead to VERY long execution times!": PRINT: PRINT
540 REM some rudimentary error trapping is provided to catch likely typos
550 INPUT "Enter FIRST target value for X|0 in cm...", X1: IF X1[=0 THEN 550
560 INPUT "Enter LAST target value for X|0 in cm...", X2: IF X2[=0 THEN 560
570 IF (X1|X2) THEN PRINT: PRINT "X2 must not be less than X1!": GOTO 550
580 INPUT "Enter STEPSIZE (|0) for X in cm...", XS: PRINT: IF XS[=0 THEN 580
590 INPUT "Enter FIRST target value for Y|0 in cm...", Y1: IF Y1[=0 THEN 590
600 INPUT "Enter LAST target value for Y|0 in cm...", Y2: IF Y2[=0 THEN 600
610 IF (Y1|Y2) THEN PRINT: PRINT "Y2 must not be less than Y1!": GOTO 550
620 INPUT "Enter STEPSIZE (|0) for Y in cm...", YS: PRINT: IF YS[=0 THEN 620

```


CARETAB Cont'd.

```

630 INPUT "Enter FIRST target value for Z|0 in cm...", Z1: IF Z1[=0 THEN 630
640 INPUT "Enter LAST target value for Z|0 in cm...", Z2: IF Z2[=0 THEN 640
650 IF (Z1|Z2) THEN PRINT: PRINT "Z2 must not be less than Z1!": GOTO 550
660 INPUT "Enter STEPSIZE (|0) for Z in cm...", ZS: PRINT: IF ZS[=0 THEN 660
670 INPUT "Enter LOWEST frequency (=|0) of BW in MHz...", F1: IF F1[0 THEN 670
680 INPUT "Enter HIGHEST frequency (|0) of BW in MHz...", F2
690 IF (F1|F2) THEN PRINT: PRINT "F1 must be greater than F2!": GOTO 670
700 CLS: LOCATE 25,10: COLOR 0,7 'position cursor and change to reverse video
710 PRINT " Press F1 to interrupt program after computing next cavity. ";
720 COLOR 7,0: PRINT: LOCATE 1,1: BEEP 'reset font and reposition cursor
730 REM =====
740 REM      Storage and Printing of Current Cavity Dimensions
750 REM =====
760 FOR X=X1 TO X2 STEP XS: FOR Y=Y1 TO Y2 STEP YS 'X and Y dimension loops
770 REM space 1 line and print column headers every ZS rows
780 PRINT: PRINT TAB(2) "X(cm)" TAB(10) "Y(cm)" TAB(18) "Z(cm)";
790 PRINT TAB(31) "TS" TAB(37) "NL" TAB(43) "TE" TAB(49) "TM" TAB(55) "EM"
800 PRINT: PRINT USING "###.## "; X;Y; 'print the X and Y dimensions
810 FOR Z=Z1 TO Z2 STEP ZS 'Z dimension loop
820 CAVS(P,1)=X: CAVS(P,2)=Y: CAVS(P,3)=Z 'store the current cavity dimensions
830 PRINT TAB(17);: PRINT USING "###.## "; Z; 'print the Z dimension
840 KEY(1) ON: KEY(1) STOP 'trap F1 and execute before starting next loop
850 REM =====
860 REM      Calculation of Resonant Frequency
870 REM =====
880 TS=0: NL=0: TE=0: TM=0: TIMES="00" 'reset all mode counters and timer
890 FOR L=0 TO FIX(X*2*F2*HZ/C)+1 STEP 1 'first mode index
900 FOR M=0 TO FIX(Y*2*F2*HZ/C)+1 STEP 1 'second mode index
910 FOR N=0 TO FIX(Z*2*F2*HZ/C)+1 STEP 1 'third mode index
920 F=(C/2)*SQR(((L/X)^2)+((M/Y)^2)+((N/Z)^2))/HZ 'resonant frequency in MHz
930 REM =====
940 REM      Mode Sorting and Counting
950 REM =====
960 REM count the total number of (mathematical) solutions to equation for F.
970 IF (F|F1) OR (F|F2) THEN 1030 ELSE TS=TS+1 'ignore if F is out of range
980 REM count the non-longitudinal modes (as Mackay, et al.)
990 IF (L|0 AND N|0) OR (M|0 AND N|0) OR (L|0 AND M|0) THEN NL=NL+1
1000 REM count TE and TM modes separately and combine them outside the loop
1010 IF (L|0 AND N|0) OR (M|0 AND N|0) THEN TE=TE+1 'count the TE modes
1020 IF (L|0 AND M|0) THEN TM=TM+1 'count the TM modes
1030 NEXT N,M,L
1040 EM=TE+TM 'compute the total number of electromagnetic modes
1050 REM =====
1060 REM      Identification of Cavities with Maximum Number of TE Modes
1070 REM =====
1080 IF TE[TEM THEN 1150 'continue if less than current maximum
1090 IF TE=TEM THEN 1100 ELSE TEC=0 'test for a tie and reset counter if not
1100 TEC=TEC+1: TEM=TE 'increment counter and establish TE as new maximum
1110 MAXTE(TEC)=P 'enter corresponding CAVS and MODS index in array MAXTE
1120 REM =====
1130 REM      Identification of Cavities with Maximum Number of TM Modes
1140 REM =====
1150 IF TM[TMM THEN 1220 'continue if less than current maximum
1160 IF TM=TMM THEN 1170 ELSE TMC=0 'test for a tie and reset counter if not
1170 TMC=TMC+1: TMM=TM 'increment counter and establish TM as new maximum
1180 MAXTM(TMC)=P 'enter corresponding CAVS and MODS index in array MAXTM
1190 REM =====
1200 REM      Identification of Cavities with Maximum Total Number of Modes
1210 REM =====
1220 IF (TE+TM)[EMM THEN 1290 'continue if less than current maximum
1230 IF EM=EMM THEN 1240 ELSE EMC=0 'test for a tie and reset counter if not
1240 EMC=EMC+1: EMM=EM 'increment counter and establish EM as new maximum

```

CARETAB Cont'd.

```

1250 MAXEM(EMC)=P 'enter corresponding CAVS and MODS index in array MAXEM
1260 REM =====
1270 REM      Storing and Printing of Results to the Screen
1280 REM =====
1290 MODS(P,1)=TS: MODS(P,2)=NL: MODS(P,3)=TE: MODS(P,4)=TM: MODS(P,5)=EM
1300 PRINT TAB(29);: PRINT USING "#### "; TS,NL,TE,TM,EM; 'print mode counts
1310 IF Z=Z1 THEN PRINT " ";TIMES ELSE PRINT 'print execution time once
1320 P=P+1 'increment array index (cavity counter)
1330 NEXT Z,Y,X
1340 REM =====
1350 REM      (Optional) Storage of Mode Count Results in file C:TEMP
1360 REM =====
1370 REM disable trapping and ask whether or not storage is required
1380 GOSUB 1960: IF PL THEN GOTO 1540 ELSE S=2 'device #2 is file TEMP
1390 FOR I=1 TO P-1 STEP 1+PIX((Z2-Z1)/ZS) 'intervals for column headers
1400 PRINT#S, 'blank line
1410 PRINT#S,TAB(12) "X(cm)" TAB(20) "Y(cm)" TAB(28) "Z(cm)"; 'column headers
1420 PRINT#S,TAB(41) "TS" TAB(47) "NL" TAB(53) "TE" TAB(59) "TM" TAB(65) "EM"
1430 PRINT#S,: PRINT#S,TAB(11); 'blank line, position cursor
1440 PRINT#S,USING "###.## "; CAVS(Q,1);CAVS(Q,2); 'print X and Y
1450 FOR J=0 TO FIX((Z2-Z1)/ZS) STEP 1 'line items per interval
1460 PRINT#S,TAB(27): PRINT#S,USING "###.## "; CAVS(Q,3); 'print Z
1470 PRINT#S,TAB(39); 'tab and print mode count results
1480 PRINT#S,USING "#### "; MODS(Q,1),MODS(Q,2),MODS(Q,3),MODS(Q,4),MODS(Q,5)
1490 Q=Q+1 'increment array index
1500 NEXT J,I
1510 REM =====
1520 REM      Printing of Cavities Identified Above
1530 REM =====
1540 S=1 'reset output device switch S to screen
1550 PRINT#S,"The cavities which support the most TE modes are:": GOSUB 2310
1560 PRINT#S,: GOSUB 2310 'call PAGEPAUSE to check line count after each line
1570 FOR I=1 TO TEC STEP 1 'print cavities with the most TE modes
1580 PRINT#S, TAB(5); 'tab and print dimensions of TE cavities
1590 PRINT#S," X=";: PRINT#S,USING "###.##"; CAVS(MAXTE(I),1);: PRINT#S," cm";
1600 PRINT#S," Y=";: PRINT#S,USING "###.##"; CAVS(MAXTE(I),2);: PRINT#S," cm";
1610 PRINT#S," Z=";: PRINT#S,USING "###.##"; CAVS(MAXTE(I),3);: PRINT#S," cm"
1620 GOSUB 2310: NEXT I
1630 PRINT#S,: GOSUB 2310: PRINT#S,"      Each cavity supports";
1640 PRINT#S,USING "####"; MODS(MAXTE(TEC),3);: PRINT#S," TE modes."
1650 GOSUB 2310: PRINT#S,: GOSUB 2310: PRINT#S,: GOSUB 2310 'blank lines
1660 PRINT#S,"The cavities which support the most TM modes are:": GOSUB 2310
1670 PRINT#S,: GOSUB 2310
1680 FOR I=1 TO TMC STEP 1 'print cavities with the most TM modes
1690 PRINT#S, TAB(5); 'tab and print dimensions of TM cavities
1700 PRINT#S," X=";: PRINT#S,USING "###.##"; CAVS(MAXTM(I),1);: PRINT#S," cm";
1710 PRINT#S," Y=";: PRINT#S,USING "###.##"; CAVS(MAXTM(I),2);: PRINT#S," cm";
1720 PRINT#S," Z=";: PRINT#S,USING "###.##"; CAVS(MAXTM(I),3);: PRINT#S," cm"
1730 GOSUB 2310: NEXT I
1740 PRINT#S,: GOSUB 2310: PRINT#S,"      Each cavity supports";
1750 PRINT#S,USING "####"; MODS(MAXTM(TMC),4);: PRINT#S," TM modes."
1760 GOSUB 2310: PRINT#S,: GOSUB 2310: PRINT#S,: GOSUB 2310 'blank lines
1770 PRINT#S,"The cavities which support the most EM modes are:": GOSUB 2310
1780 PRINT#S,: GOSUB 2310
1790 FOR I=1 TO EMC STEP 1 'print cavities with the most EM modes
1800 PRINT#S, TAB(5); 'tab and print dimensions of EM cavities
1810 PRINT#S," X=";: PRINT#S,USING "###.##"; CAVS(MAXEM(I),1);: PRINT#S," cm";
1820 PRINT#S," Y=";: PRINT#S,USING "###.##"; CAVS(MAXEM(I),2);: PRINT#S," cm";
1830 PRINT#S," Z=";: PRINT#S,USING "###.##"; CAVS(MAXEM(I),3);: PRINT#S," cm"
1840 GOSUB 2310: NEXT I
1850 PRINT#S,: GOSUB 2310: PRINT#S,"      Each cavity supports";
1860 PRINT#S,USING "####"; MODS(MAXEM(EMC),5);: PRINT#S," EM modes."

```

CARETAB Cont'd.

```

1870 GOSUB 2310: PRINT#S,: GOSUB 2310: PRINT#S,: GOSUB 2310 'blank lines
1880 IF S=2 THEN 1900 ELSE GOSUB 1970 'ask if storage in file TEMP is required
1890 IF PL THEN 1900 ELSE S=2: GOTO 1550 'rewrite results to file C:TEMP
1900 GOSUB 2100
1910 KEY ON 'replace soft key definitions
1920 END
1930 REM =====
1940 REM          SUBROUTINE SOFTCOPY
1950 REM =====
1960 KEY(1) OFF 'disable F1 trapping on first call
1970 BEEP: LOCATE 25,1: PRINT STRING$(80,0); 'get attention, clear prompt line
1980 LOCATE 25,14: COLOR 0,7 'position cursor and change to reverse video font
1990 PRINT " Do you want these results saved in the file C:TEMP? "; 'prompt
2000 COLOR 7,0 'return to normal video font
2010 INPUT " ", A2: A2=LEFT$(A2,1) 'examine first character of response A2
2020 LOCATE 25,1: PRINT STRING$(80,0); 'clear prompt line
2030 IF (A2="Y") OR (A2="y") THEN PL=0: RL=1: RETURN 'storage required
2040 IF (A2="N") OR (A2="n") THEN PL=1: RETURN 'storage not required
2050 PRINT "Please answer YES or NO (Y or N).": PRINT: GOTO 1970 'instructions
2060 RETURN
2070 REM =====
2080 REM          SUBROUTINE HARDCOPY
2090 REM =====
2100 IF RL=0 THEN RETURN 'check whether or not any results have been stored
2110 BEEP: LOCATE 25,1: PRINT STRING$(80,0); 'get attention, clear prompt line
2120 LOCATE 25,14: COLOR 0,7 'position cursor and change to reverse video font
2130 PRINT " Do you want these results sent to the printer? ";
2140 COLOR 7,0 'return to normal video font
2150 INPUT " ", A2: A2=LEFT$(A2,1) 'examine first character of response A2
2160 LOCATE 25,1: PRINT STRING$(80,0); 'clear prompt line
2170 IF (A2="Y") OR (A2="y") THEN S=4: GOTO 2200 'set device switch to printer
2180 IF (A2="N") OR (A2="n") THEN RETURN 'continue if no printing required
2190 PRINT "Please answer YES or NO (Y or N).": PRINT: GOTO 2110 'instructions
2200 BEEP: LOCATE 25,1: PRINT STRING$(80,0); 'get attention, clear prompt line
2210 LOCATE 25,14: COLOR 0,7 'position cursor and change to reverse video font
2220 PRINT " Turn the printer on and strike the SPACE BAR to start printing. ";
2230 A3=INKEY$: IF NOT(A3=CHR$(32)) THEN 2230 'pause until space bar is struck
2240 COLOR 7,0: PRINT; 'return to normal video font
2250 LOCATE 25,1: PRINT STRING$(80,0); 'clear prompt line
2260 WHILE NOT EOF(3): LINE INPUT#3,A4: PRINT#S,A4: GOSUB 2310: WEND
2270 RETURN
2280 REM =====
2290 REM          SUBROUTINE PAGEPAUSE
2300 REM =====
2310 IF S=1 AND T=|21 THEN 2340 'pause when CRT screen is full
2320 IF S=2 OR S=3 THEN RETURN 'ignore call
2330 IF S=4 AND T=|53 THEN PRINT#S,STRING$(11,10): GOTO 2340 ELSE T=T+1: RETURN
2340 BEEP: LOCATE 25,1: PRINT STRING$(80,0); 'beep attention, clear prompt line
2350 LOCATE 25,22: COLOR 0,7 'position cursor and change to reverse video font
2360 PRINT " Strike the SPACE BAR to continue. "; 'prompt
2370 A5=INKEY$: IF NOT(A5=CHR$(32)) THEN 2370 'pause until space bar is struck
2380 COLOR 7,0: PRINT 'return to normal video font
2390 LOCATE 25,1: PRINT STRING$(80,0) 'clear prompt line
2400 T=0 'reset line counter
2410 RETURN
2420 END

```

APPENDIX B. CAVITY MODE COUNT REFERENCE TABLES

Table B.1 Numerically determined mode count reference data for several rectangular cavities excited by frequencies within the range $2425 \leq f \leq 2475$ MHz. TS is the total number of mathematical solutions to the dispersion relation; NL is the number of nonlongitudinal modes; TE and TM are the actual numbers of TE and TM modes respectively; EM is the total number of electromagnetic modes.

X(cm) Y(cm) Z(cm) TS NL TE TM EM	X(cm) Y(cm) Z(cm) TS NL TE TM EM
48.50 38.50 38.50 14 13 12 10 22	48.50 39.00 38.50 15 14 12 11 23
39.00 15 14 13 10 23	39.00 18 17 15 11 26
39.50 17 16 15 10 25	39.50 17 16 14 10 24
40.00 21 20 19 14 33	40.00 20 19 17 13 30
40.50 18 17 16 14 30	40.50 17 16 14 14 28
41.00 15 14 13 11 24	41.00 13 12 10 11 21
41.50 14 13 12 10 22	41.50 13 12 10 11 21
X(cm) Y(cm) Z(cm) TS NL TE TM EM	X(cm) Y(cm) Z(cm) TS NL TE TM EM
48.50 39.50 38.50 17 16 13 12 25	48.50 40.00 38.50 21 20 17 16 33
39.00 17 16 13 11 24	39.00 20 19 16 14 30
39.50 16 15 12 10 22	39.50 19 18 15 15 30
40.00 19 18 15 15 30	40.00 19 18 15 15 30
40.50 18 17 14 16 30	40.50 17 16 13 15 28
41.00 15 14 11 12 23	41.00 15 14 11 12 23
41.50 16 15 12 14 26	41.50 16 15 12 14 26
X(cm) Y(cm) Z(cm) TS NL TE TM EM	X(cm) Y(cm) Z(cm) TS NL TE TM EM
48.50 40.50 38.50 18 17 16 14 30	48.50 41.00 38.50 15 14 13 11 24
39.00 17 16 15 13 28	39.00 13 12 11 10 21
39.50 18 17 16 14 30	39.50 15 14 13 10 23
40.00 17 16 15 13 28	40.00 15 14 13 10 23
40.50 13 12 11 11 22	40.50 12 11 10 9 19
41.00 12 11 10 9 19	41.00 13 12 11 9 20
41.50 13 12 11 10 21	41.50 13 12 11 10 21
X(cm) Y(cm) Z(cm) TS NL TE TM EM	X(cm) Y(cm) Z(cm) TS NL TE TM EM
48.50 41.50 38.50 14 13 13 9 22	49.00 38.50 38.50 16 15 14 12 26
39.00 13 12 12 9 21	39.00 18 17 16 13 29
39.50 16 15 15 11 26	39.50 18 17 16 11 27
40.00 16 15 15 11 26	40.00 19 18 17 14 31
40.50 13 12 12 9 21	40.50 18 17 16 15 31
41.00 13 12 12 9 21	41.00 14 13 12 11 23
41.50 11 10 10 10 20	41.50 16 15 14 12 26

Table B.1 Cont'd.

X (cm) Y (cm) Z (cm) TS NL TE TM EM	X (cm) Y (cm) Z (cm) TS NL TE TM EM
49.00 39.00 38.50 18 17 15 14 29	49.00 39.50 38.50 18 17 14 13 27
39.00 18 17 15 11 26	39.00 19 18 15 13 28
39.50 19 18 16 12 28	39.50 19 18 15 13 28
40.00 20 19 17 15 32	40.00 17 16 13 15 28
40.50 15 14 12 13 25	40.50 16 15 12 15 27
41.00 12 11 9 11 20	41.00 13 12 9 11 20
41.50 14 13 11 12 23	41.50 16 15 12 14 26
X (cm) Y (cm) Z (cm) TS NL TE TM EM	X (cm) Y (cm) Z (cm) TS NL TE TM EM
49.00 40.00 38.50 19 18 17 14 31	49.00 40.50 38.50 18 17 17 14 31
39.00 20 19 18 14 32	39.00 15 14 14 11 25
39.50 17 16 15 13 28	39.50 16 15 15 12 27
40.00 13 12 11 11 22	40.00 12 11 11 10 21
40.50 12 11 10 11 21	40.50 12 11 11 11 22
41.00 13 12 11 11 22	41.00 11 10 10 9 19
41.50 14 13 12 12 24	41.50 14 13 13 11 24
X (cm) Y (cm) Z (cm) TS NL TE TM EM	X (cm) Y (cm) Z (cm) TS NL TE TM EM
49.00 41.00 38.50 14 13 13 10 23	49.00 41.50 38.50 16 15 15 11 26
39.00 12 11 11 9 20	39.00 14 13 13 10 23
39.50 13 12 12 8 20	39.50 16 15 15 11 26
40.00 13 12 12 10 22	40.00 14 13 13 11 24
40.50 11 10 10 9 19	40.50 14 13 13 11 24
41.00 11 10 10 8 18	41.00 12 11 11 9 20
41.50 12 11 11 9 20	41.50 11 10 10 10 20
X (cm) Y (cm) Z (cm) TS NL TE TM EM	X (cm) Y (cm) Z (cm) TS NL TE TM EM
49.50 38.50 38.50 17 17 15 13 28	49.50 39.00 38.50 16 16 14 12 26
39.00 16 16 14 12 26	39.00 15 15 13 9 22
39.50 17 17 15 11 26	39.50 17 17 15 11 26
40.00 19 19 17 14 31	40.00 18 18 16 13 29
40.50 17 17 15 14 29	40.50 14 14 12 12 24
41.00 12 12 10 9 19	41.00 9 9 7 8 15
41.50 15 15 13 11 24	41.50 12 12 10 10 20
X (cm) Y (cm) Z (cm) TS NL TE TM EM	X (cm) Y (cm) Z (cm) TS NL TE TM EM
49.50 39.50 38.50 17 17 14 12 26	49.50 40.00 38.50 19 19 17 14 31
39.00 17 17 14 12 26	39.00 18 18 16 13 29
39.50 18 18 15 13 28	39.50 15 15 13 12 25
40.00 15 15 12 13 25	40.00 15 15 13 13 26
40.50 13 13 10 12 22	40.50 13 13 11 12 23
41.00 13 13 10 11 21	41.00 13 13 11 11 22
41.50 14 14 11 12 23	41.50 16 16 14 14 28

Table B.1 Cont'd.

X(cm) Y(cm) Z(cm) TS NL TE TM EM	X(cm) Y(cm) Z(cm) TS NL TE TM EM
49.50 40.50 38.50 17 17 16 13 29	49.50 41.00 38.50 12 12 11 8 19
39.00 14 14 13 11 24	39.00 9 9 8 7 15
39.50 13 13 12 10 22	39.50 13 13 12 9 21
40.00 13 13 12 11 23	40.00 13 13 12 10 22
40.50 8 8 7 7 14	40.50 10 10 9 8 17
41.00 10 10 9 8 17	41.00 10 10 9 7 16
41.50 13 13 12 10 22	41.50 12 12 11 9 20
X(cm) Y(cm) Z(cm) TS NL TE TM EM	X(cm) Y(cm) Z(cm) TS NL TE TM EM
49.50 41.50 38.50 15 15 14 10 24	50.00 38.50 38.50 16 16 14 12 26
39.00 12 12 11 9 20	39.00 16 16 14 12 26
39.50 14 14 13 10 23	39.50 17 17 15 12 27
40.00 16 16 15 13 28	40.00 17 17 15 13 28
40.50 13 13 12 10 22	40.50 16 16 14 13 27
41.00 12 12 11 9 20	41.00 13 13 11 10 21
41.50 12 12 11 11 22	41.50 17 17 15 13 28
X(cm) Y(cm) Z(cm) TS NL TE TM EM	X(cm) Y(cm) Z(cm) TS NL TE TM EM
50.00 39.00 38.50 16 16 14 12 26	50.00 39.50 38.50 17 17 15 12 27
39.00 18 18 16 12 28	39.00 17 17 15 12 27
39.50 17 17 15 12 27	39.50 14 14 12 10 22
40.00 18 18 16 14 30	40.00 14 14 12 13 25
40.50 13 13 11 11 22	40.50 12 12 10 11 21
41.00 11 11 9 10 19	41.00 13 13 11 11 22
41.50 14 14 12 12 24	41.50 15 15 13 13 26
X(cm) Y(cm) Z(cm) TS NL TE TM EM	X(cm) Y(cm) Z(cm) TS NL TE TM EM
50.00 40.00 38.50 17 17 16 12 28	50.00 40.50 38.50 16 16 15 12 27
39.00 18 18 17 13 30	39.00 13 13 12 10 22
39.50 14 14 13 12 25	39.50 12 12 11 10 21
40.00 14 14 13 13 26	40.00 12 12 11 11 22
40.50 12 12 11 11 22	40.50 11 11 10 10 20
41.00 12 12 11 10 21	41.00 11 11 10 9 19
41.50 14 14 13 12 25	41.50 11 11 10 8 18
X(cm) Y(cm) Z(cm) TS NL TE TM EM	X(cm) Y(cm) Z(cm) TS NL TE TM EM
50.00 41.00 38.50 13 13 12 9 21	50.00 41.50 38.50 17 17 16 12 28
39.00 11 11 10 9 19	39.00 14 14 13 11 24
39.50 13 13 12 10 22	39.50 15 15 14 12 26
40.00 12 12 11 10 21	40.00 14 14 13 12 25
40.50 11 11 10 9 19	40.50 11 11 10 8 18
41.00 11 11 10 8 18	41.00 14 14 13 11 24
41.50 14 14 13 11 24	41.50 13 13 12 12 24

Table B.1 Cont'd.

X (cm)	Y (cm)	Z (cm)	TS	NL	TE	TM	EM	X (cm)	Y (cm)	Z (cm)	TS	NL	TE	TM	EM
50.50	38.50	38.50	12	12	11	9	20	50.50	39.00	38.50	12	12	10	9	19
		39.00	12	12	11	8	19			39.00	15	15	13	9	22
		39.50	13	13	12	9	21			39.50	15	15	13	11	24
		40.00	13	13	12	10	22			40.00	15	15	13	12	25
		40.50	12	12	11	10	21			40.50	12	12	10	11	21
		41.00	10	10	9	8	17			41.00	12	12	10	12	22
		41.50	15	15	14	11	25			41.50	14	14	12	12	24
X (cm)	Y (cm)	Z (cm)	TS	NL	TE	TM	EM	X (cm)	Y (cm)	Z (cm)	TS	NL	TE	TM	EM
50.50	39.50	38.50	13	13	12	9	21	50.50	40.00	38.50	13	13	13	9	22
		39.00	15	15	14	10	24			39.00	15	15	15	10	25
		39.50	14	14	13	11	24			39.50	11	11	11	10	21
		40.00	11	11	10	11	21			40.00	10	10	10	10	20
		40.50	10	10	9	10	19			40.50	9	9	9	9	18
		41.00	12	12	11	11	22			41.00	11	11	11	10	21
		41.50	15	15	14	13	27			41.50	14	14	14	12	26
X (cm)	Y (cm)	Z (cm)	TS	NL	TE	TM	EM	X (cm)	Y (cm)	Z (cm)	TS	NL	TE	TM	EM
50.50	40.50	38.50	12	12	12	9	21	50.50	41.00	38.50	10	10	10	7	17
		39.00	12	12	12	9	21			39.00	12	12	12	10	22
		39.50	10	10	10	9	19			39.50	12	12	12	10	22
		40.00	9	9	9	9	18			40.00	11	11	11	10	21
		40.50	9	9	9	9	18			40.50	10	10	10	9	19
		41.00	10	10	10	9	19			41.00	11	11	11	9	20
		41.50	12	12	12	9	21			41.50	13	13	13	10	23
X (cm)	Y (cm)	Z (cm)	TS	NL	TE	TM	EM	X (cm)	Y (cm)	Z (cm)	TS	NL	TE	TM	EM
50.50	41.50	38.50	15	15	14	11	25	51.00	38.50	38.50	12	12	11	9	20
		39.00	14	14	13	11	24			39.00	12	12	11	9	20
		39.50	15	15	14	13	27			39.50	16	16	15	11	
		40.00	14	14	13	13	26			40.00	15	15	14	11	
		40.50	12	12	11	10	21			40.50	14	14	13	11	24
		41.00	13	13	12	11	23			41.00	14	14	13	11	24
		41.50	11	11	10	10	20			41.50	17	17	16	12	28
X (cm)	Y (cm)	Z (cm)	TS	NL	TE	TM	EM	X (cm)	Y (cm)	Z (cm)	TS	NL	TE	TM	EM
51.00	39.00	38.50	12	12	11	9	20	51.00	39.50	38.50	16	16	14	12	26
		39.00	13	13	12	8	20			39.00	15	15	13	11	24
		39.50	15	15	14	10	24			39.50	19	19	17	15	32
		40.00	15	15	14	11	25			40.00	15	15	13	14	27
		40.50	12	12	11	10	21			40.50	14	14	12	13	25
		41.00	12	12	11	11	22			41.00	14	14	12	12	24
		41.50	14	14	13	11	24			41.50	17	17	15	14	29

Table B.1 Cont'd.

X (cm)	Y (cm)	Z (cm)	TS	NL	TE	TM	EM
51.00	40.00	38.50	15	15	14	11	25
		39.00	15	15	14	11	25
		39.50	15	15	14	13	27
		40.00	13	13	12	12	24
		40.50	10	10	9	9	18
		41.00	13	13	12	11	23
		41.50	15	15	14	12	26
X (cm)	Y (cm)	Z (cm)	TS	NL	TE	TM	EM
51.00	40.50	38.50	14	14	13	11	24
		39.00	12	12	11	10	21
		39.50	14	14	13	12	25
		40.00	10	10	9	9	18
		40.50	8	8	7	7	14
		41.00	10	10	9	8	17
		41.50	13	13	12	9	21
X (cm)	Y (cm)	Z (cm)	TS	NL	TE	TM	EM
51.00	41.00	38.50	14	14	13	11	24
		39.00	12	12	11	11	22
		39.50	14	14	13	11	24
		40.00	13	13	12	11	23
		40.50	10	10	9	8	17
		41.00	12	12	11	9	20
		41.50	14	14	13	10	23
X (cm)	Y (cm)	Z (cm)	TS	NL	TE	TM	EM
51.50	38.50	38.50	16	16	14	12	26
		39.00	16	16	14	12	26
		39.50	17	17	15	12	27
		40.00	17	17	15	13	28
		40.50	15	15	13	12	25
		41.00	17	17	15	14	29
		41.50	19	19	17	14	31
X (cm)	Y (cm)	Z (cm)	TS	NL	TE	TM	EM
51.50	39.00	38.50	16	16	14	12	26
		39.00	17	17	15	11	26
		39.50	18	18	16	13	29
		40.00	17	17	15	13	28
		40.50	13	13	11	11	22
		41.00	13	13	11	12	23
		41.50	16	16	14	13	27
X (cm)	Y (cm)	Z (cm)	TS	NL	TE	TM	EM
51.50	40.00	38.50	17	17	16	12	28
		39.00	17	17	16	12	28
		39.50	14	14	13	12	25
		40.00	10	10	9	9	18
		40.50	12	12	11	11	22
		41.00	13	13	12	11	23
		41.50	16	16	15	13	28
X (cm)	Y (cm)	Z (cm)	TS	NL	TE	TM	EM
51.50	40.50	38.50	15	15	14	11	25
		39.00	13	13	12	10	22
		39.50	12	12	11	10	21
		40.00	12	12	11	11	22
		40.50	12	12	11	11	22
		41.00	12	12	11	10	21
		41.50	14	14	13	10	23
X (cm)	Y (cm)	Z (cm)	TS	NL	TE	TM	EM
51.50	41.00	38.50	17	17	16	13	29
		39.00	13	13	12	11	23
		39.50	12	12	11	10	21
		40.00	13	13	12	11	23
		40.50	12	12	11	10	21
		41.00	16	16	15	13	28
		41.50	14	14	13	10	23

Table B.2 Numerically determined mode count reference data for several rectangular cavities excited by frequencies within the range $900 \leq f \leq 930$ MHz. TS is the total number of mathematical solutions to the dispersion relation; NL is the number of nonlongitudinal modes; TE and TM are the actual numbers of TE and TM modes respectively; EM is the total number of electromagnetic modes.

X(cm)	Y(cm)	Z(cm)	TS	NL	TE	TM	EM	X(cm)	Y(cm)	Z(cm)	TS	NL	TE	TM	EM
48.50	38.50	38.50	3	2	2	2	4	48.50	39.00	38.50	3	2	2	2	4
		39.00	3	2	2	2	4			39.00	3	2	2	2	4
		39.50	3	2	2	2	4			39.50	3	2	2	2	4
		40.00	2	1	1	1	2			40.00	2	1	1	1	2
		40.50	2	1	1	1	2			40.50	2	1	1	1	2
		41.00	2	1	1	1	2			41.00	2	1	1	1	2
		41.50	2	1	1	1	2			41.50	2	1	1	1	2
X(cm)	Y(cm)	Z(cm)	TS	NL	TE	TM	EM	X(cm)	Y(cm)	Z(cm)	TS	NL	TE	TM	EM
48.50	39.50	38.50	3	2	2	2	4	48.50	40.00	38.50	2	1	1	1	2
		39.00	3	2	2	2	4			39.00	2	1	1	1	2
		39.50	3	2	2	2	4			39.50	2	1	1	1	2
		40.00	2	1	1	1	2			40.00	1	0	0	0	0
		40.50	1	0	0	0	0			40.50	1	0	0	0	0
		41.00	1	0	0	0	0			41.00	1	0	0	0	0
		41.50	1	0	0	0	0			41.50	1	0	0	0	0
X(cm)	Y(cm)	Z(cm)	TS	NL	TE	TM	EM	X(cm)	Y(cm)	Z(cm)	TS	NL	TE	TM	EM
48.50	40.50	38.50	2	1	1	1	2	48.50	41.00	38.50	2	1	1	1	2
		39.00	2	1	1	1	2			39.00	2	1	1	1	2
		39.50	1	0	0	0	0			39.50	1	0	0	0	0
		40.00	1	0	0	0	0			40.00	1	0	0	0	0
		40.50	1	0	0	0	0			40.50	1	0	0	0	0
		41.00	1	0	0	0	0			41.00	1	0	0	0	0
		41.50	1	0	0	0	0			41.50	1	0	0	0	0
X(cm)	Y(cm)	Z(cm)	TS	NL	TE	TM	EM	X(cm)	Y(cm)	Z(cm)	TS	NL	TE	TM	EM
48.50	41.50	38.50	2	1	1	1	2	49.00	38.50	38.50	3	2	2	2	4
		39.00	2	1	1	1	2			39.00	3	2	2	2	4
		39.50	1	0	0	0	0			39.50	3	2	2	2	4
		40.00	1	0	0	0	0			40.00	2	1	1	1	2
		40.50	1	0	0	0	0			40.50	2	1	1	1	2
		41.00	1	0	0	0	0			41.00	2	1	1	1	2
		41.50	1	0	0	0	0			41.50	2	1	1	1	2

Table B.2 Cont'd.

X (cm)	Y (cm)	Z (cm)	TS	NL	TE	TM	EM	X (cm)	Y (cm)	Z (cm)	TS	NL	TE	TM	EM
49.00	39.00	38.50	3	2	2	2	4	49.00	39.50	38.50	3	2	2	2	4
		39.00	3	2	2	2	4			39.00	3	2	2	2	4
		39.50	3	2	2	2	4			39.50	3	2	2	2	4
		40.00	2	1	1	1	2			40.00	2	1	1	1	2
		40.50	2	1	1	1	2			40.50	1	0	0	0	0
		41.00	2	1	1	1	2			41.00	1	0	0	0	0
		41.50	2	1	1	1	2			41.50	1	0	0	0	0
X (cm)	Y (cm)	Z (cm)	TS	NL	TE	TM	EM	X (cm)	Y (cm)	Z (cm)	TS	NL	TE	TM	EM
49.00	40.00	38.50	2	1	1	1	2	49.00	40.50	38.50	2	1	1	1	2
		39.00	2	1	1	1	2			39.00	2	1	1	1	2
		39.50	2	1	1	1	2			39.50	1	0	0	0	0
		40.00	1	0	0	0	0			40.00	1	0	0	0	0
		40.50	1	0	0	0	0			40.50	1	0	0	0	0
		41.00	1	0	0	0	0			41.00	1	0	0	0	0
		41.50	1	0	0	0	0			41.50	1	0	0	0	0
X (cm)	Y (cm)	Z (cm)	TS	NL	TE	TM	EM	X (cm)	Y (cm)	Z (cm)	TS	NL	TE	TM	EM
49.00	41.00	38.50	2	1	1	1	2	49.00	41.50	38.50	2	1	1	1	2
		39.00	2	1	1	1	2			39.00	2	1	1	1	2
		39.50	1	0	0	0	0			39.50	1	0	0	0	0
		40.00	1	0	0	0	0			40.00	1	0	0	0	0
		40.50	1	0	0	0	0			40.50	1	0	0	0	0
		41.00	1	0	0	0	0			41.00	1	0	0	0	0
		41.50	1	0	0	0	0			41.50	1	0	0	0	0
X (cm)	Y (cm)	Z (cm)	TS	NL	TE	TM	EM	X (cm)	Y (cm)	Z (cm)	TS	NL	TE	TM	EM
49.50	38.50	38.50	3	2	2	2	4	49.50	39.00	38.50	3	2	2	2	4
		39.00	3	2	2	2	4			39.00	3	2	2	2	4
		39.50	3	2	2	2	4			39.50	3	2	2	2	4
		40.00	2	1	1	1	2			40.00	2	1	1	1	2
		40.50	2	1	1	1	2			40.50	2	1	1	1	2
		41.00	2	1	1	1	2			41.00	2	1	1	1	2
		41.50	2	1	1	1	2			41.50	2	1	1	1	2
X (cm)	Y (cm)	Z (cm)	TS	NL	TE	TM	EM	X (cm)	Y (cm)	Z (cm)	TS	NL	TE	TM	EM
49.50	39.50	38.50	3	2	2	2	4	49.50	40.00	38.50	2	1	1	1	2
		39.00	3	2	2	2	4			39.00	2	1	1	1	2
		39.50	3	2	2	2	4			39.50	1	0	0	0	0
		40.00	1	0	0	0	0			40.00	1	0	0	0	0
		40.50	1	0	0	0	0			40.50	1	0	0	0	0
		41.00	1	0	0	0	0			41.00	1	0	0	0	0
		41.50	1	0	0	0	0			41.50	1	0	0	0	0

Table B.2 Cont'd.

X (cm)	Y (cm)	Z (cm)	TS	NL	TE	TM	EM	X (cm)	Y (cm)	Z (cm)	TS	NL	TE	TM	EM
49.50	40.50	38.50	2	1	1	1	2	49.50	41.00	38.50	2	1	1	1	2
		39.00	2	1	1	1	2			39.00	2	1	1	1	2
		39.50	1	0	0	0	0			39.50	1	0	0	0	0
		40.00	1	0	0	0	0			40.00	1	0	0	0	0
		40.50	1	0	0	0	0			40.50	1	0	0	0	0
		41.00	1	0	0	0	0			41.00	1	0	0	0	0
		41.50	1	0	0	0	0			41.50	1	0	0	0	0
X (cm)	Y (cm)	Z (cm)	TS	NL	TE	TM	EM	X (cm)	Y (cm)	Z (cm)	TS	NL	TE	TM	EM
49.50	41.50	38.50	2	1	1	1	2	50.00	38.50	38.50	3	2	2	2	4
		39.00	2	1	1	1	2			39.00	3	2	2	2	4
		39.50	1	0	0	0	0			39.50	3	2	2	2	4
		40.00	1	0	0	0	0			40.00	2	1	1	1	2
		40.50	1	0	0	0	0			40.50	2	1	1	1	2
		41.00	1	0	0	0	0			41.00	2	1	1	1	2
		41.50	1	0	0	0	0			41.50	2	1	1	1	2
X (cm)	Y (cm)	Z (cm)	TS	NL	TE	TM	EM	X (cm)	Y (cm)	Z (cm)	TS	NL	TE	TM	EM
50.00	39.00	38.50	3	2	2	2	4	50.00	39.50	38.50	3	2			
		39.00	3	2	2	2	4			39.00	3	2			
		39.50	3	2	2	2	4			39.50	3	2			
		40.00	2	1	1	1	2			40.00	1	0	0	0	0
		40.50	2	1	1	1	2			40.50	1	0	0	0	0
		41.00	2	1	1	1	2			41.00	1	0	0	0	0
		41.50	2	1	1	1	2			41.50	1	0	0	0	0
X (cm)	Y (cm)	Z (cm)	TS	NL	TE	TM	EM	X (cm)	Y (cm)	Z (cm)	TS	NL	TE	TM	EM
50.00	40.00	38.50	2	1	1	1	2	50.00	40.50	38.50	2	1	1	1	2
		39.00	2	1	1	1	2			39.00	2	1	1	1	2
		39.50	1	0	0	0	0			39.50	1	0	0	0	0
		40.00	1	0	0	0	0			40.00	1	0	0	0	0
		40.50	1	0	0	0	0			40.50	1	0	0	0	0
		41.00	1	0	0	0	0			41.00	1	0	0	0	0
		41.50	1	0	0	0	0			41.50	1	0	0	0	0
X (cm)	Y (cm)	Z (cm)	TS	NL	TE	TM	EM	X (cm)	Y (cm)	Z (cm)	TS	NL	TE	TM	EM
50.00	41.00	38.50	2	1	1	1	2	50.00	41.50	38.50	2	1	1	1	2
		39.00	2	1	1	1	2			39.00	2	1	1	1	2
		39.50	1	0	0	0	0			39.50	1	0	0	0	0
		40.00	1	0	0	0	0			40.00	1	0	0	0	0
		40.50	1	0	0	0	0			40.50	1	0	0	0	0
		41.00	1	0	0	0	0			41.00	1	0	0	0	0
		41.50	1	0	0	0	0			41.50	1	0	0	0	0

Table B.2 Cont'd.

X(cm) Y(cm) Z(cm) TS NL TE TM EM	X(cm) Y(cm) Z(cm) TS NL TE TM EM
50.50 38.50 38.50 2 2 2 2 4	50.50 39.00 38.50 2 2 2 2 4
39.00 2 2 2 2 4	39.00 2 2 2 2 4
39.50 2 2 2 2 4	39.50 2 2 2 2 4
40.00 1 1 1 1 2	40.00 1 1 1 1 2
40.50 1 1 1 1 2	40.50 1 1 1 1 2
41.00 1 1 1 1 2	41.00 1 1 1 1 2
41.50 1 1 1 1 2	41.50 1 1 1 1 2
X(cm) Y(cm) Z(cm) TS NL TE TM EM	X(cm) Y(cm) Z(cm) TS NL TE TM EM
50.50 39.50 38.50 2 2 2 2 4	50.00 40.00 38.50 1 1 1 1 2
39.00 2 2 2 2 4	39.00 1 1 1 1 2
39.50 0 0 0 0 0	39.50 0 0 0 0 0
40.00 0 0 0 0 0	40.00 0 0 0 0 0
40.50 0 0 0 0 0	40.50 0 0 0 0 0
41.00 0 0 0 0 0	41.00 0 0 0 0 0
41.50 0 0 0 0 0	41.50 0 0 0 0 0
X(cm) Y(cm) Z(cm) TS NL TE TM EM	X(cm) Y(cm) Z(cm) TS NL TE TM EM
50.50 40.50 38.50 1 1 1 1 2	50.50 41.00 38.50 1 1 1 1 2
39.00 1 1 1 1 2	39.00 1 1 1 1 2
39.50 0 0 0 0 0	39.50 0 0 0 0 0
40.00 0 0 0 0 0	40.00 0 0 0 0 0
40.50 0 0 0 0 0	40.50 0 0 0 0 0
41.00 0 0 0 0 0	41.00 0 0 0 0 0
41.50 0 0 0 0 0	41.50 0 0 0 0 0
X(cm) Y(cm) Z(cm) TS NL TE TM EM	X(cm) Y(cm) Z(cm) TS NL TE TM EM
50.50 41.50 38.50 1 1 1 1 2	51.00 38.50 38.50 2 2 2 2 4
39.00 1 1 1 1 2	39.00 2 2 2 2 4
39.50 0 0 0 0 0	39.50 2 2 2 2 4
40.00 0 0 0 0 0	40.00 1 1 1 1 2
40.50 0 0 0 0 0	40.50 1 1 1 1 2
41.00 0 0 0 0 0	41.00 1 1 1 1 2
41.50 0 0 0 0 0	41.50 1 1 1 1 2
X(cm) Y(cm) Z(cm) TS NL TE TM EM	X(cm) Y(cm) Z(cm) TS NL TE TM EM
51.00 39.00 38.50 2 2 2 2 4	51.00 39.50 38.50 2 2 2 2 4
39.00 2 2 2 2 4	39.00 2 2 2 2 4
39.50 2 2 2 2 4	39.50 0 0 0 0 0
40.00 1 1 1 1 2	40.00 0 0 0 0 0
40.50 1 1 1 1 2	40.50 0 0 0 0 0
41.00 1 1 1 1 2	41.00 0 0 0 0 0
41.50 0 0 0 0 0	41.50 0 0 0 0 0

Table B.2 Cont'd.

X (cm) Y (cm) Z (cm) TS NL TE TM EM	X (cm) Y (cm) Z (cm) TS NL TE TM EM
51.00 40.00 38.50 1 1 1 1 2	51.00 40.50 38.50 1 1 1 1 2
39.00 1 1 1 1 2	39.00 1 1 1 1 2
39.50 0 0 0 0 0	39.50 0 0 0 0 0
40.00 0 0 0 0 0	40.00 0 0 0 0 0
40.50 0 0 0 0 0	40.50 0 0 0 0 0
41.00 0 0 0 0 0	41.00 0 0 0 0 0
41.50 0 0 0 0 0	41.50 0 0 0 0 0
X (cm) Y (cm) Z (cm) TS NL TE TM EM	X (cm) Y (cm) Z (cm) TS NL TE TM EM
51.00 41.00 38.50 1 1 1 1 2	51.00 41.50 38.50 1 1 1 1 2
39.00 1 1 1 1 2	39.00 0 0 0 0 0
39.50 0 0 0 0 0	39.50 0 0 0 0 0
40.00 0 0 0 0 0	40.00 0 0 0 0 0
40.50 0 0 0 0 0	40.50 0 0 0 0 0
41.00 0 0 0 0 0	41.00 0 0 0 0 0
41.50 0 0 0 0 0	41.50 0 0 0 0 0
X (cm) Y (cm) Z (cm) TS NL TE TM EM	X (cm) Y (cm) Z (cm) TS NL TE TM EM
51.50 38.50 38.50 2 2 2 2 4	51.50 39.00 38.50 2 2 2 2 4
39.00 2 2 2 2 4	39.00 2 2 2 2 4
39.50 2 2 2 2 4	39.50 1 1 1 1 2
40.00 1 1 1 1 2	40.00 1 1 1 1 2
40.50 1 1 1 1 2	40.50 1 1 1 1 2
41.00 1 1 1 1 2	41.00 1 1 1 1 2
41.50 2 2 2 1 3	41.50 1 1 1 0 1
X (cm) Y (cm) Z (cm) TS NL TE TM EM	X (cm) Y (cm) Z (cm) TS NL TE TM EM
51.50 39.50 38.50 2 2 2 2 4	51.50 40.00 38.50 1 1 1 1 2
39.00 1 1 1 1 2	39.00 1 1 1 1 2
39.50 0 0 0 0 0	39.50 0 0 0 0 0
40.00 0 0 0 0 0	40.00 0 0 0 0 0
40.50 0 0 0 0 0	40.50 0 0 0 0 0
41.00 0 0 0 0 0	41.00 0 0 0 0 0
41.50 1 1 1 0 1	41.50 1 1 1 0 1
X (cm) Y (cm) Z (cm) TS NL TE TM EM	X (cm) Y (cm) Z (cm) TS NL TE TM EM
51.50 40.50 38.50 1 1 1 1 2	51.50 41.00 38.50 1 1 1 1 2
39.00 1 1 1 1 2	39.00 1 1 1 1 2
39.50 0 0 0 0 0	39.50 0 0 0 0 0
40.00 0 0 0 0 0	40.00 0 0 0 0 0
40.50 0 0 0 0 0	40.50 0 0 0 0 0
41.00 0 0 0 0 0	41.00 0 0 0 0 0
41.50 1 1 1 0 1	41.50 1 1 1 0 1

Table B.3 A comparison of mode count reference data for several cavities of typical sizes used in domestic microwave ovens.

CAVITY DIMENSIONS			2400 ≤ f ≤ 2500 MHz					902 ≤ f ≤ 928 MHz				
X (cm)	Y (cm)	Z (cm)	TS	NL	TE	TM	EM	TS	NL	TE	TM	EM
28.00	36.00	38.00	11	11	10	8	18	1	1	1	0	1
		39.00	9	9	8	7	15	1	1	1	0	1
		40.00	12	12	11	9	20	2	2	2	0	2
		41.00	15	15	14	11	25	2	2	2	0	2
		42.00	14	14	13	11	24	1	1	1	0	1
28.00	38.00	38.00	14	14	12	8	20	0	0	0	0	0
		39.00	14	14	12	10	22	0	0	0	0	0
		40.00	16	16	14	10	24	1	1	1	0	1
		41.00	19	19	17	12	29	1	1	1	0	1
		42.00	16	16	14	12	26	0	0	0	0	0
28.00	40.00	38.00	16	16	13	11	24	1	1	0	1	1
		39.00	19	19	16	15	31	1	1	0	1	1
		40.00	20	20	17	15	32	2	2	1	1	2
		41.00	18	18	15	14	29	2	2	1	1	2
		42.00	17	17	14	14	28	1	1	0	1	1
30.00	36.00	38.00	8	8	8	5	13	1	1	1	0	1
		39.00	9	9	9	7	16	2	2	2	0	2
		40.00	13	13	13	10	23	1	1	1	0	1
		41.00	14	14	14	11	25	1	1	1	0	1
		42.00	13	13	13	10	23	1	1	1	0	1
30.00	38.00	38.00	15	15	13	9	22	0	0	0	0	0
		39.00	16	16	14	12	26	1	1	1	0	1
		40.00	18	18	16	12	28	0	0	0	0	0
		41.00	17	17	15	11	26	0	0	0	0	0
		42.00	17	17	15	13	28	0	0	0	0	0
30.00	40.00	38.00	18	18	15	13	28	0	0	0	0	0
		39.00	20	20	17	16	33	1	1	1	0	1
		40.00	22	22	19	17	36	0	0	0	0	0
		41.00	15	15	12	12	24	0	0	0	0	0
		42.00	15	15	12	12	24	0	0	0	0	0
32.00	36.00	38.00	15	15	14	10	24	2	2	2	0	2
		39.00	15	15	14	11	25	1	1	1	0	1
		40.00	16	16	15	13	28	1	1	1	0	1
		41.00	12	12	11	10	21	1	1	1	0	1
		42.00	11	11	10	8	18	1	1	1	0	1
32.00	38.00	38.00	24	24	20	16	36	2	2	1	1	2
		39.00	22	22	18	16	34	1	1	0	1	1
		40.00	23	23	19	17	36	1	1	0	1	1
		41.00	20	20	16	15	31	1	1	0	1	1
		42.00	22	22	18	18	36	1	1	0	1	1
32.00	40.00	38.00	23	23	20	16	36	1	1	1	0	1
		39.00	24	24	21	18	39	0	0	0	0	0
		40.00	22	22	19	17	36	0	0	0	0	0
		41.00	19	19	16	17	33	0	0	0	0	0
		42.00	18	18	15	15	30	0	0	0	0	0

Table B.4 Variations in the mode count data presented in Tables B.1,2,3.

BANDWIDTH (MHz)	RANGE OF CAVITY DIMENSIONS			RANGE OF MODE COUNTS				
	X (cm)	Y (cm)	Z (cm)	TS	NL	TE	TM	EM
$2425 \leq f \leq 2475$	48.50-52.00	38.50-41.50	38.50-41.50	8-21	8-20	7-19	8-16	14-33
$900 \leq f \leq 930$	48.50-52.00	38.50-41.50	38.50-41.50	0-3	0-2	0-2	0-2	0-4
$2400 \leq f \leq 2500$	28.00-32.00	36.00-40.00	38.00-42.00	8-24	8-24	8-21	5-18	13-39
$902 \leq f \leq 928$	28.00-32.00	36.00-40.00	38.00-42.00	0-2	0-2	0-2	0-1	0-2

APPENDIX C. ON THE CROSS-COUPLING PROBLEM

Solid state microwave power applicators have been technologically feasible for over a decade. However, in order to make them economically feasible (even the present or slightly advanced state of the art), efficient means must be devised for combining the outputs of several medium power microwave sources. The simplest method is to use the cavity itself as the power combining network, by separately coupling each source to the cavity through an independent feed structure. The "cross-coupling problem" is thus defined as achieving this independence.

Several methods have been hypothesized which should, theoretically, reduce the cross-coupling between multiple sources. For example, operating each source at widely different frequencies (e.g. 915 vs. 2450 MHz) or using cross-polarized antennae are commonly cited [48]. However, to the author's knowledge, no one has examined the problem experimentally to determine the severity (or nonseverity) of this problem qualitatively. Part of the reason for this lack of information may be the difficulty in generalizing any experimental data. And for this reason, the remainder of the discussion which follows is primarily conjecture, but is based on observations made while conducting the measurements of Chapter 4.

The measurement system described in Chapter 4 is easily modified to observe the cross-coupling between any two antennae. Basically, a transmission loss measurement can be performed by connecting the output of a receiving antenna to channel B of the swept amplitude analyzer through a second detector as indicated in Figure 4.1.

It was found that when the receiving probe was very short, and the cavity was empty, only cross-coupling through normal cavity eigenmodes can occur. In this case, the transmission spectrum is discrete and differs mainly in magnitude from the input spectrum. The degree of cross-coupling for some of the modes within the domain of Figure 4.2 were classified as strong (S), medium (M) or weak (W) as indicated in Figure C.1. The actual level of transmission loss was small.

When the receiving probe was a realistic length (≈ 10 cm), and a mode stirrer was included, the transmission spectrum was observed to be virtually continuous, and the transmission loss was much higher than in the above case. The continuous spectrum can probably be explained as a result of the length and proximity of the two antennae which allowed cross-coupling through near fields or evanescent modes (which is enhanced by the mode stirrer). This observation would seem to indicate that the cross-coupling problem is indeed severe in a practical case. However, many

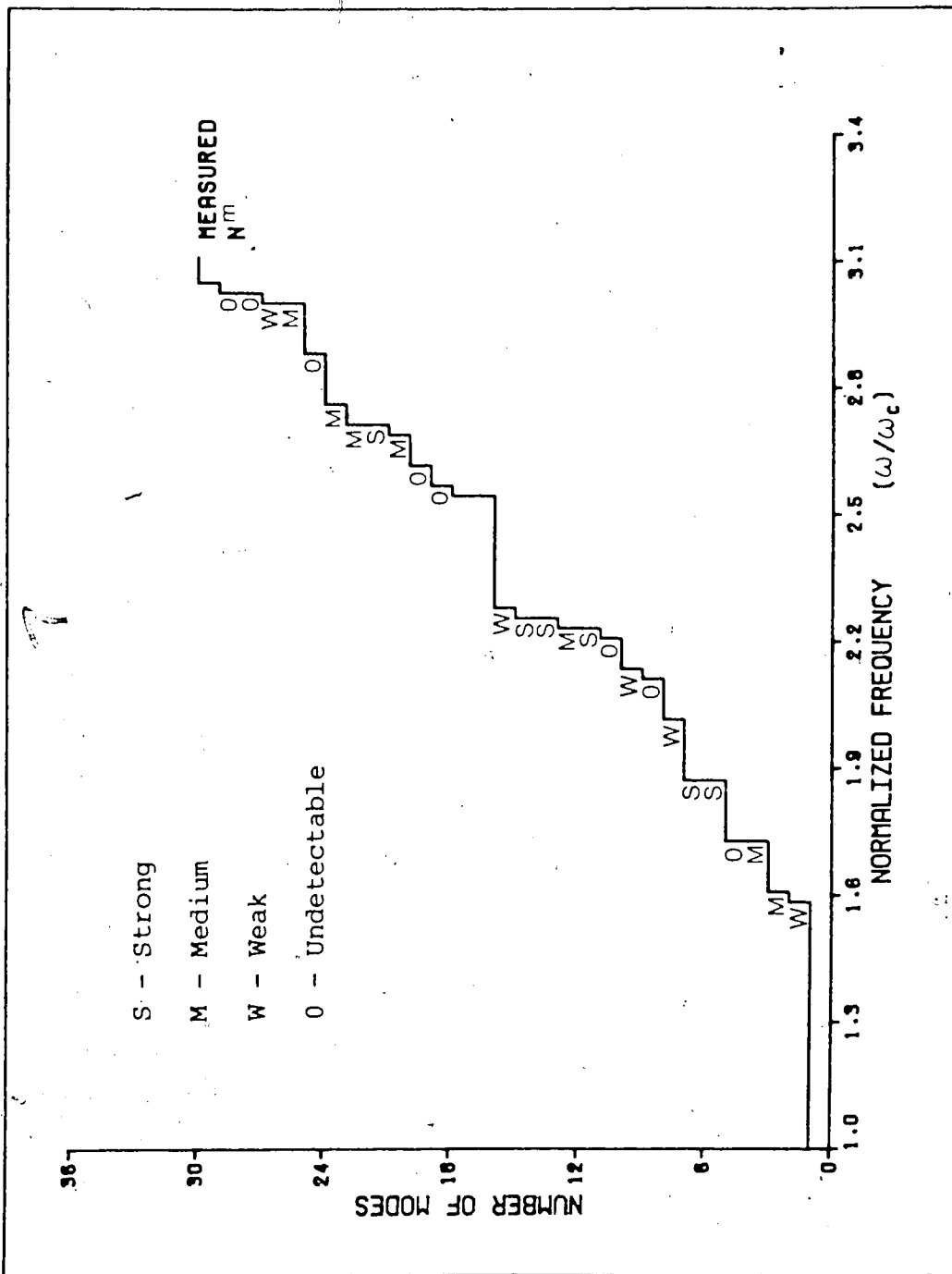


Figure C.1 Measured spectral distribution of modes (N^m), for the experimental cavity discussed in Chapters 4 and 5, showing the relative cross-coupling between top and side oriented antennae. The receiving antenna is less than 1 cm length.

new power transistors can withstand infinite VSWR in a class C mode (at least temporarily). And when the cavity is heavily loaded with lossy dielectric, the actual level of received power due to the cross-coupling effect would presumably be much less than the output capability of the source. In any case, the output spectrum of solid state power amplifiers is broad enough that much power is reflected from an empty cavity even when the input is perfectly matched to the cavity (at the eigenfrequencies). Hence, although the cross-coupling per se can be serious, it may not necessarily be detrimental to the operation of a solid state applicator. More thorough experimental studies with transistor sources are required in order to determine the true extent of this problem.

Numerical Models

Since general results are difficult to obtain, either experimentally or analytically, it would be extremely useful if a numerical algorithm were available that could parametrically model the cross-coupling between two (or more) antennae. Again, a completely general model could not be obtained with a finite number of parameters, but perhaps certain classes of antennae could be modeled.

It may be possible to base such a model on a perturbation-type analysis, where the perturbed

eigenfunctions are numerically integrated over the receiving antenna. However, some philosophical problems regarding the applicability of perturbation theory to a cavity which is not a closed thermodynamic system, may exist. A more complicated approach, but one which is (probably) free of philosophical questions, is to employ the image theory of Kelvin. That is, once all of the image antennae are determined, the theory of antennae arrays could perhaps be used to compute the image currents on the receiving antennae due to the exciting antennae. If this method is feasible, it may be the most general since free space radiation patterns for arbitrarily shaped antennae can be determined empirically.

APPENDIX D. ASYMPTOTIC FORMULAE FOR WAVEGUIDES

Recall that the two dimensional EM boundary value problem leads to an eigenvalue equation for the cutoff frequencies of waveguide modes. Asymptotic formulae for the spectral distribution and density of these eigenfrequencies can be derived in exactly the same manner as that used in Chapter 5 to obtain the asymptotic formulae for cavity modes.

The number of characteristic points in a two dimensional p-space, to first order, is just the area enclosed in the first quadrant by the ellipse described by Eq.(2.29), viz.

$$\frac{1}{4} \pi \left[\frac{L_1}{\pi} \frac{\omega}{c} \frac{L_2}{\pi} \frac{\omega}{c} \right] = \frac{A}{4\pi} \frac{\omega^2}{c^2} \equiv N_0^W(\omega) \quad (D.1)$$

where A is the cross-sectional area of the guide (normal to the x_3 axis). $N_0^W(\omega)$ is thus the two dimensional counterpart of $N_0(\omega)$, the ambivalent first term of the asymptotic expansion for cavity modes.

Correcting for the undercounting/overcounting of characteristic points on the coordinate axes of p-space, one obtains

$$N_{TM}(\omega) = N_0^W(\omega) - \frac{(L_1+L_2)}{2\pi} \frac{\omega}{c} + \frac{1}{4} \quad (D.2)$$

for the TM modes, and

$$N_{TE}(\omega) = N_0^W(\omega) + \frac{(L_1+L_2)}{2\pi} \frac{\omega}{c} - \frac{3}{4} \quad (D.3)$$

for the TE modes. Thus the total number of EM modes with cutoff frequencies not greater than ω is approximately

$$N_{EM}(\omega) = 2N_0^W(\omega) - \frac{1}{2} \quad (D.4)$$

and the total number of EM modes with cutoff frequencies between ω and $\omega+\delta\omega$ is approximately

$$D_{EM}(\omega)\delta\omega = \frac{A}{\pi} \frac{\omega}{c^2} \delta\omega = 2D_0^W(\omega)\delta\omega \quad (D.5)$$

where $D_0^W(\omega)$ is the two dimensional counterpart to $D_0(\omega)$ as defined in Chapter 5. Hence, the spectral density function for waveguide modes is

$$D_{EM}(\omega) = 2D_0^W(\omega) \quad (D.6)$$

which is just the derivative of $N_{EM}(\omega)$ with respect to ω .